



جمهورية العراق  
وزارة التعليم العالي والبحث العلمي  
جامعة بابل  
كلية التربية للعلوم الصرفة  
قسم الفيزياء

تصميم معوض خسائر بصري للألياف الضوئية بالاعتماد على  
الشبكات العصبية الاصطناعية البصرية

رسالة مقدمة

إلى مجلس كلية التربية للعلوم الصرفة في جامعة بابل  
وهي جزء من متطلبات نيل درجة دكتوراه فلسفه  
في التربية / الفيزياء

من قبل الطالبة

**زينب عادل عباس جاسم**

ماجستير تربية فيزياء  
2015 م

بإشراف

أ.د. ابراهيم عبد الله  
مرداس

أ.د. طالب محسن عباس

2023م

1445هـ

Republic of Iraq  
Ministry of Higher Education



and Scientific Research  
University of Babylon  
College of Education for Pure Sciences  
Department of physics

# Design of Optical Loss Compensation for Optical Fibers Based on Optical Artificial Neural Networks

*A Thesis*

*Submitted to the Council of the College of Education  
for Pure Sciences, University of Babylon in Partial  
Fulfillment of the Requirements for the Degree  
of Doctor of Philosophy in Education/Physics*

By

**Zainab Adil Abbas Jasim**

*Master of Education Physics  
University of Babylon (2015)*

*Supervised by*

**Prof. Dr. Talib Mohsen Abbas**

**Prof. Dr. Ibrahim Abdullah Murdas**

**2023 A.D**

**1445 A.H**

سورة الاسراء



﴿٨٤﴾ وَبَسَّ الْوُزْنُكَ عَنِ الرُّوحِ ۖ قُلِ الرُّوحُ مِنْ أَمْرِ رَبِّي وَمَا

أُوتِيتُمْ مِنَ الْعِلْمِ إِلَّا قَلِيلًا ﴿٨٥﴾

صدق الله العظيم

(سورة الاسراء : ٨٥)

# Dedication

## Sincerity

I dedicate this effort to

The mother who did not give birth to me “my aunt”

My children

My aunts and uncle

My sister, my cousins and my brothers

My country is Iraq

For my teachers

Who provides me with the keys to success

*Zainab* ✍

## Acknowledgments

First of all, I thank the gracious God for helping me complete this letter.

After that, I would like to express my sincere appreciation and deep gratitude to my supervisors Prof. Dr. Talib Mohsen Abbas and Prof. Dr. Ibrahim Abdullah Murdas for suggesting the topic of this thesis and for the guidance, suggestions and continuous encouragement throughout the research work.

A word of thanks to the faculty members of the Department of Physics, College of Education for Pure Sciences.

*Zainab* ✍

## Summary

This study focused on the compensation techniques in optical fiber channels for linear and nonlinear impairments. The work in this study falls into two main parts based on the compensation technique used. The first part deals with using the proposed design for compensation method based on optical phase conjugation (optical inversion spectrum) to mitigate the optical fiber losses (linear and nonlinear) in the second part using the artificial intelligent method such as neural network to compensate the fiber losses. In optical fiber systems, the optical fiber is the communication channel in which light propagates. As with any other transmission medium, attenuation, dispersion, self-phase modulation and cross phase modulation are determining factors for the efficiency of the optical fiber.

The achievement of low-loss optical fibers is not restricted only in the field of optical communications, but rather in the emergence of a new field of science that is nonlinear fiber optics, and the benefit of this new field of science is the continuous development of the basics of the technologies necessary for information management.

The nonlinear effects as well as the linear effects of optical fibers are among the important points that must be taken care of, because most of the optical fiber applications depend on them. Therefore, when studying optical fibers in the field of communications or in the field of medical applications, the signal transmission process within the optical fiber is very important because the transmitted signal within the optical fiber suffers from attenuation and weakness due to these effects, which restrict the work of optical fibers in the field of communications.

In this work, a loss compensation was proposed for both types of linear losses within the optical fiber, such as dispersion, attenuation, and absorption. Dispersion compensation fiber dispersion compensation fiber DCF loss compensators were

designed and implemented to eliminate dispersion within the optical fiber with an appropriate compensation coefficient. Optical semiconductor amplifiers were used to compensate for losses resulting from signal attenuation. As for the nonlinear losses, two types of compensators were proposed, designed, and implemented. The first is the opacity compensation process based on the optical phase coupling method. An optical compensator was designed based on highly nonlinear fiber HNLF and implemented in two configurations, one in the middle of the path and the other on both ends of the system. Good compensation results were obtained, and the system's signal transmission performance was also improved. A second loss compensator was proposed based on the technique of artificial neural networks, where these networks train on the outputs of the system and then improve the performance of the system by controlling the transmitted power and controlling the nonlinear phase change, as shown in the results. The programs used in this work are Optisystem 19 and Matlab with the help of Python code.

## Supervisor's certificate

We certify that this thesis entitled " **Design of Optical Loss Compensation for Optical Fibers Based on Optical Artificial Neural Networks**" is prepared by the student (**Zainab Adil Abbas jasim**) under our supervision at the College of Education for Pure Sciences, University of Babylon as partial fulfillment of the requirements for the Degree of doctorate of philosophy in Physical Sciences.

**Signature:**

Name: Dr. Talib Mohsen Abbas

Title: Professor

(Supervisor)

Date: / / 2023

**Signature:**

Name: Dr. Ibrahim Abdullah Murdas

Title: Professor

(Supervisor)

Date: / / 2023

---

**Head of the Department Certificate**

---

In view of the available recommendations, I forward this thesis for debate by the examining committee.

**Signature:**

Name: Dr. Khalid Haneen Abbas

Title: Professor

(Head of Physics Department)

Date: / / 2023

## ***Certification of Linguistic Expert***

I certify that I have read this dissertation entitled “**Design of Optical Loss Compensation for Optical Fibers Based on Optical Artificial Neural Networks**” and corrected its grammatical mistakes, therefore it has qualified for debate.

Signature:

Name: Dr.

Title:

Address:

Date:        /        / 2023

## ***Certification of Scientific Expert***

I certify that I have read the scientific content of this thesis “**Design of Optical Loss Compensation for Optical Fibers Based on Optical Artificial Neural Networks**” and I have approved this dissertation is qualified for debate.

Signature:

Name: Dr.

Title:

Address:

Date:        /        / 2023

## ***Certification of Scientific Expert***

I certify that I have read the scientific content of this thesis “**Design of Optical Loss Compensation for Optical Fibers Based on Optical Artificial Neural Networks**” and I have approved this dissertation is qualified for debate.

Signature:

Name: Dr.

Title:

Address:

Date:        /        / 2023

### *Examining Committee Certification*

We certify that we have read this thesis entitled “**Design of Optical Loss Compensation for Optical Fibers Based on Optical Artificial Neural Networks**” and as a committee examined the student “**Zainab Adil Abbas Jasim**” its contents and that in our opinion, it meets the standards of a thesis for the Degree Doctor of Philosophy Education / Physics.

Signature:  
Name: Dr.  
Title:  
Address:  
Date: / / 2023  
(Chairman)

Signature:  
Name: Dr.  
Title:  
Address:  
Date: / / 2023  
(Member)

Signature:  
Name: Dr.  
Title:  
Address:  
Date: / / 2023  
(Member)

Signature:  
Name: Dr.  
Title:  
Address:  
Date: / / 2023  
(Member)

Signature:  
Name: Dr.  
Title:  
Address:  
Date: / / 2023  
(Member)

Signature:  
Name: Dr.  
Title:  
Address:  
Date: / / 2023  
Member / Supervisor

Signature:  
Name: Dr.  
Title:  
Address:  
Date: / / 2023  
Member / Supervisor

Approved by the Council of the College of Education for Pure Sciences.

Signature:  
Name:  
Dean of the College of Education for Pure Sciences  
Title:  
Address:  
Date: / / 2023

# Contents

NO	Subject	Page No.
	Contents	I
	List of Figures	VI
	List of Tables	IX
	List of Symbols	XI
	List of Abbreviations	XIII
	Chapter One: Introduction and Literature Review	
1.1	Introduction	1
1.2	History of optical fiber	1
1.3	Advantage of optical fiber	4
1.4	Problem statements	5
1.5	Literature review of optical phase conjunction	5
1.6	Literature review of optical neural network	10
1.7	Research aims	14
	Chapter Two: Theoretical Part	
2.1	Introduction	15
2.2	Theory involving ray transmission	15
2.2.1	Total internal reflection	15
2.3	Wave propagation in optical fiber	18
2.4	Types of fiber impairments	21

2.4.1	Linear impairments in optical fibers	21
2.4.1.1	Power attenuation in fibers	21
2.4.1.2	Absorption losses in silica glass fibers	22
2.4.1.3	Linear scattering loss	23
2.4.1.4	Dispersion effects in optical fibers	23
2.4.1.5	Mode dispersion MD	24
2.4.1.6	Chromatic dispersion CD	24
2.4.1.7	Material dispersion	25
2.4.1.8	Waveguide dispersion	26
2.4.2	Nonlinear impairments in optical fibers	26
2.4.2.1	Light kerr effect in optical fiber	27
2.4.2.1.1	Self phase modulation	27
2.4.2.1.2	Cross phase modulation	28
2.4.2.1.3	Four wave mixing	29
2.5	All optical neural network	30
2.5.1	Deep learning of optical neural network	32
2.5.1.1	The previously dimensionality curse	33
2.5.1.2	Regularization of local constancy and smoothness	33
2.5.1.3	An information set for training	33
2.6	Convolutional neural network	34
2.6.1	Basic Convolutional neural network structure elements	35
2.6.2	Convolutional neural network component	35
2.7	Structure of artificial neural networks	37
2.8	Algorithm training for Back-propagation	39

2.9	Typical all-optical neural network AONN Organization	39
2.10	Operation of linear optics	40
2.11	Putting optical back – propagation in to practice	42
	<b>Chapter Three: The Proposed System Design</b>	
3.1	Optical spectrum inversion technique	43
3.2	Techniques for light inversion spectrum	44
3.3	Methods based on fiber nonlinearities	45
3.3.1	Optical spectrum inversion based four wave mixing	46
3.3.1.1	Four wave regenerative mixing in reverse	47
3.3.2	Enhanced backwards scattering	48
3.4	Design of dispersion optical compensator based optical spectrum inversion	49
3.5	Compensation design based optical spectrum inversion	51
3.6	Implementation the optical spectrum inversion	53
3.6.1	Effect of two pump source	56
3.6.2	Approximate analysis of the four wave mixing - optical spectrum inversion system	56
3.7	Neural network artificially	58
3.8	Optical neural network	62
3.8.1	Hybrid optic-electronic neural network	63
3.9	Challenge for implementing all-optical neural network	63
3.10	Training algorithms (backpropagation algorithm)	63

3.11	Optical neural network implementation	65
3.12	Training network	67
	Chapter Four: Results and Discussion	
4.1	Introduction	69
4.2	Fiber losses compensator	69
4.3	Compensation of linear fiber impairments by DCF OOK	69
4.4	One optical spectrum inversion (MiD fiber) compensation control	75
4.5	Compensation using MID-HNLF-OPC OOK at different Bitrate	76
4.6	Compensation using MID-HNLF-OPC OOK at different Fiber Length	82
4.7	Multiple-(2- optical spectrum inversion) Compensation Scheme for different bit rate	87
4.7.1	Effect of multiple optical spectrum inversion for 40 Gb/s	88
4.7.2	Effect of multiple optical spectrum inversion for 80 Gb/s	90
4.8	Multiple-(2- optical spectrum inversion) compensation scheme for different fiber length	93
4.8.1	Effect of multiple optical spectrum inversion for 200 Km	93

4.8.2	Effect of multiple optical spectrum inversion for 400 Km	95
4.9	Compensation using artificial neural networks	97
4.9.1	Neural network compensator	97
4.9.2	Neural network results	99
4.10	Results and discussion of optical neural network	101
4.11	Comparison between Optical neural networks ONNs and artificial neural networks ANNs	106
	Chapter Five: Conclusion and Future work	
5.1	Conclusion	110
5.2	Suggestion for future work	111
	References	112

## List of Abbreviations

Abbreviation	Definition
ANN	Artificial neural network
AONN	All optical neural network
BL	Band line width product
CCE	Categorical cross entropy
CD	Chromatic dispersion
CNN	Convolutional neural network
CO-OFDM	Coherent optical orthogonal frequency division multiplexing
DB	Decibels
DCF	Dispersion compensation fiber
FTTH	Fiber to the home
FWHM	Full width half maximum
FWM	Four wave mixing
GVD	Group velocity dispersion
HNLF	Highly nonlinear fiber
HONN	Hybrid optic electronic network
InGaAsP	Indium gallium arsenide phosphide
ISI	Inter symbol interferences
MAE	Mean absolute error
MMF	Multi-mode fiber
MD	Mode dispersion
MZM	Mach Zehnder modulator
NLS	Nonlinear Schrödinger equation

Abbreviation	Definition
NN	Neural network
ONN	Optical neural network
OOK	On off key
OPC	Optical phase conjugation
OSI	Optical spectrum inversion
PCW	Phase conjugate wave
PDM	Polarization division multiplexing
QAM	Quadrature amplitude modulation
SBS	Stimulated Brillouin scattering
SMF	Single mode fiber
SRS	Stimulated Raman scattering
SOA	Semiconductor optical amplifier
SPM	Self-phase modulation
TIR	Total internal reflection
WDM	Wavelength division multiplexing
XPM	Cross phase modulation

## List of Figures

No. Of Figures	Name	Page
1-1	Through several generations of photonics systems, the BL product grew during 1975 and 1980	2
2-1	(a) Shows light rays striking a contact with a high to low refractive index, such as glass and air. (b) Refraction, its limiting situation in which the crucial beam appears at an angle of $\phi_c$ , (c) total internal reflection in which $\phi > \phi_c$ .	16
2-2	Shows how a light beam travels through a flawless optical fiber	17
2-3	Attenuation in relation to wavelength	22
2-4	Shows the wavelength-dependent values of the dispersion parameters for a standard single-mode fiber's material dispersion parameter (DM), waveguide dispersion parameter (DW), and total dispersion parameter (DT) for a common single-mode fiber	25
2-5	Block digrame of fiber nonlinearities	26
2.6	Shows the AONN structure. (a) The D2 NN's general structure. (b) Using D2 NN as an image classifier. (b) The application of D2NN in imaging. (d) The distinction between electronic NN and diffractive ONN	31
2.7	Single-layer feed-forward network	38
2.8	Multi-layer feed-forward networks	38
2.9	(a) Typical two layer neural network is an AONN. (b) Diagram of a nonlinear and linear optical neuron implementation under investigation	40
2.10	Shows the optical setup performing the linear operations	41

3.1	Show the OSI signal (left, L1) and conjugate are included in the schematics of a straightforward two-span transmission system (right, L2).	45
3.2	Optical inversion spectrum based four wave mixing	46
3.3	Show degenerate of four-wave mixing produces phase-conjugate wave	47
3.4	Schematic of midspan phase conjugation	50
3.5	The proposed compensated design	55
3.6	Optical spectrum of the signals	55
3.7	Artificial neural network operation theory. (A) A diagram of a biological neuron. (b) A schematic illustration of a synthetic neuron. (c) Feed-forward artificial neural networks' architecture	61
3.8	The classification of optical neural network	62
3.9	Block diagram of the neural network system	64
3.10	Method of import libraries	66
3.11	Process of the neural network system	68
4.1	Simulation of optical fiber system with DCF only	70
4.2	Illustrate Dispersion compensation fiber DCF at 30 Gb/s	73
4.3	Illustrate Dispersion compensation fiber DCF at 60 Gb/s	75
4.4	Schematic diagram of MiD fiber OSI Compensation control	76
4.5	Simulation of optical fiber system with optical MID-OSI	77
4.6	Illustrate MiD-OSI compensation fiber at 30 Gb/s	78
4.7	Illustrate OSI compensation fiber at 60 Gb/s	80

4.8	Illustrate the effect of OSI compensator on fiber length at 200 Km.	84
4.9	Illustrate MiD-OSI compensation fiber at 400 Km	86
4.10	Simulation of optical fiber system with Multiple-optical OSI	87
4.11	Illustrate Multi-OSI compensation fiber at 40Gb/s	90
4.12	Illustrate Multi-OSI compensation fiber at 80 Gb/s	92
4.13	Illustrate Multi-OSI compensation fiber at 200Km	94
4.14	Illustrate Multi-OSI compensation fiber at 400Km 80Gb/s	96
4.15	A CNN sequence to classify handwritten digits	100
4.16	The accuracy and loss of first dataset in ANN.	100
4.17	The losses and accuracy of second dataset in ANN.	101
4.18	The accuracy and loss of first dataset in ONN	103
4.19	The accuracy and loss of second dataset in ONN	105
4.20	Training of convolutional neural network	108

## List of Symbols

Symbols	Definitions
$A$	Complex envelop of propagated signal
$A_{\text{eff}}$	Effective area of fiber core
$A^*$	Complex conjugated envelop of propagated signal
$\widetilde{A}^*$	Fourier transform of $A^*$
$C$	Light velocity
$E$	Electrical fields
$f_c$	Frequency phase-conjugated wave
$f_p$	Frequency of pump wave
$f_s$	Frequency of signal wave
$g$	Parameter coefficient of the gain
$K$	Wave number
$L$	Number of layer
$L_1$	Fiber length of OPC
$\mathcal{L}$	Loss function
$M$	Material dispersion
$n_1$	Core refractive index
$n_2$	Cladding refractive index
$N$	Gain term
$P$	Induce polarization
$P_L$	Linear part
$P_{NL}$	Nonlinear part
$Q$	Quality factor

Symbols	Definitions
$V_j$	Input layer nodes in the linear operation
$\alpha$	Loss coefficient
$\beta$	Propagation constant
$\beta_2$	Chromatic dispersion
$\beta_3$	Third order dispersion parameter
$\xi$	Power on the long fiber
$\chi$	Susceptibility
$\lambda$	Wave length
$\omega$	Angular frequency
$\gamma$	Nonlinear coefficient
$\epsilon, \epsilon_0$	Permittivity, Permittivity of vacuum
$\phi_1, \phi_c$	Angle of incident, critical angle
$F_1$	Filter size
$k_{\text{eff}}$	Effective length
$k_{\text{out}}$	Output size
$\Delta k$	Nonlinear Phase loss
$\phi_{\text{NL}}$	Nonlinear phase shift
$P_a$	Number of padding
$S_t$	Number of stride
$w^l$	Weight matrix
$y_i$	Output optical fiber
$\delta_i$	Error of term
$\mu$	Permeability
$\mu_0$	Permeability for vacuum

## List of Tables

No. Of Tables	Name	Page
3.1	Represent the Parameter values of the proposed system	56
4.1	200 km Fiber length, with dispersion compensation fiber DCF only, at bit rate 30 Gb/s	71
4.2	200 km Fiber length, with dispersion compensation fiber DCF ,at bit rate 60 Gb/s	73
4.3	200 km Fiber length, with MiD-OSI fiber ,at bit rate 30 Gb/s	78
4.4	200 km Fiber length, with MiD-OSI fiber ,at bit rate 60 Gb/s	81
4.5	200 km Fiber length, with MiD-OSI fiber ,at bit rate 30 Gb/s	83
4.6	400 km Fiber length, with MID-OSI fiber ,at bit rate 30 Gb/s	85
4.7	400 km Fiber length, with Multiple-OSI fiber ,at bit rate 40 Gb/s	88
4.8	400 km Fiber length, with Multiple-OSI fiber ,at bit rate 80 Gb/s	91
4.9	200 Km Fiber length, with Multiple-OSI fiber ,at bit rate 80 Gb/s	93
4.10	400 km Fiber length, with Multiple-OSI fiber ,at bit rate 80 Gb/s	95

4.11	Results of artificial neural networks	99
4.12	Results of dataset in ONN (learning rate $1 \times 10^{-3}$ )	103
4.13	Results of first dataset in ONN (learning rate $1 \times 10^{-4}$ )	105
4.14	A comparison between artificial neural networks (ANNs) and Optical Neural Networks (ONNs)	107
4.15	Illustrate the performance enhancement of the system for different laser power and fiber length	109

## الخلاصة

ركزت هذه الأطروحة على تقنيات التعويض في قنوات الألياف الضوئية للخسائر الخطية وغير الخطية. ينقسم العمل في هذه الأطروحة إلى جزأين رئيسيين بناءً على تقنية التعويض المستخدمة. يتناول الجزء الأول استخدام التصميم المقترح لطريقة التعويض القائمة على اقتران الطور البصري (طيف الانعكاس البصري) لتخفيف خسائر الألياف الضوئية (الخطية وغير الخطية) في الجزء الثاني باستخدام طريقة الذكاء الاصطناعي مثل الشبكة العصبية لتعويض خسائر الألياف الضوئية. فلألياف الضوئية هي قناة الاتصال التي ينتشر فيها الضوء كما هو الحال مع أي وسيط إرسال آخر، يعد التوهين والتشتت وتضمين الطور الذاتي وتضمين الطور المتقاطع عوامل محددة لكفاءة الألياف الضوئية. لا يقتصر تحقيق خسائر الألياف الضوئية في مجال الاتصالات الضوئية فحسب، بل في ظهور مجال علمي جديد هو الألياف الضوئية غير الخطية، وتتمثل فائدة هذا المجال الجديد من العلم في التطوير المستمر لـ أساسيات التقنيات اللازمة لإدارة المعلومات.

تعتبر التأثيرات غير الخطية وكذلك التأثيرات الخطية للألياف الضوئية من بين النقاط المهمة التي يجب الاهتمام بها، لأن معظم تطبيقات الألياف الضوئية تعتمد عليها. لذلك، عند دراسة الألياف الضوئية في مجال الاتصالات أو في مجال التطبيقات الطبية، فإن عملية نقل الإشارة داخل الألياف الضوئية مهمة للغاية لأن الإشارة المرسله داخل الألياف الضوئية تعاني من التوهين والضعف بسبب هذه التأثيرات التي تقيد عمل الألياف الضوئية في مجال الاتصالات.

في هذا العمل، تم اقتراح تعويض الخسارة لكلا النوعين من الخسائر الخطية، مثل التشتت والتوهين والامتصاص. تم تصميم معوضات فقدان التشتت DCF وتنفيذها للقضاء عليه داخل بمعامل تعويض مناسب. وتم استخدام مضخمات أشباه الموصلات الضوئية لتعويض الخسائر الناتجة عن توهين الإشارة. أما بالنسبة للخسائر غير الخطية فقد تم اقتراح وتصميم وتنفيذ نوعين من المعوضات. الأول هو عملية تعويض الخسائر على أساس طريقة اقتران الطور البصري. تم تصميم المعوض البصري على أساس الألياف غير الخطية HNLF وتم تنفيذه في تكوينين، أحدهما في منتصف المسار والآخر على طرفي النظام. تم الحصول على نتائج تعويض جيدة، كما تم تحسين أداء الإشارة المرسله.

تم اقتراح معوض خسارة ثان بالاعتماد على تقنية الشبكات العصبية الاصطناعية، حيث تتدرب هذه الشبكات على مخرجات النظام ومن ثم تحسين أداء النظام من خلال التحكم في القدرة المرسله والتحكم في تغير الطور غير الخطي، كما هو موضح في النتائج.

البرامج المستخدمة في هذا العمل هي Optisystem 19 و Matlab بلاستعانه بكوند البايتون Python code.

### 1.1 Introduction

Since its inception, optical fiber systems have grown in response to the increasing demand for ultra-high-speed data transmission in fiber communications [1]. The need for ultra-high bit data transmission in optical fiber communication required high bandwidth and has grown significantly globally during the last few decades. The majority of the expansion took place in the most recent few years, whenever data began to rule the internet traffic.

### 1.2 History of Optical Fiber

Ever since God created the earth and those on it without Him, light has been utilized for communication won't look around a limited amount of information has been sent via signs, reflective mirrors, and bulbs, but this information can also be seen by others [2]. Furthermore, to the detrimental effects of the environment a blog serves as the first real attempt in order to transfer information over a distance of 200 km, Aloud Chabe first employed signs in France in 1791 it takes him roughly 15 minutes to send one piece of information using this system.

John Tyndale carried out a straightforward experiment in 1854 to demonstrate that light may be bent if the right medium is found. In 1880 A light beam was used by Alexander Graham Bell to transmit sound [3], and this century saw numerous attempts to use optical communication. However, it was unsuccessful because there were not enough tools available and weather conditions including rain, snow, dust, and fog made it difficult to operate.

Theodore Maiman's 1960 invention of the laser sparked renewed interest in optical fiber communication, and Charles Cowe and George Hockam proposed making low loss glass fibers in 1966 [4], a silica optical fiber was produced in 1970 with a loss of 20 dB per kilometer as opposed to 1000 dB per kilometer at that point in time in ten years 1550 nm-wavelength fibers with losses of up to 20 dB were produced. The development of fiber-optic communication technologies started around 1975. The

massive advancements made between 1975 and 2000 over a 25-year span can be divided into numerous separate generations. The growth in the band line width (B.L) output throughout this time period is illustrated in Figure 1.1 and was evaluated via many laboratory experiments, the BL product doubles yearly according to the straight line. Every generation sees an initial rise in (B.L), but as the technology develops, it begins to saturate [5]. Every generation offers a fundamental change that assists to further improving system performance.

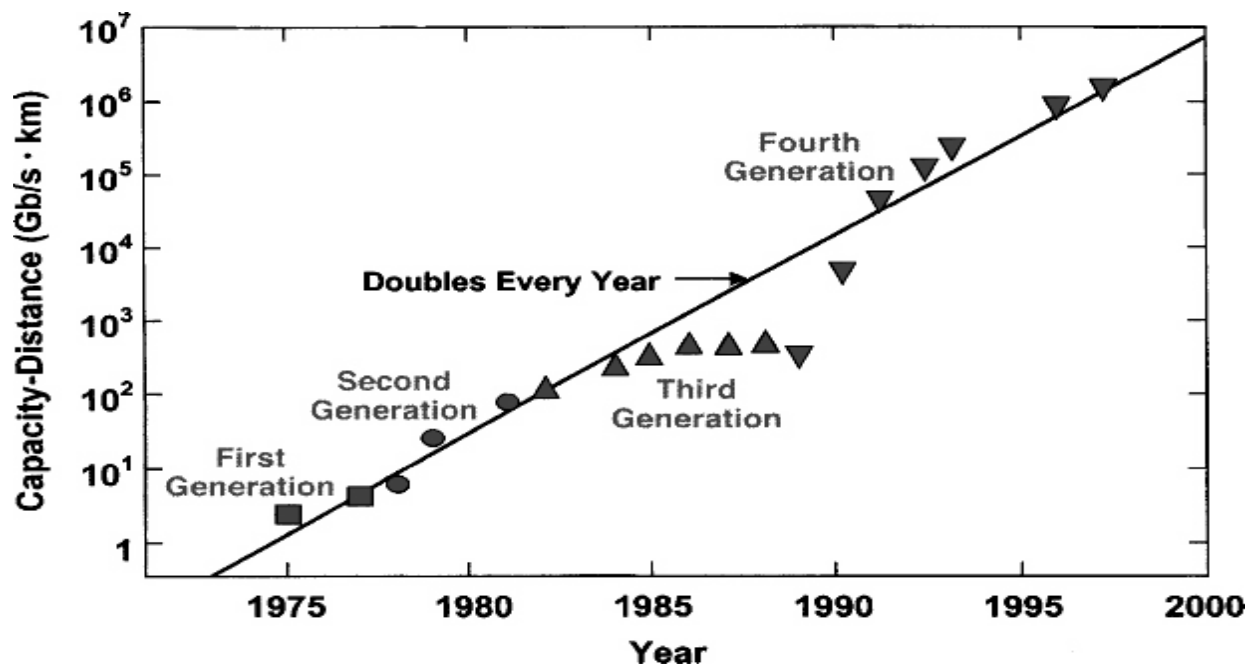


Figure 1.1: Through several generations of photonics systems, the (B.L) product grew during 1975 and 1980. The symbols used for succeeding generations change [6].

The initial generation of photonics systems employed GaAs semiconductor lasers and operated at wavelengths about 800 nm. Following multiple field tests between 1977 and 1979, such devices were made commercially available in 1980 [7].

They permitted repeaters to be spaced apart by up to 10 km and functioned to the tune of 45 Mb/s. System designers were strongly influenced by the larger repeater spacing compared to coaxial systems' 1-km spacing since it lowered the cost of each

repeater's construction and upkeep [6]. Early in the 1980s, the 2 G of Since fiber-optic networks for communication first became available, their bit rates were limited to fewer than 100 Mb/s because to dispersion in multimode fibers. Single mode fibers (SMF) were used to work around this limitation. In a 1981 lab test, transmission of 2 Gb/s over 44 km of SMF has been shown available commercially systems soon after were introduced. Second-generation light wave systems, with repeater spacing of approximately 50 km and, bit rates, of up to 1.7 Gb/s, were commercially available by 1987 [8]. However, due to significant fiber dispersion close to 1550 nm, the development of that wavelength's 3rd-generation light wave systems were launched much later. Due to the concurrent oscillation of many continuity modes, pulse spreading prevented the use of conventional in GaAsP semiconductor lasers. Either utilizing dispersion shifted fibers with a minimal the wavelength dispersion issue can be resolved by dispersion near 1550 nm or by restricting the laser spectrum to a single longitudinal mode.

Both approaches were taken during the 1980s by 1985, laboratory experiments indicated that information could be transmitted at bit rates of up to 4 Gbit/s over distances of more than 100 km. 3<sup>th</sup> generation light wave systems work at 2.5 Gbit/s became commercially produce in 1990 These systems are capable of operating at bit rates up to 10 Gbit/s Utilizing dispersion-shifted fibers yields the optimum performance. Using a laser that only oscillates in one longitudinal mode [9].

The disadvantage of 3rd generation 1550 nm systems is that Using electronic repeaters, the signal is regularly reproduced that are typically spaced 60-70 km away making use of a symmetric or heterogeneous detection approach might increase repeater spacing because using it increases the receiver's empathy.

4<sup>th</sup> generation wave propagation use of technologies Wavelength Division Multiplexing (WDM) to boost bitrate and optical amplification to expand repeater spacing. The development of the Wavelength Division Multiplexing technique in

1992 sparked a revolution that saw the system capacity double roughly every six months and resulted in by 2001, 10 Tb/s data rates were being reached by light wave systems [10].

### 1.3 Advantage of Optical Fiber

As depicted in previously optical fibers have replaced the majority of wireless media as the central component of information and communications network infrastructure. There is a very high demand for channel capacity because of the exponential growth in its use, in particular because of the tremendous increase in Internet-based data traffic. Due to its distinct qualities which include the following, optical fiber connection is specifically the most efficient way to achieve this high bandwidth [11]. In this context, we start with the benefits that were initially anticipated before looking at new characteristics that have emerged as the technology has advanced [10-12].

1. A huge bandwidth and extremely high data rate.
2. Small size and the object's weight Optical fibers are usually barely larger than the diameter of a human hair.
3. Electrical separation: Since glasses and occasionally polymer plastics are electrical insulators, optical fibers produced of these materials do not have the same issues with interfaces as their metallic counterparts.
4. Telecommunication safety: Optical fibers provide a high level of signal security because their light does not radiate significantly.
5. Low transmission loss: Over the past 20 years, optical fiber technology has allowed for the creation of optical fiber lines with extremely low attenuation losses  
Electrical separation: Since glasses and occasionally polymer plastics are electrical insulators, optical fibers produced of these materials do not have the same issues with interfaces as their metallic counterparts.
6. Coaxial cable has a shorter lifespan.

7. Greater range when compared to coaxial copper, without the need for repeaters.
8. Reliability of the system and ease of maintenance.
9. Inexpensive: The glass that typically serves as the transmission medium for optical fibers is made from sand, which is not a scarce resource. In contrast to copper connections, optical fibers have the potential to offer low-cost line communication.

### **1.4 Problem Statements**

The problem losses in optical fiber that limit the fiber system performance such as, dispersion, dispersion slope, and nonlinearities was compensated by taking into account an electrical field inside the fiber, it is possible to derive the mathematical model for fiber transmission. Fiber dispersion and nonlinear distortion compensation can considerably boost transmission performance in high-capacity, long-distance fiber-optic networks, this is done to correct both linear and nonlinear distortions. These distortions result from the interaction between fiber nonlinearity and dispersion, which is brought on by the Kerr effect. The steps below can be used to do this.

- Constructing numerical and analytical models to describe optical nonlinearities and dispersion's effects on fiber transmission characteristics.
- Use of compensating techniques in fiber-optic systems to offset fiber nonlinearities applying optical phase conjugation techniques (OPC) and artificial neural network (ANN)

### **1.5 Literature Review of Optical Phase Conjunction OPC**

In 1995, Arnoldus [13], present the fundamental foundation of Kerr media optical phase inversion It is thought about how A Kerr medium may accomplish optical phase inversion through four-wave mixture. Two powerful counterpropagating lasers pump a nonlinear medium and excite the third-order polarization. The incident field's phase-conjugated image is then created by combining with a weak incident field. It is demonstrated how a geometrical both the

polarization of the pumps and the tensorial structure of the nonlinear interaction can be explained by the polarization tensor.

In 1997, Hsiung [14], introduce a study included many applications, such as optical resonators and aberration correction in real-time holography, are attracted to optical phase conjugation (OPC), which is quick, effective, and low power.

In 1999, Kanprachar [15], suggested a different model for optical fiber impairments. The signal may be subjected to a variety of degradation. System performance is decreased as a result of these flaws, such as high bit-error rates or power penalties.

In ,2001 Guang [16] provide a complete description of It is referred to as optical phase conjugation when two coherent optical beams moving in opposing directions have the same transverse amplitude distributions and a wave front that has been inverted. The backward phase-conjugate beam can now be produced effectively using three main technical methods. The first methodology uses deteriorate (or somewhat degenerate) four-wave mixing processes, the second technique uses various backward simulations of scattering processes (Brillouin, Raman, Rayleigh-wing, or Kerr), and the third technique uses single-photon or multi-photon pumped backward stimulated emission (lasing) techniques.

In 2001, Claudio [17] give the Given that the light is constrained in a very tiny area over extended interaction lengths due to the exceptionally low attenuation coefficient and the presence of optical amplifiers, the nonlinear effects in optical fibers can be noticed even at low powers. This is the reason that when thinking about light propagation in optical fibers, nonlinear effects cannot be disregarded.

In 2003, Bo Xu, [18] introduce various impacts of the fiber with an emphasis on effective ways to compute the system degradations caused by these nonlinear effects, Kerr nonlinearity on optical fiber communication systems has been studied. There

are several analysis tools that are crucial for understanding optical fiber systems. The nonlinear Schrödinger (NLS) equation, which describes how optical pulses travel through optical fiber channels, is the main focus of these analysis tools.

In 2004, Kurtinaitis and F. Ivanauskas [19] introduce an approximate solution of nonlinear Schrödinger equations based on A system of the nonlinear Schrödinger (NLS) equations can be solved using finite difference techniques. The definitions include explicit, implicit, Hopscotch-type, Crank-Nicholson-type, and other types of schemes.

In 2005, J. Toulouse [20], suggest a model for various optical nonlinearities that can occur in fibers while highlighting the crucial material and fiber characteristics that govern them. We highlight the variations in each type of nonlinearity's effects for various values of crucial parameters as we describe their respective effects.

In 2005, Xiao and et al [21] presented a method to eliminate the inter and intra channel impairments by using optical phase conjugation techniques in power symmetric systems to suppress the dominant nonlinearity, the transmission connection must be optimized using OPC. By adjusting the pump wavelength close to the HNLF's zero dispersion wavelength, researchers were able to experimentally generate the phase conjugation of the dispersed 300 fs pulses.

In 2007, J. B. H Tahar [22] introduced an employ a theoretical model that accounts for transmission speed, physical penalty, and system factors in order to create simulation tools. These simulation approaches make it possible to examine different compensation strategies and show how they affect system performance.

In 2009 I. Cristiani [23] provided a mathematical model for optical fiber communication system to eliminate the fiber nonlinearities by using phase-

conjugation-based nonlinear effects compensation in optical communication systems.

In 2011, A. Supe and J. Porins [24] describe a method for estimation the optical fiber nonlinearities. The central wavelength from the third optical transparency window, equal 1550 nm, has been used in the calculations and experiments for the research effort.

In 2013, Sugumaran and et al [25], propose study of the nonlinear Schrödinger equation and Four Wave Mixing Efficiency (FWM) for various fiber lengths and channel spacing for waves two and three, the FWM design was simulated. The effects of non-linear refractive index on the four-wave mixing (FWM) properties in semiconductor optical amplifiers have also been studied (SOAs).

In 2013, Salah Al-Deen and et al [26], introduce a simulation by using the MATLAB software package, explore the various effects on pulse propagation in optical transmission systems. Effects of Dispersion and Attenuation are investigated.

In 2013, Maxime Gazeau [27], The stochastic Manakov equation, which has been deduced as the limit of the Manakov PMD equation, controls how the slowly varying envelopes evolve. The purpose of this work is to examine how the PMD affects Manakov's solitons and the propagation of soliton wave trains.

In 2016, H. Eliasson [28], study Mitigation of nonlinear fiber distortion using phase conjugation By sending a phase-conjugated copy along with the original signal and then superimposing it coherently, we reduce the nonlinear distortion caused by the Kerr effect.

In 2017, John C. and et al [29] suggested a digital signal processing methods for coherent optical fiber transmission systems that account for, control for, and take advantage of fiber nonlinearities.

In 2017 Adnan [30], provided a solution of the optical Phase Conjugation-Based Distortion Mitigation in WDM Systems where the optical fiber impairments processed and compensated.

In 2018, Francesco and et al [31], presented a method depend on optical phase conjugation recent studies on the effects of sub-optimal transmission links and our efforts to implement the optical phase conjugator itself have focused on integrated silicon waveguides rather than highly nonlinear fibers.

In 2021, P.M. Kaminski [32], propose Nonlinearity Lumped Compensation Using Optical Phase Conjugation It has been demonstrated that compensating for Kerr nonlinearity-induced distortions enables increases in transmission rate and range, with optical compensation approaches being especially appealing for broadband wavelength-division multiplexed (WDM) scenarios.

In 2021, J. Wang and et al [33] Experimental evaluation was done to ascertain the quantitative assessment (HNLF) for the 640 Gbps 16-QAM coherent-optical orthogonal frequency-division multiplexing (CO-OFDM) across 800 km of optical fiber with mid-link optical phase conjugation (OPC) using extremely nonlinear fiber.

In 2021 S. Kumar [34], provided a complete survey about fiber nonlinearities Attenuation and chromatic dispersion are the most frequent linear effects, while the Kerr effect is the most prevalent nonlinear impact. Where thorough introduction covers the theoretical underpinnings of pulse propagation in optical fiber, the Kerr nonlinearity effect, the parameters of the optical fiber channel, and the numerical and analytical approaches for solving the pulse propagation equation.

In 2022, Feng Wen and et al [35], introduce the nonlinear bidirectional semiconductor optical amplifier subsystem (SOA), where the optical phase conjugation (OPC) process is carefully examined, showing the conjugation

conversion through the two ports of the SOA, concurrently. Through simulation in a nonlinear bidirectional setup, the nonlinear power curves and the conjugated quality optimization are examined.

### 1.6 Literature Review of Optical Neural Network ONN

A. Jha and et al (2016) [36] suggested silicon nitride to create a photonic reservoir node on an integrated non-linear photovoltaic device. Its non-linear dynamics originate from the Kerr effect which is brought on by optical intensity dependence and cavities. Due to its completely passive optical construction, it does information processing very quickly allowing for time delay reservoirs with swift virtual nodes and low latency. The researchers experimentally show how the reservoir node in time-delay architecture can successfully complete two benchmark tasks: (1) Binary classification on a dataset of earthquake sensor time series. (2) Time series prediction using a non-linear autoregressive moving average (NARMA-10) with a normalized root mean square error of 0.183. These results pave the way for non-linear photonic node-based photonic computing with high throughput and minimal latency.

G. Fennessy, (2018) [37] create an innovative optical neural network (ONN) framework that has a degree of scalar invariance to picture classification estimates. Images are divided into several levels of different zoom based on a focal point, taking inspiration from the human eye which has superior resolution near the center of the retina. An identical convolutional neural network (CNN) is used to process each level in a Siamese fashion, and the combined results yield a highly accurate estimate of the item class. Since ONNs act as a wrapper around CNNs, they can be used for a variety of a wide range of existing algorithms to generate noticeable accuracy gains without modifying the underlying architecture.

J. Chang and et al (2018) [38] suggested a technique for utilizing the intrinsic convolution of a linear spatially invariant imaging system to produce One that is convolutional photonic layer with an optimizable phase mask to test their architecture, they first employ two simulated image classification models. The study found that the primary use of the convolutional layer consists of a single convolutional layer that matches image templates, an optical link that has been studied for optical target recognition and tracking. They show how the supplied Opt-Conv layer may integrate into a larger hybrid optoelectronic CNN by feeding the output of the convolutional layer into a digital fully connected layer. The study convincingly shows that, in both instances, the simulated optoelectronic implementation of the identical network structure competes with an unrestricted electronic implementation in terms of classification accuracy.

S. Geoffroy-Gagnon and et al (2019) [39] to describe the presented optical neural network, a synthetic dataset was produced the data set consists of four Gaussian distributions, each of which is filled with a set of four-dimensional points designated as IER. The different Gaussian distribution classes are one-hot encoded so that the ground PH OER is the truth vector for a single sample and 1 is set as a different value for each class. A single-layer neural network that is created using a traditional computer accurately classifies this dataset. To better comprehend the benefits and constraints of this optical neural network, it is now possible to compare it to a perfect classifier.

R. Hamerly and et al (2019) [40] suggested a new coherent detection based photonic accelerator with large (gigahertz) speeds and little (subattojoule) energy per multiplied and accumulated (MAC) and scalable to enormous ( $N \gtrsim 10^6$ ) networks. This accelerator makes use of the substantial spatial multiplexing that is offered by standard free-space optical components. Unlike earlier techniques both inputs and

weights are optically recorded making it possible to quickly retrain the network. Optical neural networks have a "typical quantum limit" that is determined by photo detector shot noise. That limit which can be as low as 50 ZJ/MAC demonstrates the possibility of this technology to execute thermodynamic (Landauer) constrained digital irreversible computing. The suggested accelerator supports both convolutional and fully connected networks, the study also offers a back-propagation and training scheme that utilizes the same gear this design will make it possible to develop new ultralow energy deep learning processors. Introduced a silicon-based fully connected optical neural network (ONN) which can be used to classify and recognize images it is built on a completely connected neural network. In chip design, the one-layer model has been employed as long as photons are big enough chip simulations demonstrate that precision will not be impaired, this structure has the potential to be used in deep learning.

M. Y.-S Fang and et al (2019) [41] suggested training two ONN to categorize handwritten digits, one with a more customizable design (GridNet) and one with improved fault-tolerance(FFTNet) when replicated flawlessly, GridNet outperforms FFTNet in terms of accuracy. However, the more fault tolerant FFTNet surpasses Grid Net when there is a slight inaccuracy in their photonic components.

M. Paraschiv and et al (2020) [42] suggested creating and improving deep learning for the categorization, or species identification of fish photos acquired by underwater camera arrays. The Symbiosis project, which is concerned with the identification and classification of pelagic fish in the Mediterranean Sea and the Atlantic Ocean is the context for our work. In this project, mooring is used to drop an autonomous system below the water's surface the researchers used two camera arrays like sonars and other sensors, the system monitors the species of each fish within a specified

radius in real time. A remote observation station receives aggregated data from the computation of real-time statistics.

H. Zhang and et al (2021) [43] proposed to highlight an optical neural chip (ONC) that uses neural networks with genuinely complicated values. The researchers evaluate efficiency of their complex-valued ONC in four different scenarios: including simple Boolean operations, the classification of species in an Iris dataset, identification of handwriting, and the classification of non-linear datasets (Circle and Spiral). When it comes to powerful learning capacities their complex the valued ONC performs better than its real-valued counterpart, for example (quick convergence, high accuracy, as well as the ability to establish non-linear decision limits).

T. Wang and et al, (2022) [44] provided a method for image classification using on average  $<1$  photon detected for each scalar multiplication and required specialized experimental instrumentation to execute optical vector-vector dot products. This approach is in line with theoretical forecasts for ONNs' quantum-limited optimal efficiency.

### 1.7 Research Aims

1. Developed a mathematical model for the optical fiber impairments that based on interaction of fiber light intensity with optical fiber caused by Kerr effect.
2. Design optical compensator for linear and nonlinear impairment losses in optical fiber large-capacity, long-haul fiber-optic systems.
3. Developing a numerical model based on optical spectrum inversion defines as optical phase conjugation technique to mitigate fiber losses the models included characterize fiber transfer properties in the presence of optical nonlinearities, attenuation, and dispersion and compensation by using artificial neural networks.
4. Execution of the proposed model for compensation the fiber impairments linear and system irregularities in fiber optics. By utilizing the suggested mitigating techniques for fiber-optic system based on Optical spectrum inversion and artificial neural networks.

### 2.1 Introduction

In this chapter, the theoretical part of pulse propagation in optical fiber was explained and introduce the mathematical model for wave travelling in optical fibers. The study of light wave transmission technology in optical fiber was focused in this chapter and how optical fibers function as dominant in fiber communication light wave systems.

### 2.2 Theory involving Ray Transmission

#### 2.2.1 Total Internal Reflection (TIR)

When assessing how light moves through an optical fiber using the ray theory model, the refractive index of the dielectric material must be taken into consideration. The difference between the speed of light in a vacuum and the velocity of light in the fiber medium is called the medium's refractive index [36]. The refractive index measures how much slower a light ray moves through an optically thick substance compared to one that is less dense, refraction occurs when a beam encounters a boundary between two distinct refractive indices of dielectrics (like glass and air), as seen in in Figure 2.1. (a)

The ray travelling through the material as it approaches the interface may be seen with a refractive index of  $n_1$ , and that it is angled at an angle of  $\phi_1$  with respect to the surface normal. In the lower index medium, the beam path will be oblique an angle  $\phi_2$  if the dielectric on the opposite side of the contact has a refractive index, to the normal  $n_2$  that is less than  $n_1$ , where  $n_2$  is less than  $n_1$ .

According to Snell's law of refraction as shown in equation (2.1) the situation's angles  $\phi_1$  and refraction  $\phi_2$  are connected to one another and Snell's law of refraction applies to the dielectrics' refractive indices [37]:

$$n_1 \sin \phi_1 = n_2 \sin \phi_2 \quad (2.1)$$

$$\frac{\sin \phi_1}{\sin \phi_2} = \frac{n_2}{n_1} \quad (2.2)$$

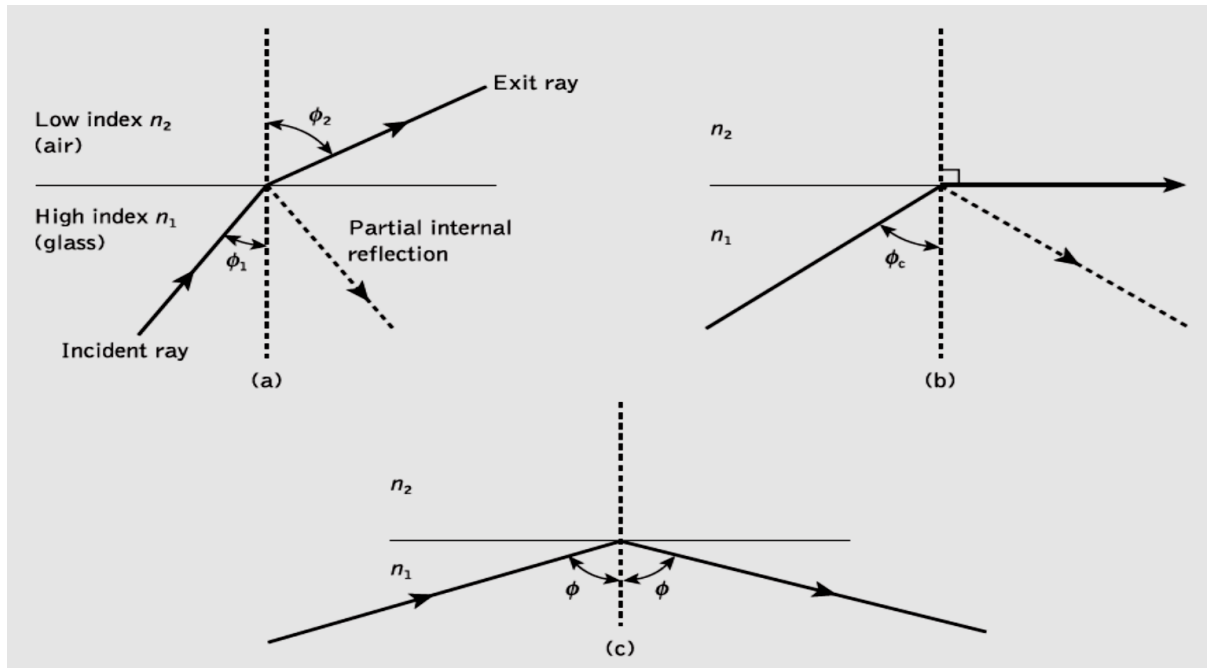


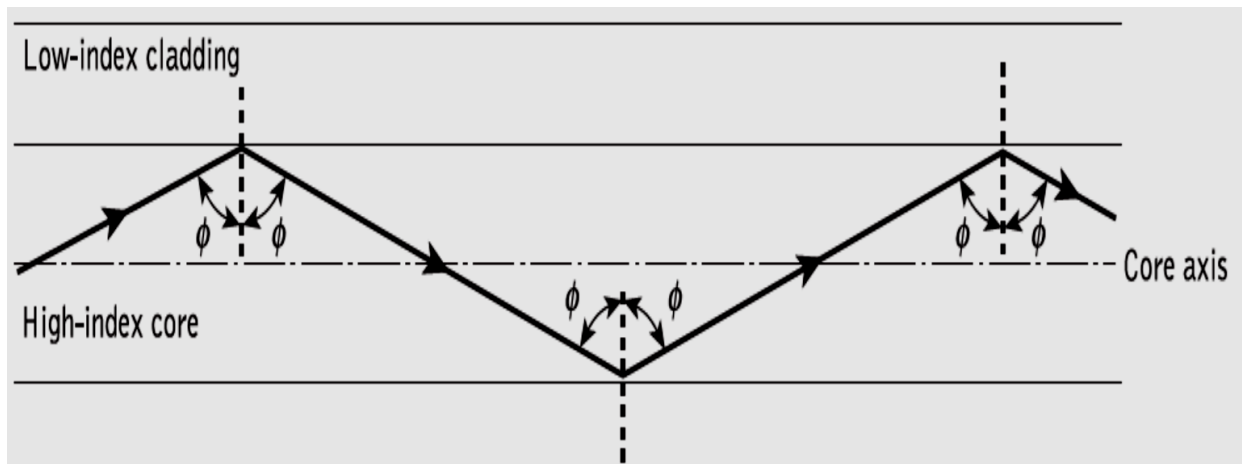
Figure 2.1 (a) Shows light rays striking a contact with a high to low refractive index, such as glass and air. (b) Refraction, its limiting situation in which the crucial beam appears at an angle of  $\phi_c$ , (c) total internal reflection in which  $\phi > \phi_c$  [14]

Figure 2.1(a) also demonstrates that some light is reflected back into the initial dielectric medium (internal reflection in section) since the angle of incidence is always smaller than the angle of refraction  $n_1$  is greater than  $n_2$  as a result, when the angle of refraction is 90 degrees and the refracted ray appears parallel to the dielectric interface, the angle of incidence must be less than 90 degrees. [38].

The critical angle  $\phi_c$  which is depicted in figure 2.1(b) is the angle of incidence in this limiting instance of refraction, the incidence angle above which 100% internal reflection occurs called the critical angle. The value of the critical angle is given by equation (2.3), where [39]:

$$\sin\phi_c = \frac{n_2}{n_1} \quad (2.3)$$

Total internal reflection is the highly efficient (about 99.9%) process by which Angles of incidence greater than the critical angle cause light to reflect back into the original dielectric medium. As a result, it is possible to see in figure 2.1(c) that total internal reflection TIR happens at the junction of two dielectrics with different refractive indices when a ray of light from a higher index dielectric strikes a lower index dielectric and its angle of incidence is greater than a critical value it is by this mechanism that light at an angle less than  $90^\circ$  can be said to pass along an optical cable with little loss [40]. At the intersection of the slightly lower refractive index silica cladding and core, total internal reflections show how an optical fiber is used to transfer light in Figure( 2.2). The angle of reflection of the ray is the same to the normal and has an larger than the critecal angle of incidence at the interface as the light beam travels through the fiber core's axis, it is referred to as a meridional ray [41,16],in this work used single mode fiber (SMF) .



**Figure (2.2) Shows how a light beam travels through a flawless optical fiber [16].**

### 2.3 Wave Propagation in Optical Fiber

The pulse propagation that have electromagnetic field inside the optical fiber is controlled by the wave equation as in equation (2.4), Maxwell's Equations provide as a general model of electromagnetic field transmission through an optical fiber from which we extract the wave equation [42].

$$\nabla \times \nabla \times \vec{E}(\vec{r}, t) = -\frac{1}{c} \frac{\partial^2 \vec{E}(\vec{r}, t)}{\partial t^2} - \mu_0 \frac{\partial^2 \vec{p}(\vec{r}, t)}{\partial t^2} \quad (2.4)$$

Where  $c$  : velocity of light ,  $E$  : electric field ,  $p$  induce polarization .

$$c = \frac{1}{\sqrt{\mu_0 \epsilon_0}}$$

Where  $\mu_0$  permabilty ,  $\epsilon_0$  permitivity

A phenomenological relationship can frequently be used but typically a quantum-mechanical examination of the link between  $E_r$  and  $P_r$  is necessary as shown in equation (2.5) [43]:

$$\vec{P} = \epsilon_0 (\chi^1 \vec{E} + \chi^2 : \vec{E} \vec{E} + \chi^3 : \vec{E} \vec{E} \vec{E} + \dots) \quad (2.5)$$

Where the parameter  $\chi^j$  is the  $j$  represent the order susceptibility, the term experssion  $j=1$  the linear relationship is illustrated by it alters the fiber's attenuation coefficient and refractive index [44].  $SiO_2$  has a small second order susceptibility, which prevents optical fibers from generating second order harmonics. The vulnerability of the third order  $\chi(3)$ , is It is in charge of events like third order harmonic generation, nonlinear refraction and four wave mixing (Kerr effect) [45,5]. This last result shows how the refractive index fluctuates with intensity as equation (2.6):

$$\tilde{n}(\omega |\vec{E}|^2) = n(\omega) + n_2 |\vec{E}|^2 \quad (2.6)$$

Where the value of  $n(\omega)$  expressed the part of the linear effect as contribution and the parameter  $n_2$  represent the nonlinear index part and related to  $\chi(3)$ .

If non linear influences are taken into account, the induced polarization is created by combining two, the first part is linear  $P_L(r,t)$ , the second part represent the non-linear part  $P_{NL}(r,t)$ ,  $P(r,t) = (P_L(r,t) + (P_{NL}(r,t))$  .

The nonlinear and linear coefficients are related to the electrical field by [46]:

$$\vec{P}_L(\vec{r}, t) = \varepsilon_o \int_{-\infty}^{+\infty} \chi^1(t - \dot{t}) \vec{E}(\vec{r}, \dot{t}) d\dot{t} \quad (2.7)$$

$$\begin{aligned} \vec{P}_{NL}(\vec{r}, t) = \varepsilon_o \int \int \int_{-\infty}^{+\infty} \chi^3(t - t_1, t - t_2, t - t_3) \\ : \vec{E}(\vec{r}, t_1) \vec{E}(\vec{r}, t_2) \vec{E}(\vec{r}, t_3) dt_1 dt_2 dt_3 \end{aligned} \quad (2.8)$$

Consider the unreliable term as a minor a change to the overall polarization to conduct a more condensed analysis. In that regard, it makes sense to start by figuring out how to solve the electrical field in a linear medium. Only take into account the field's wave equation along the propagation axis (z), in accordance with the analysis in [47]:

$$\tilde{E}_z(\vec{r}, \omega) = A(\omega) F(\rho) e^{\pm im\phi} e^{i\beta z} \quad (2.9)$$

where the  $\tilde{E}_z$  field represent the electronic field ,  $F(\rho)$  component represent the Fourier transform ,  $A(\omega)$ is represent the normalization constant , the parameter  $\beta$  is proliferating constant and m an integer[47]. When thinking about the transmission of short pulses, nonlinear effects in optical fibers are especially crucial (from 10ns to 10fs). Nonlinearities and group-delay dispersion both have an impact on the shape and spectrum of these pulses as they pass through the fiber. Construct the wave equation, which takes into account both linear and nonlinear effects, according to above analysis [47].

The scalar nonlinear Schrödinger equation (NLSE) can be used to simulate how an electric field propagates in an optical fiber without taking into account polarization [48, 21].

$$\frac{\partial \tilde{E}(z,t)}{\partial z} = -j \frac{\beta_2}{2} \frac{\partial^2 \tilde{E}(z,t)}{\partial t^2} + \frac{\beta_3}{6} \frac{\partial^3 \tilde{E}(z,t)}{\partial t^3} + \frac{g(z) - \alpha(z)}{2} \tilde{E}(z,t) + j\gamma |\tilde{E}(z,t)|^2 \tilde{E}(z,t) \quad (2.10)$$

Dispersion

Power evolution

Kerr effect

It is well known that a wide range of physical phenomena are described by the nonlinear Schrodinger equation (NLSE) such as, water waves' modulational instability, the movement of a very thin vortex filament in a helical pattern, the transmission of heat pulses in anharmonic crystals, the nonlinear modulation of collisionless plasma waves, and a light beam in a color-dispersive system self-capturing [49,22]

The nonlinear Schrodinger equation is a general wave equation that first appeared in the research on the propagation of unidirectional wave packets in an energy-efficient, dispersive medium. The Kerr effect is a feature that occurs in some dielectric components where the refractive n index rises according to the electric field's square. The refractive index can then be expressed as equation (2.11) [50].

A pulse ( peak power represent amplitude square , wave number K) moving through a fiber of length L experiences a phase change that is power reliant due to the power dependency of the refractive index [51, 17]:

$$\phi(P) = \phi_l \phi_{nl} = n_0 kL + n_2 kL_{eff} \frac{P}{A_{eff}} m \quad (2.11)$$

the effective length  $L_{eff} = 1/\alpha [1 - \exp(-\alpha L)]$ , with fiber loss coefficient  $\alpha$  accounts for fiber losses. The test fiber's polarization properties and the signal's polarization state both affect the polarization parameter m.

### 2.4 Types of Fiber Impairments

#### 2.4.1 Linear Impairments in Optical Fibers

This section focuses specifically on the causes and consequences of two different types of linear impairments on the optical signal field travelling through optical fibers [52].

##### 2.4.1.1 Power attenuation in fibers

Since it has an important effect on the maximum transmission distance before signal restoration when constructing an optical fiber system, it is essential to consider the attenuation of a light signal as it passes through a fiber. Optical energy for light signal are the core attenuation processes in a fiber due to absorption, scattering and radiative losses. While scattering is connected to both the optical waveguide's structural defects and fiber composition, absorption is related to the fiber material. Radiative attenuation results from changes of the fiber geometry, both microscopic and macroscopic [53,25].

Similar to metallic conductors, the decibel's logarithmic unit is typically used to indicate signal attenuation within optical fibers. For a specific optical wavelength, the decibel where two power levels are contrasted can be characterized as the proportion of optical power received from a fiber to optical power supplied (sent) into the fiber as equation (2.12):

$$\alpha_{dB} = \frac{10}{z} \log_{10} \frac{P_i}{P_o} \quad (2.12)$$

The Beer-Lambert law governs how the optical field in the fiber changes in power.

$$P(z) = P(0) \exp(-\alpha z) \quad (2.13)$$

Where  $\alpha$  denotes attenuation.

The general attenuation curve in Figure(2.3) illustrates that attenuation is a function of wavelength.

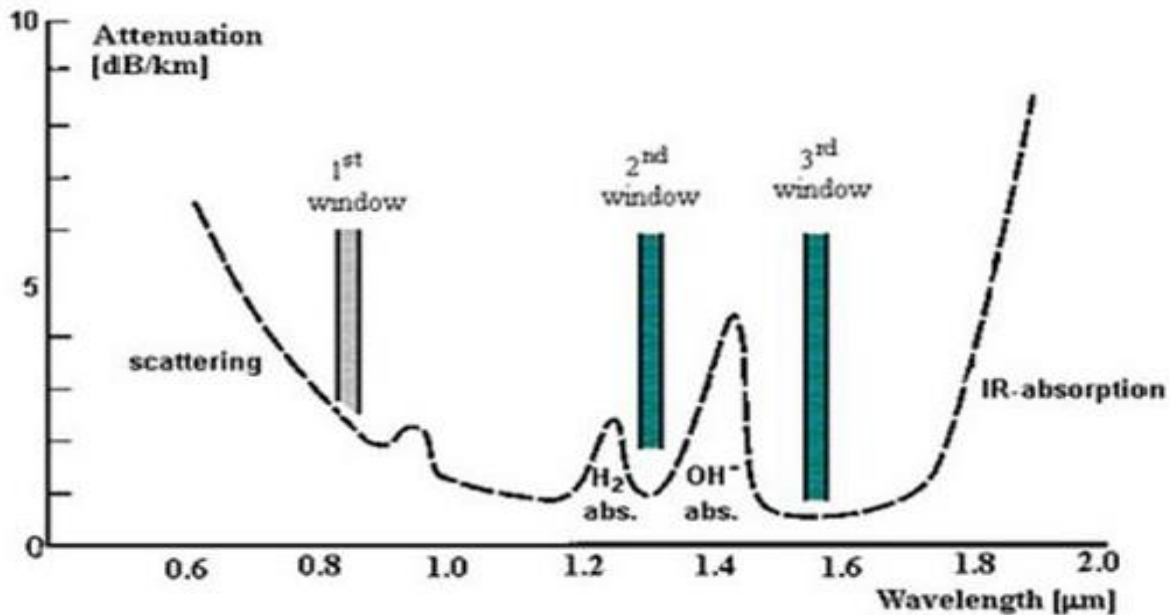


Figure (2.3) : Attenuation in relation to wavelength [13]

During transmission there is attenuation or loss of power of the light signal. Passive media components that cause attenuation include cables, cable splices, and connections. Although optical fiber attenuation is far smaller than that of other media, both multimode and single-mode transmission still involves it. An optical data link needs access to enough light to overcome attenuation in order to be effective [54,26].

### 2.4.1.2 Absorption losses in silica glass fibers

A loss as absorption causes some of the optical power that is transmitted to be dissipated as heat in the waveguide, absorption is connected to the material formulation and production methods of the fiber following are the categories of light absorption [55].

Absorption caused by atomic flaws in the chemical makeup of glass internal caused by the glass's primary components interacting with one or more of them extraneous caused by impurities within the glass[56].

### 2.4.1.3 Linear scattering losses

One propagating mode's optical power can be partially or completely the transfer is linear proportional to the mode power into another mode by use of linear scattering processes. This mechanism tends to attenuate the transmitted light because the transfer may be in a leaky or radiation mode, which does not continue to propagate within the fiber core but is radiated from the fiber [56].

It should be emphasized that like with all linear processes, scattering does not alter with frequency (elastic scattering). The two primary types of linear scattering are Rayleigh scattering and Mie scattering both result from the manufactured fiber's less than ideal physical characteristics which are currently difficult or even impossible to eliminate[56].

### 2.4.1.4 Dispersion effects in optical fibers

When building a fiber optic system, the capacity of information transmission and fiber loss are crucial factors. The highest achievable bit rate or modulation frequency is largely determined by the fiber's dispersion.

Three different dispersion types exist [57].

1. Mode dispersion (MD).
2. Chromatic dispersion (CD).
  - a. Dispersion due to material dispersion
  - b. Waveguide dispersion effect
3. Polarization mode dispersion (PMD)

Mode dispersion is result from differences at the times of propagation of distinct modes. Mode dispersion would be the only dispersion present if the source were completely monochromatic. In truth, all sources especially modulated ones emit light over a range of optical wavelengths and this spectrum of wavelengths causes other kinds of dispersion. Material dispersion is caused by the variation in transmission

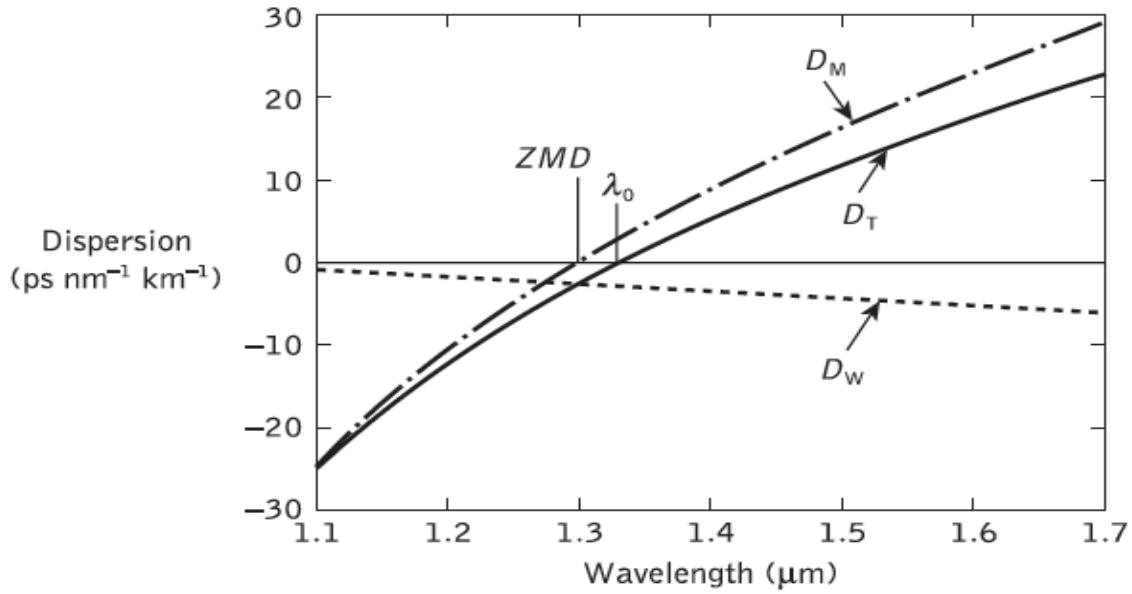
time brought on by the refractive index's wavelength dependency. Waveguide dispersion results from of the propagation pattern's wavelength dependence [58].

### 2.4.1.5 Mode dispersion (MD)

The most extreme meridional ray and the axial ray which are event at the crucial angle of the core cladding interface  $c$ , can be used to represent the step index fiber's quickest and slowest modes of propagation, respectively, according to the ray theory model depicts the routes travelled through these two rays in a step index fiber with flawless structure the broadening of the pulse brought on by intermodal dispersion within the fiber can be estimated using the difference in delay between these two rays as they move through the fiber core given that both rays are moving at the same speed inside the core of a fiber with a fixed refractive index, the delay difference is linearly correlated with each ray's individual path length inside the fiber [59]. Now obtain an approximation of the time spread caused by intermodal dispersion from the length of time it takes the path of the axial ray down a fiber of and the length  $L$  This gives us the minimum delay time  $T_{\text{Min}}$ . [60, 32]

### 2.4.1.6 Chromatic dispersion (CD).

According of the optical source's limited spectral linewidth, chromatic and the intramodal dispersion can happen in all. types of optical fiber appear in Figure (2.4) the fact that optical sources do not emit at a single frequency means that there may be variations in the propagation delays of the different spectral components of the transmitted signal rather than a single frequency as in the case of the injection laser only a small percentage of but for the LED it is likely to represent a sizeable portion of the central frequency [61,33]. Each transmitted mode is widened as a result, leading to intramodal dispersion , the material dispersion of the waveguide material and the guidance effects inside the fiber structure may both contribute to the delay differences (waveguide dispersion).



Figure(2.4) Displays the wavelength-dependent values of the material dispersion parameter (DM), waveguide dispersion parameter (DW), and total dispersion parameter (DT) for a common single-mode fiber [34].

### 2.4.1.7 Material dispersion

Given the material dispersion, the varied group velocities of the different spectrum components fired into the fiber from the optical source create pulse broadening. A substance has material dispersion if the second differential of the refractive index with respect to wavelength is not zero, which happens when the phase velocity of the wavelength of a plane wave in a dielectric medium fluctuates nonlinearly. Through material dispersion, the rms pulse broadening is provided by [62]:

$$\sigma_m = \frac{\sigma_{\lambda} L}{c} \left| \lambda \frac{d^2 n_1}{d\lambda^2} \right| \quad (2.14)$$

However, it could be expressed in terms of a parameter called M for material [63]: dispersion, which is defined as follows[63]

$$M = \frac{1}{L} \frac{d\tau_m}{d\lambda} = \frac{\lambda}{c} \left| \frac{d^2 n_1}{d\lambda^2} \right| \quad (2.15)$$

### 2.4.1.8 Waveguide dispersion

Chromatic dispersion may also be induced by the fiber's waveguide, this happens when the group velocity of a specific mode shifts with wavelength. The angle between the ray and the fiber axis changes as a result of the wavelength which subsequently influences the rays' transmission times and as a result, their dispersion according to the ray theory approach [64, 36].

### 2.4.2 Non- Linear Impirments in Optical Fibers

There are two different types of nonlinearities in optical fibers, the optical Kerr effect is caused by fluctuations in the refractive index with optical power and the first is stimulated scattering (Raman and Brillouin) as shown in Figure (2.5). The nonlinear refractive index causes the intensity dependent phase shift of the optical signal whereas stimulated scatterings cause the intensity dependent gain or loss. The threshold energy output at which the nonlinear effects exhibit themselves in stimulated scatterings are dissimilar from those in the Kerr effect which does not, this is a critical distinction between scattering effects and the Kerr effect [65].

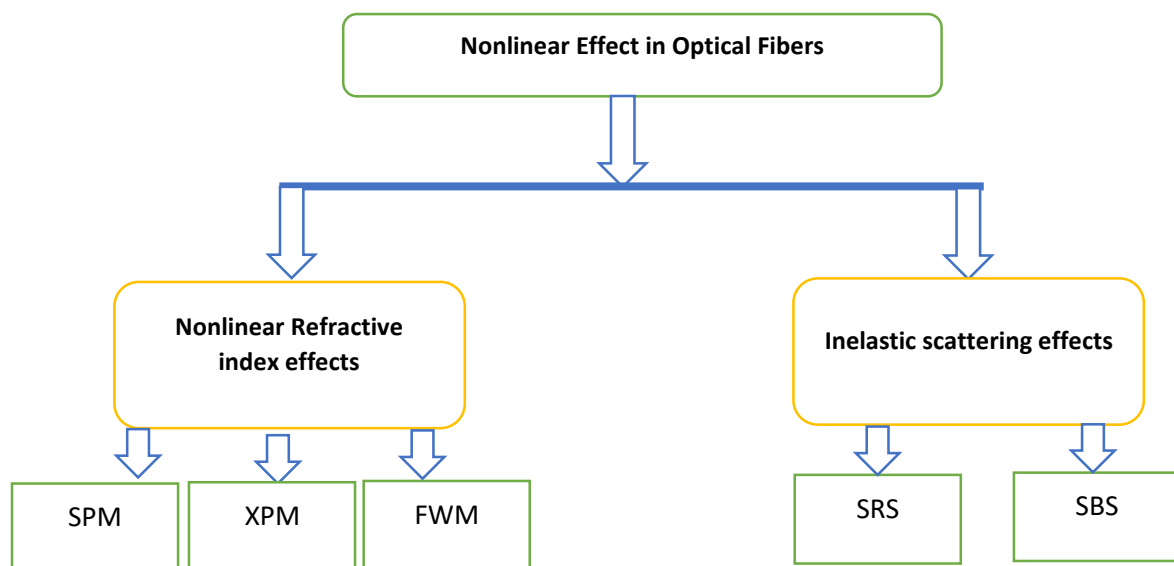


Figure (2.5) Block digrame of fiber nonlinearities[65]

### 2.4.2.1 Light kerr effect in optical fiber

Silica fiber's refractive index for optical systems has a weak relationship with optical intensity and is provided as [66]

$$n = n_0 + n_2 I(t) \quad (2.16)$$

Where  $I(t)$  optical intensity,  $n_0$  refractive index,  $n_2$  nonlinear refractive index.

In modern optical fiber systems, the refractive index is no longer unimportant despite being a very minor function of signal power due to increased power from optical amplifiers and vast transmission distances. In fact, self phase modulation (SPM), cross phase modulation (XPM) and multiple mixing are some of the nonlinear effects caused by phase modulation caused by intensity dependent refractive index (FWM).

#### 2.4.2.1.1 Self phase modulation

Self-phase modulation (SPM) is a nonlinear optical result of the interaction between light and matter due to the optical Kerr effect, an ultrashort pulse of light will cause the medium's refractive index to change while it travels across it [1]. The pulse's phase will shift as a result of this fluctuation in refractive index, changing the pulse's frequency spectrum [67, 39]. Silica's index of refraction depends only very weakly on intensity so that it has the form and the index where the result of self phase modulation is depicted as a change in the optical pulse's phase as a result of the refractive index change brought on by the pulse's intensity. The optical Kerr effect is what causes the medium's fluctuating refractive index, the pulse's frequency spectrum changes as a result of the phase shift brought on by changing the refractive index, the description of this refractive index change is [68]:

$$n = n_0 + n_2 \frac{P}{A_{eff}} \quad (2.17)$$

For silica fibers, the coefficient  $n_2$  is  $2.6 * 10^{-20} \text{ m}^2/\text{W}$ , this number accounts for the polarization state of the light averaging out as it passes through the fiber. For light

travelling in a fiber of glass, the nonlinear contribution to the index of refraction causes a phase change [69, 41].

$$\Phi_{NL} = \gamma PL_{eff} \quad (2.18)$$

where we have defined the nonlinear coefficient  $\gamma = \frac{2\pi n_2}{\lambda A_{eff}}$ .

When an optical fiber carries an intensity modulated signal SPM happens. The peak of a pulse moves more slowly (or more rigorously collects phase more fast) than the wings because of the nonlinear index of refraction. When accounting for fiber loss with effective length and neglecting dispersion, the nonlinear phase shift brought on by SPM on the propagating field is determined [70].

$$\Phi_{NL}^{SPM}(L) = \frac{2\pi}{\lambda} \tilde{n}_2 |E|^2 L_{eff} = \gamma PL_{eff} \quad (2.19)$$

where P is the power of the propagating wave.

Dispersion must be considered, especially for data signals, and in this case, the NLSE needs to be numerically determined.

### 2.4.2.1.2 Cross phase modulation

When the phase change of one beam is impacted by the intensity of another beam this phenomenon is known as cross phase modulation. It is essentially the change in optical phase of one light beam caused by interaction with another beam in a nonlinear medium more precisely a Kerr medium Cross-phase modulation is another way in which intensity fluctuations impact the phase of a signal [71]. In this instance the WDM system's other channels' modulation is what causes the intensity fluctuations that are to blame, this can be explained by a change in the refractive index of [72, 44]:

$$\Delta n(\lambda_2) = 2n_2 I(\lambda_1) \quad (2.20)$$

In 1985, there was a first experimental confirmation of XPM in WDM systems, XPM takes place and uses a similar principle to SPM.

In this instance, changes in optical power in a WDM channel are transformed into changes in phase in other copropagating WDM channels XPM giving as equation (2.21) [73] :

$$\frac{\partial E_1}{\partial z} = j\gamma[P_1(z, t) + 2 \sum_{i=2}^M P_i(z, t)]E_1 \quad (2.21)$$

the SPM contribution is shown by the first term in the equation, while the XPM effect is shown by the second term. For a given power, the factor 2 in the XPM expression demonstrates that XPM has a twice as large impact as SPM [74].

### 2.4.2.1.3 Four wave mixing

A scattering mechanism known as four-wave mixing (FWM) is thought to involve the mixing of three photons to produce a fourth wave. This occurs when the four waves' momenta meet the requirement for maximum power transfer, often known as phase-matching [75]. In nonlinear optics, a phenomena known as four-wave mixing (FWM) occurs when interactions between two or three wavelengths result in the creation of one or two new wavelengths [76] . It is comparable to the electrical system's third-order intercept point, the intermodulation distortion in conventional electrical systems can be compared to four wave mixing.

When two or more light frequencies (or wavelengths) are sent via a fiber simultaneously FWM develops. The power from the original frequencies is used to generate a new frequency of light provided that the phase matching requirements are met [77, 49]. If we suppose the two co-polarized co-propagating fields,  $E_1$  and  $E_2$  with frequencies  $f_1$  and  $f_2$  and propagation constants  $\beta_1$  and  $\beta_2$  in the optical fiber produces an intensity beating at frequencies  $f_2 - f_1$  which leads to variation in the refractive index due to the Kerr effect [50].

The phase matching condition is the requirement that  $k_1 + k_4 = k_2 + k_3$ , which can be simplified to the requirement that zero GVD frequency needs to be at the center of the four waves by expanding the wave vectors  $k_j$  near the center of the four frequencies [78, 51].

The dispersion at the center frequency should be a little out of the ordinary when the nonlinear phase shift is taken into consideration. Non-degenerate FWM processes feature optical fields oscillating at distinct frequencies, whereas degenerate processes involve two fields oscillating at the same frequency [79,3].

If we take the three waves new fields are generated at frequencies

$$f_{jkl} = f_j + f_k - f_l \quad (2.22)$$

The non-degenerate FWM processes,  $j, k, l \in \{1,2,3\}, j \neq k, j \neq l, k \neq l$  and the degenerate FWM processes  $j, k, l \in \{1,2,3\}, j = k \neq l$  create three unique new frequency fields each [80].

### 2.5 All Optical Neural Network (AONN)

This type of neural network represent recent type where the kind of ONN that doesn't need photoelectric conversion devices to transmit data during computation is the all-optical neural network. All computations are performed using optical equipment. Based on how optical devices are used, AONN may be divided into three different types of neural networks: nanphotonic neural networks, optical scattering neural networks, and passive diffraction neural networks [42]

The construction of the Diffractive Deep Neural Network is depicted in Figure (2.6.a). There are several diffractive surface layers in it. By interacting with these diffraction surfaces, it is possible to produce computing functions in the form of photons. Utilizing a digital computer, the training is carried out. Following training, each diffraction layer of the network is modelled in three dimensions using Poisson

Surface Reconstruction with D2 NN parameters. A 3D printer is then used to print the models. The neural network diffraction layers are shown in figures. (2.6.b) and (2.6.c), where each printed layer can be categorized as either projective or reflective. Neurons that can transmit and reflect light waves are represented by the points on a layer. Through optical diffraction, these locations are connected to subsequent layers, enabling forward propagation to carry out a range of sophisticated function processes at the speed of light [44].

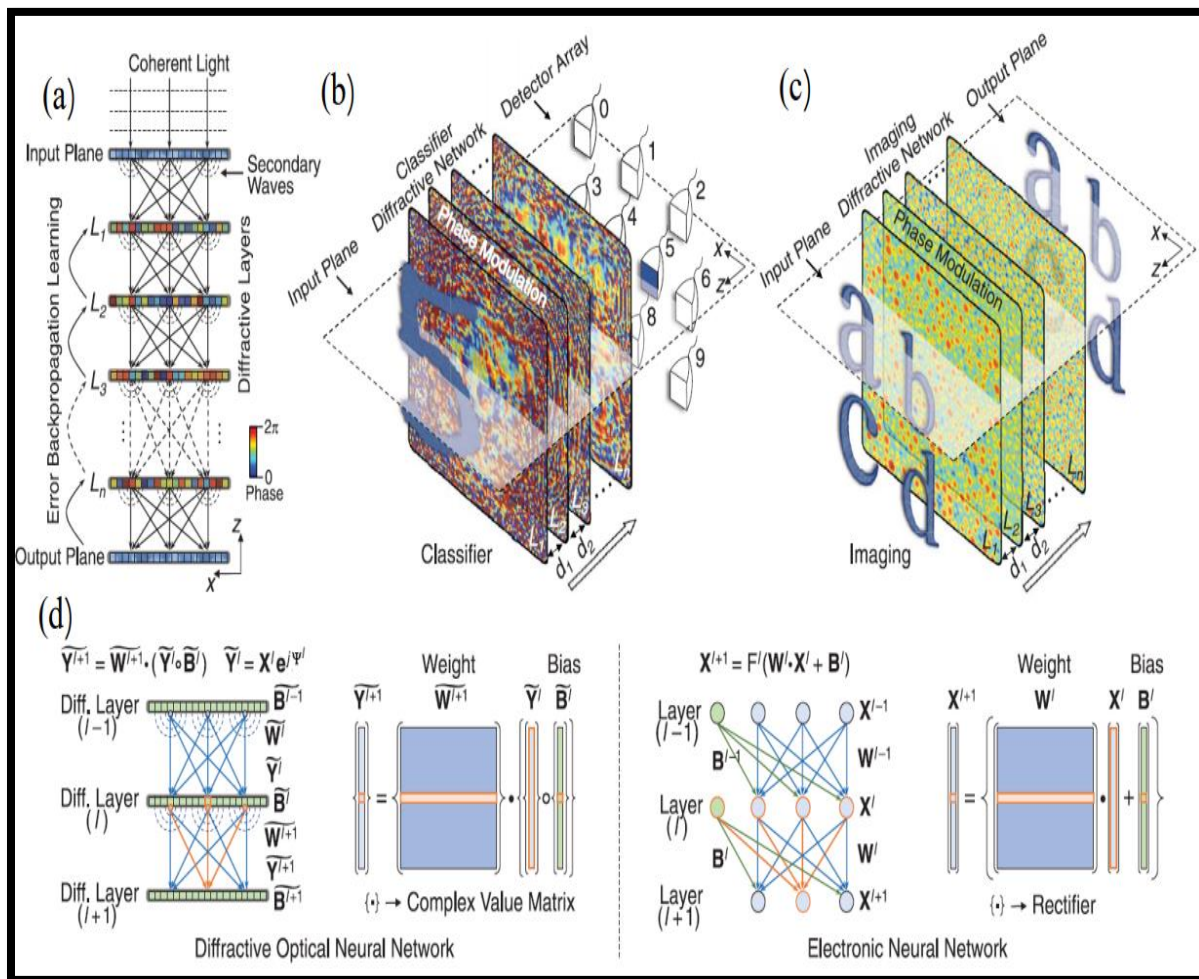


**Figure (2.6) Shows the AONN structure. (a) The D2 NN's general structure. (b) Using D2 NN as an image classifier. (c) The application of D2NN in imaging. (d) The distinction between electronic NN and diffractive ONN [44].**

### 2.5.1. Deep learning of optical neural network

Deep learning is a type of machine learning, which is an aspect of artificial intelligence in and of itself. It has a tiered architecture, where each higher layer builds on the lower layer below it, giving it the name "hierarchical learning" for the first time. Deep learning first appeared in 2007. A complex problem can be solved using deep learning, which is currently used by major technological companies including Facebook, Microsoft, Amazon, Baidu, and Google. Deep learning enhanced a wide range of applications, including drug discovery, automatic machine translation, object recognition, and object detection.

Deep learning can extract high-level features from the input data since it manages data in a nonlinear manner due to the hierarchical representation of the neural network. Applications for deep learning in image processing include edge extraction, image segmentation, shape identification, and face verification [41,43].

Due to the automated function taught without the requirement for human computing effort as it does in typical machine learning approaches, deep learning algorithms such as the Convolution Neural Network (CNN) increase its efficiency above conventional algorithms. The handcrafted features must be retrieved and then fed into a classifier because the traditional machine learning technique requires a feature vector corresponding to the raw data (intensity pixel values in the case of an image) as an input to recognize and process it.

These traits can be readily learned by deep learning systems. Deep learning algorithms are intended to solve issues that conventional machine learning algorithms have not been able to. The most significant issues that deep learning solved [42,44].

### 2.5.1.1 The previously dimensionality curse

The issue of curse dimensions affects numerous disciplines, including machine learning, data processing, and numerical analysis. The common thread of curse dimensional problems is that when the dimensionality rises, the amount of space increases so quickly that the accessible data become scant. This issue has been resolved by deep learning thanks to the vast versatility of its algorithms[40].

### 2.5.1.2 Regularization of local constancy and smoothness

Algorithms for machine learning must be motivated by prior assumptions about the kind of function they can learn. One of the most widely held ideas is that things are smooth or consistent locally. If the learned function should not change much within a small region, an algorithm is considered to be smooth. Many easier machine learning methods rely on local consistency assumptions to generalize successfully, and as a result, these algorithms are unable to handle more difficult AI problems. To go around, you may apply deep learning several issues with computer vision applications. Deep learning has helped to solve some of these problems. include picture segmentation, image classification, object identification, object detection, and image captioning. Numerous more applications include speech recognition, generative models, manufacturing, biometrics recognition systems, similarity learning, and gaming[37,41].

### 2.5.1.3 An information set for training

Selecting the proper dataset for a specific classification assignment is crucial for a generalization performance. In the end, the model's ability to accurately identify unseen data is significantly influenced by the quality of the underlying dataset itself. The ground truth labels that go with each color or grayscale image ( $Y$ ) are the network's input  $X$  for an image classification task. Image  $X$  can be viewed as a  $(c, h, w)$  tensor of integers with corresponding height and width for each color channel. The three channels in a color image represent the red, green, and blue (RGB)

intensities at each pixel. A grayscale image's single channel serves as a representation of the grayscale intensity. The complete dataset is typically divided into three subsets: the training set, validation set, and test set [41].

### *A) Practice Set*

The raw data used to train machine learning models is called the training set. Lowering the tolerances between output predictions and base truth labels provided in a training data set is accomplished by specifying learnable parameters in convolutional layers and weights in fully connected layers.

### *B) Set of validation*

Model parameters are evaluated and optimized using the validation set.

### *C) Set for Tests*

A collection of data known as a testing set is one that is not used during training. When model parameters and hyperparameters are fully defined, it is often used just once to assess how well the model generalizes [39].

## **2.6 Convolutional Neural Network (CNN)**

A particular feed forward neural network is what makes CNN a type of deep learning architecture. The investigation into the visual cortex of the brain had an impact on the concept for CNN [36].

Using CNNs for image and video processing as well as image classification and recognition is a promising technique.

The extraction function and the prediction function are the two tasks that the CNN completes. To accomplish a certain goal, each function made use of particular layers. Convolution, nonlinear (activation), pooling, and fully connected layers make up these layers.

### 2.6.1 Basic convolutional neural network structure elements

Feature extractor and forecast are the two key components that make up the CNN architecture.

#### A) Part of an attribute harvester

It is the first component of the CNN architecture, and it turns image features into feature maps. One or more convolution layers make up the structure of the CNN feature extractor, which is used to separate each hidden layer's relevant features from the special signal in that layer [44].

The convolution layer is used in the first stage of CNN to combine the filter with the picture and produce feature maps, which are then used in the pooling layer to minimize the feature maps. Using the same procedure to them as input feature maps, it continues to traverse layer by layer, still extracting powerful features, and produces smaller-sized feature maps[39].

#### B) part of an estimate

The low dimensional feature vector was supplied into a prediction portion after extracting feature maps and lowering dimensions by choosing the best features among them. A conventional fully connected artificial neural network is used for the prediction component. Depending on the sort of task the network is being trained for, the prediction portion performs either the classification or the regression task. It returns the likelihood of the class to which the input image may belong when used as a classifier[38].

### 2.6.2 Convolutional neural network component

The CNN's convolution layer is a feature extractor that takes different features out of the input image. A mathematical technique called convolutional combines two groupings of data. Convolutional filtering methods are used to obtain features from input images and learn these features via input data arrays. These filters are then

used for creating feature maps, which allow for the cultivation of the spatial relationships between each feature in the image [39].

The output size of the convolution layer is controlled by a number of hyperparameters that are part of the CNN architecture.

- Filters: A variety of suitable numbers of filters in various sizes can be employed.
- Filter width: The filter or kernel size must be more than 2 and squared  $L * L$ , smaller than the input picture, and squared  $L * L$ . By filling at the input boundary, zero-padding is an effective method for regulating the dimensionality of output volumes by [38].
- Stride: The quantity of cells (pixels) the kernel must pass through or descend at once. The receptive field will be reduced if the stride. Equation (2.23) calculated the output size of matrix [35,36].

$$K_{out} = \frac{Inz - Fl + 2Pa}{St} + 1 \quad (2.23)$$

$K_{out}$ : Output size ,  $Inz$ : Input size ,  $Fl$ : Filter size ,  $St$ : Number of stride.

$Pa$ : Number of padding

The rectangular unit (ReLU) function, sigmoid function, and other functions are carried out by non-linear layers. These methods are used to identify the particular characteristics of each buried layer.

- Layering Ponds: The goal of the pooling layer or subsampling layer is to generate a reduced dimension output feature map by dimensionally reducing the input feature map while maintaining just the most crucial data.

This layer employs the maximum pooling and median pooling techniques to minimize the number of dimensions.

An array of a specific size is converted into a one-dimensional array at the flattening layer before being sent into the following layer.

The final layers of CNN are completely connected layers, which are used to carry out the prediction stage of CNN.

The output feature map from earlier levels serves as the input for these layers in a multi-layer neural network. The output layer, the final layer of fully-connected layers, is in charge of making a choice and forecasting the values of the output [39].

### **2.7 Structure of Artificial Neural Networks (ANN)**

During the information-processing stage of neural networks, which are made up of trillions of neurons (nerve cells), the exchange of electrical pulses between cells, known as action potentials, takes place. Artificial neural networks (ANNs), which are brain-inspired algorithms, are used to anticipate issues and estimate intricate patterns. The deep learning method, also known as ANN, was founded on the idea that biological neural networks exist in the human brain.. ANN was developed in an effort to replicate how the human brain works [44]. Artificial and biological neural networks function in remarkably similar ways, despite certain differences. Only structured and quantitative information is accepted by the ANN algorithm.

In a single-layer feed-forward network, the inputs and outputs are connected by a number of weights in a single layer. Each input is linked to each output by weight-carrying synaptic connections as shown in figure (2.7).

It is considered to be a feed-forward network. It is referred to as a "feed-forward system" since information is only transmitted from input to output .

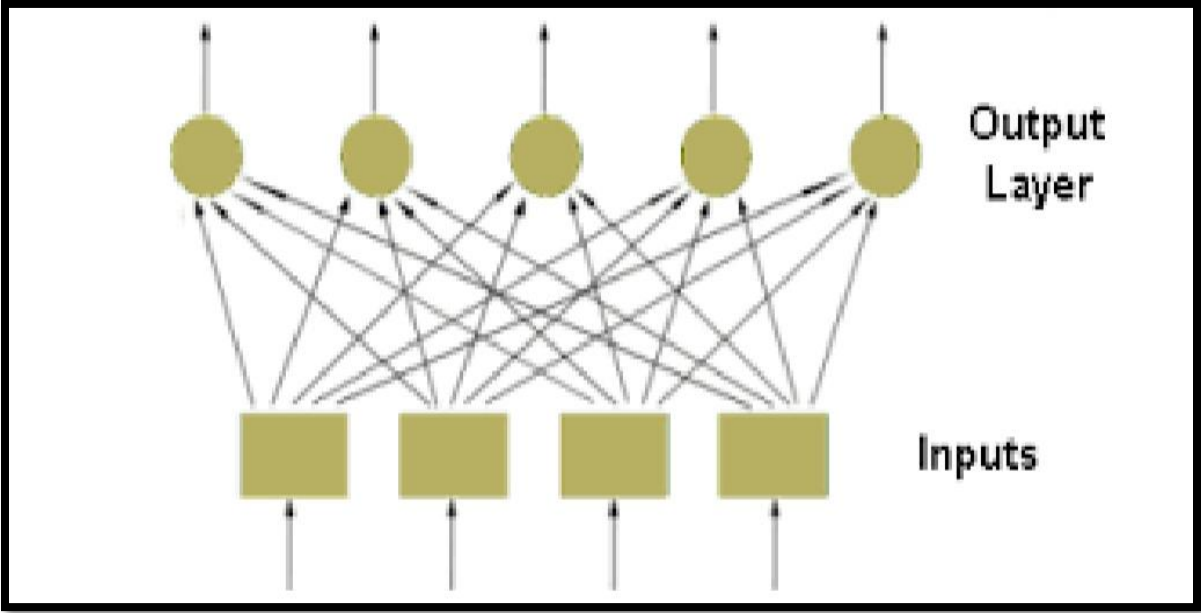


Figure ( 2.7) Single-layer feed-forward network [40]

Multiple layers are present in multi-layer feed-forward networks. In addition to input and output layers, this class of networks' architecture also includes one or more intermediate levels known as hidden layers, as shown in figure( 2.8) .

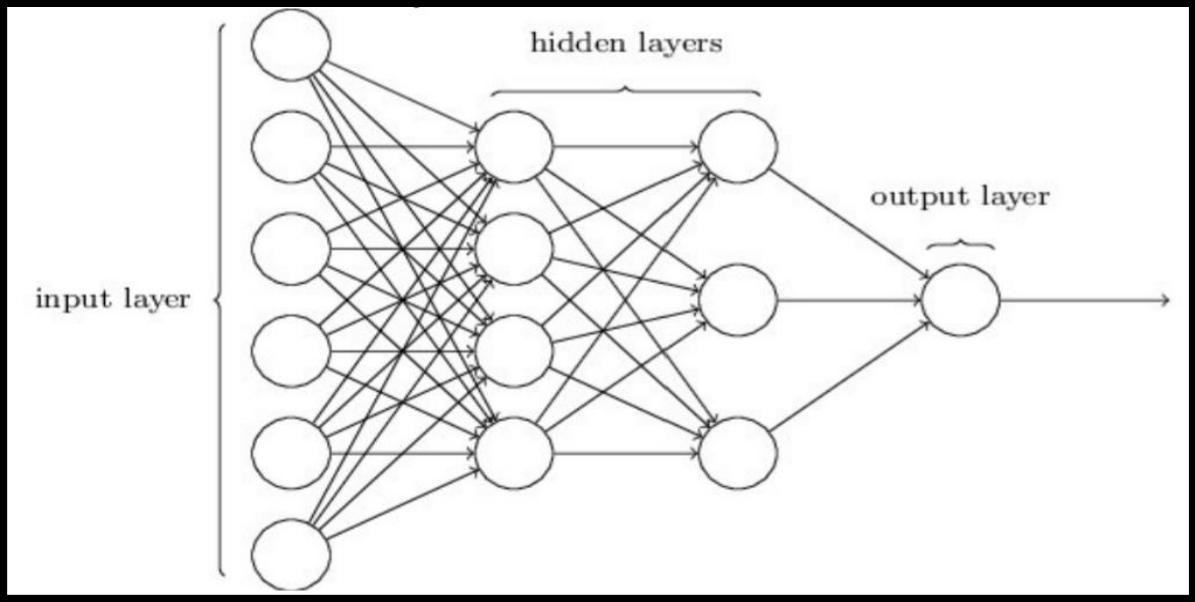


Figure (2.8) Multi-layer feed-forward networks [45]

### 2.8 Algorithm Training for Back-Bropagation

The researcher notes that, despite the fact that  $E_p$  reflects the node's real output  $w_{ij}$ , which originating from node  $i$  to node  $j$ ,  $E_p$  reflects the error function for pattern  $P_i$ , the anticipated results for the model  $PT_{pj}$  on node  $j$ .

Step 1: Configure the offsets and weights.

both node offsets and all weights should be set to low random values.

Step 2: State the input and intended outcome.

Calculate the real outputs in step three.

Step 3: The sigmoid nonlinearity is employed by the researcher.

Step 4: Adjust weights

Iteratively, the researcher moves from the output nodes to the first concealed layer.

Step 5: Resume by performing step 2.

Where  $\eta$  is a gain term,  $\delta_j$  is an error for term for node  $j$ ,  $x'_i$  is either the output of node  $i$  or an input, and  $w_{ij}(t)$  is the weight coming from a hidden node  $i$  or a node  $j$  input at time  $t$  [38,40,44].

### 2.9 Typical All Optical Neural Network Organization (AONN)

The neurons in a typical ANN are typically layered in organization patterns without linkages within a layer of neurons between neurons, as shown in figure (2.9). The neurons in the layer above provide input to the neurons in the layer below.

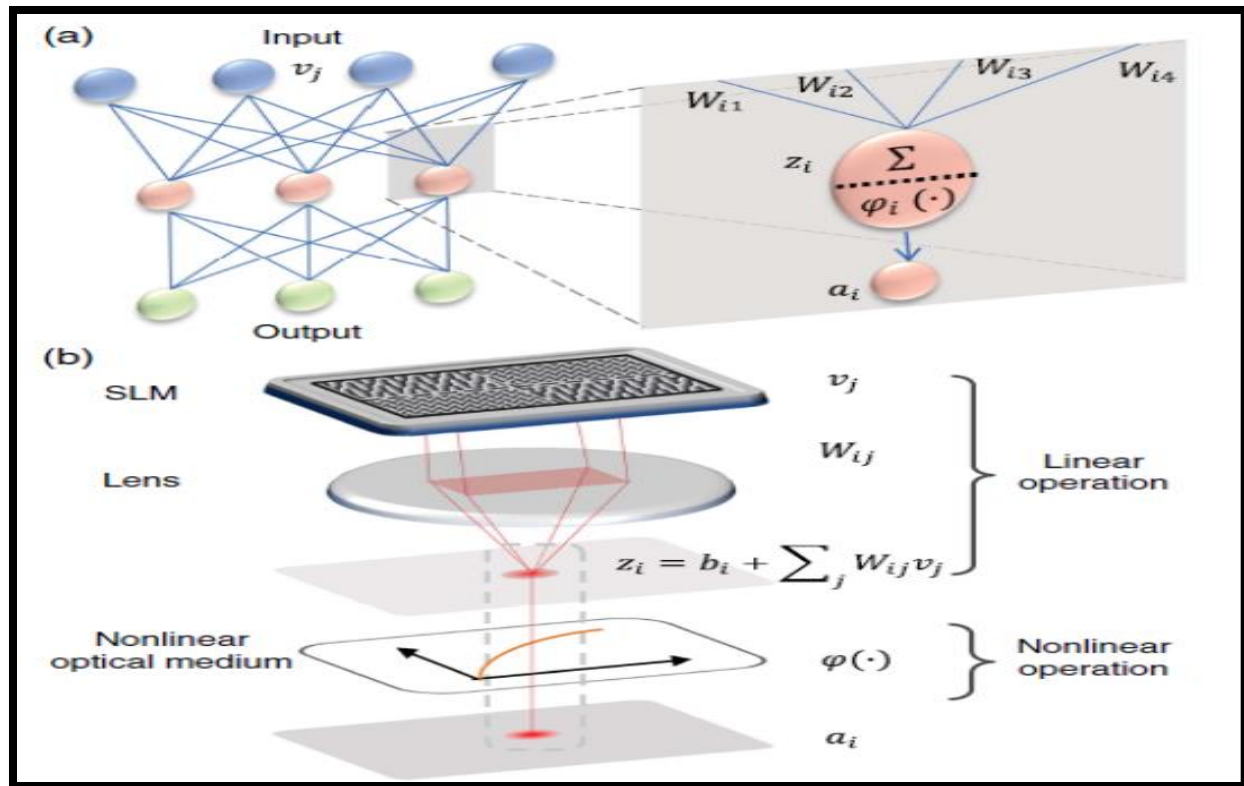


Figure (2.9) (a) Typical two layer neural network is an AONN. (b) Diagram of a nonlinear and linear optical neuron implementation under investigation [39]

The artificial neuron operating standard can be abstracted using the next two steps. used a linear process with a specific bias  $b_i$  to receive input signals  $v_j$  from neurons in the layers above that are multiple weighted  $w_{ij}$  [25].

While examining all of the input signals, a new output signal is produced using non-linear activation functions.

## 2.10 Operation of Linear Optics

The input layer nodes  $v_j$  in the linear operation process will be represented by the incident light intensities at various positions in the SLM. The incident light beams  $v_i$  may be divided into a number of directions  $j$  with weight  $w_{ij}$  by superimposing different phase grating. The SLM was placed at the lens's reverse focal plane, running Fourier transforms, and linearly summing all of the diffracted beams into a

single point at the front picture plane. Adding inputs may help acquire the linear biases  $b_i$ . The given matrix elements  $w_{ij}$  are acquired using the Gerchberg-Saxton increasing with time technique[37,44].

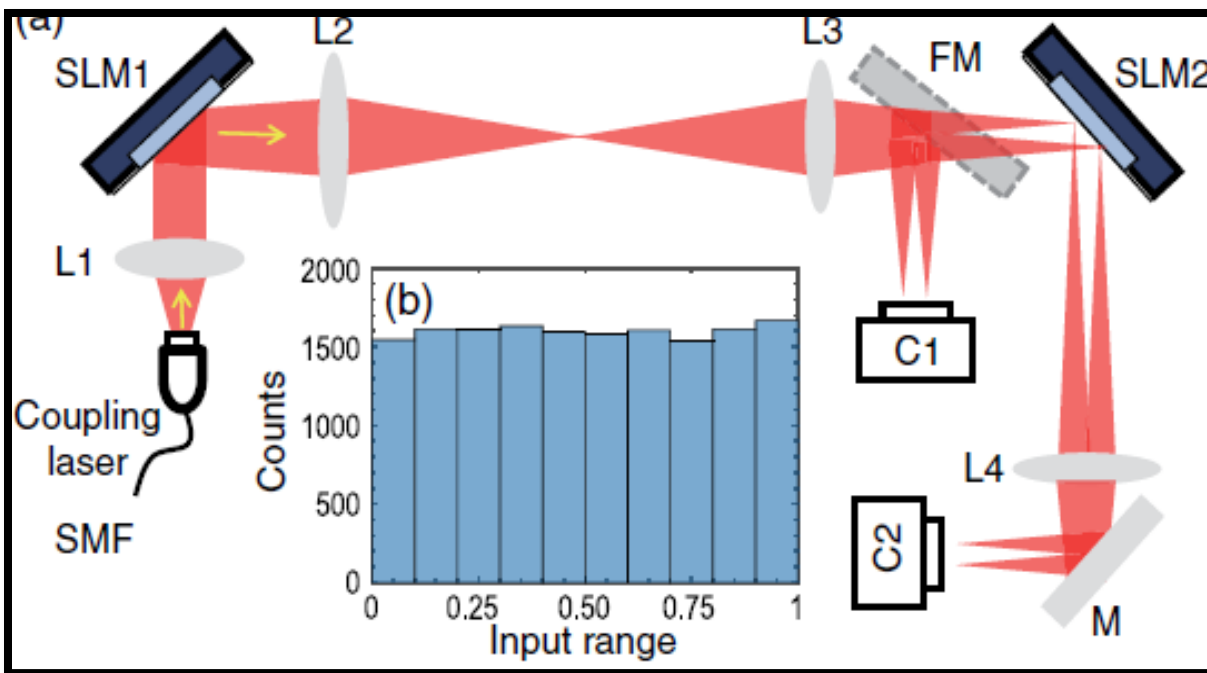


Figure (2.10) Shows the optical setup for performing the linear operations [43]

Optical setup, linear optical operation, and characterization. Single-mode fiber (SMF), flip mirror (FM), mirror (M), optical lens (L1–L4), and camera (C1–C2) Figure (2.10) represent the shows the optical setup for performing the linear operations. The researchers make use of 8-to-4 linear operations to maintain generality. A collimated single-mode fiber (SMF) coupling laser beam that selects eight different beam points and causes the first SLM (SLM1) to occur. These eight points are projected on to the next S.L.M (SLM2) as the input  $v_j$  via a 4-f optical lens arrangement (L2 and L3).  $v_j$  is measured and monitored using the first camera (C1) and flip mirror (FM). At the Fourier plane of lens L2, stray coupling light is prevented. All laser beams are split into four different beams following SLM2. The

summing process is carried out via the Fourier lens L4, while the second camera records the four output points (C2) [49].

### 2.11 Putting Optical Back-propagation into Practice

Forward-propagation translates neuron activations from layer  $l - 1$  to neuron inputs at layer  $l$  as a function of data seeded at the input layer ( $a^{(0)}$ ) as in equation (2.24)[34]:

$$z_j^{(l)} = \sum_i w_{ji}^{(l)} a_i^{(l-1)} \quad (2.24)$$

Prior to each neuron receiving a non-linear activation function,  $a_j^{(l)} = g(z_j^{(l)})$  using a weight matrix  $w^{(l)}$  (with subscripts labeling individual neurons). Equation (2.25) illustrates how the researchers assess the loss function  $\mathcal{L}$  and calculate its gradient with regard to the weights at the output layer [34].

$$\frac{\partial \mathcal{L}}{\partial w_{ji}^{(l)}} = \frac{\partial \mathcal{L}}{\partial z_j^{(l)}} \frac{\partial z_j^{(l)}}{\partial w_{ji}^{(l)}} = \delta_j^{(l)} a_i^{(l-1)} \quad (2.25)$$

Where  $\delta_j^{(l)} \equiv \partial \mathcal{L} / \partial z_j^{(l)}$ , also known as the error, is located at the  $j - th$  neuron in the  $l - th$  layer. Equation (2.26) represents the chain rule as follows [44]:

$$\delta_j^{(l)} = \sum_k \frac{\partial \mathcal{L}}{\partial z_k^{(l+1)}} \frac{\partial z_k^{(l+1)}}{\partial z_j^{(l)}} = g'(z_j^{(l)}) p_j^{(l+1)} \quad (2.26)$$

Where  $p_j^{(l+1)} = \sum_k \delta_k^{(l+1)} w_{kj}^{(l+1)}$ . Equation (2.26) is used to successively compute the errors  $\delta^{(L-1)}, \dots, \delta^{(1)}$  for each preceding layer given the error at the output layer,  $\delta^{(L)}$ , which is directly acquired from of the loss function. These errors enable to calculate the gradients Equation (2.26) of the error function with respect to all weights to be calculated, it is followed by the usage of gradients descent. They also allow to determine the activation  $a^{(l-1)}$  of all neurons [44].

### 3.1 Optical Spectrum Inversion (OSI) Technique

The opposite direction of the wave front characteristic of an optical wave that is propagating backwards to a wave that is moving onward is commonly referred to as optical phase conjugation (OPC).

In reality, a variety of physical processes such as backward four wave merging, reverse stimulated radiation (lasing) and backward stimulated scattering can be used to generate backward conjugate waves with phase (PCWs).

However, the forward PCWs is possible to create utilizing forward four wave mixing the unique three wave, or both combining photon-echo, a second order nonlinear medium, and resonant medium processes [54].

The optical inversion spectrum technique based on reverse the spectrum of propagated signals in optical fiber channel. Get as a result the dispersion effect and also Kerr effect accumulated in optical fiber as signal propagate through the fiber and need to compensate using conjugated signal along propagation path [55]. Here the optical inversion spectrum as optical phase conjugation is used to compensate this effect in optical fiber and to avoided the Kerr effect such as cross phase variation, self-phase modification, and four wave merging and other nonlinear effects. The propagation of optical pulse in dielectric media can be govern by nonlinear by the Nonlinear Schrödinger Equation (NLSE) as shown in eq. (3.1) [56]:

$$\frac{\partial A}{\partial Z} = -\frac{\alpha}{2}A - i\frac{\beta_2}{2}\frac{\partial^2 A}{\partial t^2} + \frac{\beta_3}{6}\frac{\partial^3 A}{\partial t^3} + j\gamma|A|^2.A \quad (3.1)$$

Where  $\alpha$  represent the absorption coefficient of fiber core, and  $A$  represents the complex envelop of propagated signal, the parameters  $\beta_2$  and  $\beta_3$  represent the chromatic dispersion and third-order dispersion parameter [57].

The nonlinear effect classified into two types: where the fiber Kerr effect represented one of them and produce as a result of  $\gamma$  effect can define it as  $\gamma = \frac{2\pi n_2}{\lambda A_{eff}}$  [58]. In our work can write the complex conjugate as follows [60]:

$$\frac{\partial A^*}{\partial z} = -\frac{\alpha}{2}A^* + i\frac{\beta_2}{2}\frac{\partial^2 A^*}{\partial t^2} + \frac{\beta_3}{6}\frac{\partial^3 A^*}{\partial t^3} - j\gamma|A^*|^2 \cdot A^* \quad (3.2)$$

The symbol \* in above nonlinear Schrodinger equation stands for the complex conjugate operation. While the Kerr effect term  $\gamma$  and the chromatic dispersion term ( $\beta_2$ ) have the opposite sign [61].

The induce linear effect (dispersion) in optical fiber channel results a chirp and also the Kerr effects produce nonlinear phase shift as a refractive index fluctuation. The optical phase conjugation will be cancelled accumulated chirp effects and Kerr effects after passing through highly nonlinear media that make phase conjugation of the propagated signals.

### 3.2 Techniques for Light Spectrum Inversion

The inversion of the spectrum can have performed as optical phase-conjugated light wave can be created using a number of techniques. There are a number of methods such as using the nonlinear effect such as four wave mixing, and SBS Brillouin and electrical phase conjugated waveform in the transmitter receiver and fiber [62]

### 3.3 Methods Based on Fiber Nonlinearities

To create the phase-conjugated Four Wave Mixing (FWM) is frequently used in fiber optics among a signal wave and a high power pump wave in an extremely nonlinear fiber (HNLF). The movement of the phase-conjugated waveform via this manner similar to the direction of the initial wave, and the three waves' transportable frequency are in harmony [63]:

$$f_s + f_c = 2f_p \quad (3.3)$$

where:  $f_s$ : Signal Frequency,  $f_c$ : Copy signal frequency conjugate,  $f_p$ : Pump signal frequency.

Are, the corresponding the signal wave's harmonics, the phase-conjugated wave, and the pump wave. Phase-locking is a crucial characteristic of the signal and phase-conjugated waves produced by FWM [64].

The only option to apply dispersion pre compensation to the signal as well as the phase-conjugated wave using this technique is all optically, utilizing devices like DCFs or FBGs, which has the disadvantage of restricting the amount of pre compensation for dispersion [65,10].

The three steps that make up the compensatory approach are as follows [66]:

- a) building up nonlinearities in the first span
- b) using OSI to reverse the sign of the built-up nonlinearities
- c) adding more nonlinearities in the second span

If the nonlinearities in both spans are the same and are in fact reversed by optical inversion spectrum OSI, the compensation is successful as shown in figure (3.1).

When both requirements are met, the nonlinearity's deteriorating effects are suppressed, and the system performance is anticipated to significantly improve [67].

The nonlinear Schrodinger equation (NLSE), which contains the important propagation properties, such as the fiber loss, the group velocity dispersion, and the Kerr nonlinearity, is used to determine the compensation criterion [68].

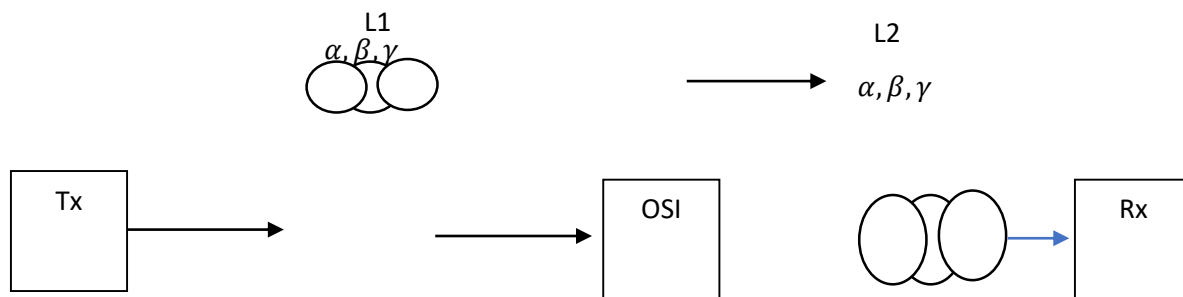


**Figure (3.1) The optical spectrum inversion signal (left, L1) and conjugate are included in the schematics of a straightforward two-span transmission system (right, L2) [68].**

### 3.3.1 Optical spectrum inversion based four wave mixing

An essential nonlinear process known as FWM takes place in optical fibers. It is helpful for a variety of tasks, including wavelength conversion and phase conjugation. Two pumps and a weak signal are concurrently introduced into the medium in the traditional non-degenerate Four Wave Mixing(FWM) operations in an unsteady medium [74]. When the phase-matching condition is met, these waves can interact nonlinearly and produce an idler or conjugate wave. Having been impacted by nonlinear nature and fiber dispersion, by reestablishing the temporal pulses in optical fibers, the pulse shape can be recovered [75]. The color dispersion and fiber nonlinearity are reversed as a result caused by the initial pulse by restoring the shape of the propagated pulse in a fiber as after conjugating its phase, the pulse travels through a separate fiber.

the pulse propagates through a different fiber after conjugating its phase. Due to these crucial characteristics, FWM-based OSI has drawn a lot of interest in long-haul fiber-optic communication systems. With relatively high input powers, a phase conjugation with high efficiency becomes feasible, which could result in the ideal fiber length for maximum conversion efficiency [76].

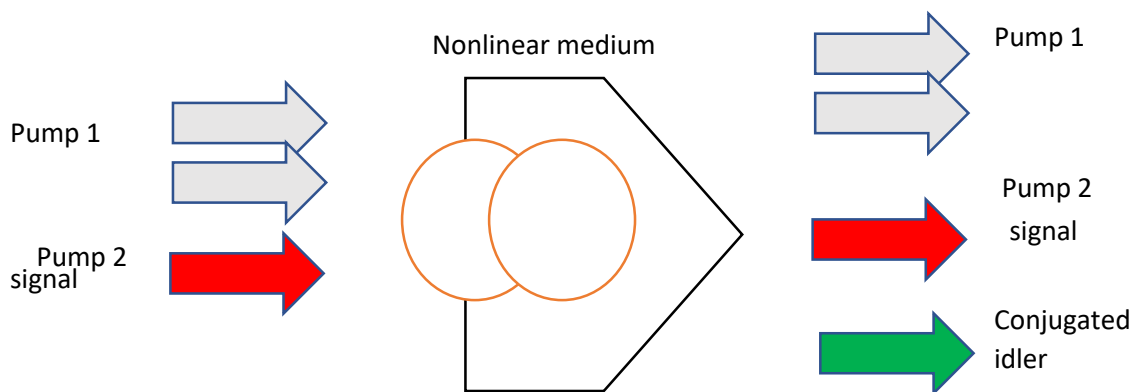


Figure (3.2) Optical inversion spectrum based four wave mixing [77]

Think about non-degenerate four wave mixing in a very nonlinear fiber where the two pumps, the frequencies of the idler, signal, and idler are all distinct [77].

In the operation the waves of pump at frequency  $F_{\text{pump1}}$  and  $F_{\text{pump2}}$  and signal frequency  $F_s$  are entered into highly nonlinear fibers to produce idler signal at frequency  $F_{\text{idler}} = F_{\text{pump1}} + F_{\text{pump2}} - F_s$  [78]

### 3.3.1.1. Four-wave regenerative mixing in reverse

The referred to as four-wave reverse degenerate mixing, first developed by Hellwarth in 1977, is the most often used technique to produce a backward degenerate PCW [69].

In this scenario, as depicted a third-order nonlinear media is concurrently shown in figure (3.3) as lit by two powerful plane waves that are travelling in opposite directions furthermore, a signal beam with arbitrary wave front distortion [70].

A newly formed wave with the same frequency and going in the opposite direction might be visible to us of the signal beam If the frequency ranges of these three incident waves match  $\omega$  [71].

the degenerate reverse harmonic phase conjugate wave (PCW) of the incident signal beam is easily demonstrated by the following derivation [72].

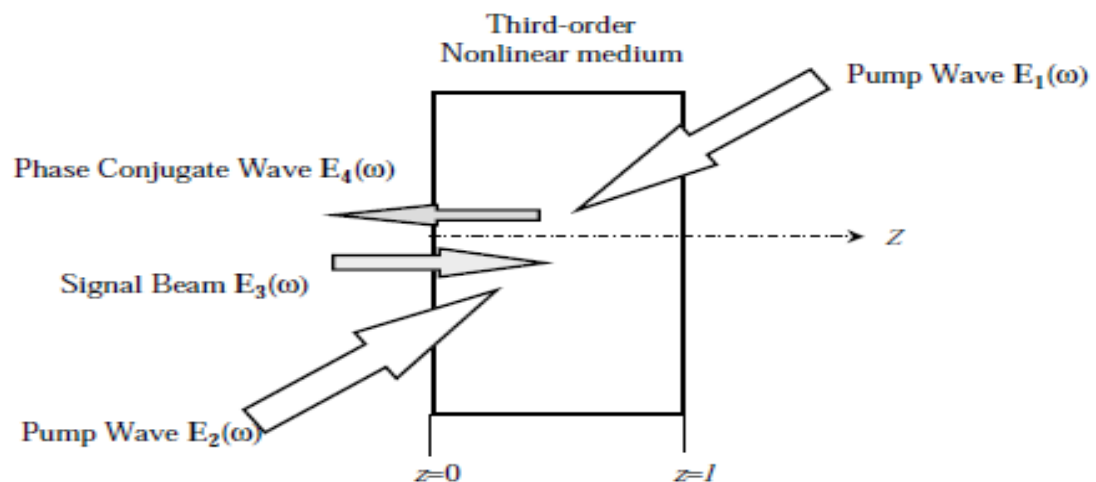


Figure (3.3) Show degenerate of four-wave mixing produces phase-conjugate waves [72].

It is theoretically demonstrated in the section above of this paragraph that a P.C.W can be produced by a unique layout of a degenerate FWM in a third-order curvilinear medium. The association of four photons is fundamentally connected to such a process [73].

### **3.3.2 Enhanced backwards scattering**

It is widely known that many types of stimulated scattering can be seen in suitable scattering medium when powerful and highly directional laser energy is excited [79].

The accelerated Kerr, Rayleigh scatterings, Brillouin, and Raman scatterings are all examples of stimulated scattering are the most prevalent among them. In general, stimulated scattering displays the same characteristics as stimulated emission (lasing) example [80].

Pump intensity must meet a threshold, tiny signals must be amplified exponentially within the gain medium, and the output coherent beam must have high directionality and brightness [81].

From a historical perspective, the investigation involving Brillouin bouncing with a backward stimuli (SBS) in 1972 yielded the earliest detection OPC characteristic, optical phase coupling. Since that time, researchers discovered that the same OPC behavior may be seen on the reverse output of many stimulated scattering types [82,83].

These experimental findings demonstrated that the pump laser beam's aberration influence may be automatically cancelled in the beam of reversibly stimulated scattering. There is a remarkable resemblance between stimulated scattering and stimulated emission, as was discussed in the prior subsection. The formation of stimulated scattering does not require such population inversion in a scattering medium, whereas stimulated emission does. This is the only distinction between

these two processes the reverse stimulated emission when circumstances are right [84,85,6].

### 3.4 Design of Dispersion Optical Compensator Based Optical Spectrum

#### Inversion

Any dispersion management strategy's fundamental premise is quite straightforward. This is clear from the equation describing pulse propagation used to enlarge the pulse generated by the dispersion [87,88 ,2].

$$\frac{\partial A}{\partial Z} + \frac{i\beta_2}{2} \frac{\partial^2 A}{\partial t^2} - \frac{\beta_3}{6} \frac{\partial^3 A}{\partial t^3} = 0 \quad (3.4)$$

where  $\beta_3$  represent the dispersion effects of third-order.

The above equation's complex conjugate can be applied to determine the simplest explanation of how OSI can correct for the GVD [89,90].

$$\frac{\partial A^*}{\partial Z} - \frac{i\beta_2}{2} \frac{\partial^2 A^*}{\partial t^2} - \frac{\beta_3}{6} \frac{\partial^3 A^*}{\partial t^3} = 0 \quad (3.5)$$

Analyzing equations above reveals that for the group velocity dispersion GVD parameter  $\beta_2$ , the  $A^*$  describe the phase conjugated field that propagates at reversible sign.

This observation can see immediately to the effect that if the optical field is phase-coupled as seen in Figure (3.4), in the center of the fiber link, then the second half of the fiber link will perfectly correct for the second order dispersion (GVD) collected over the first half [91,92].

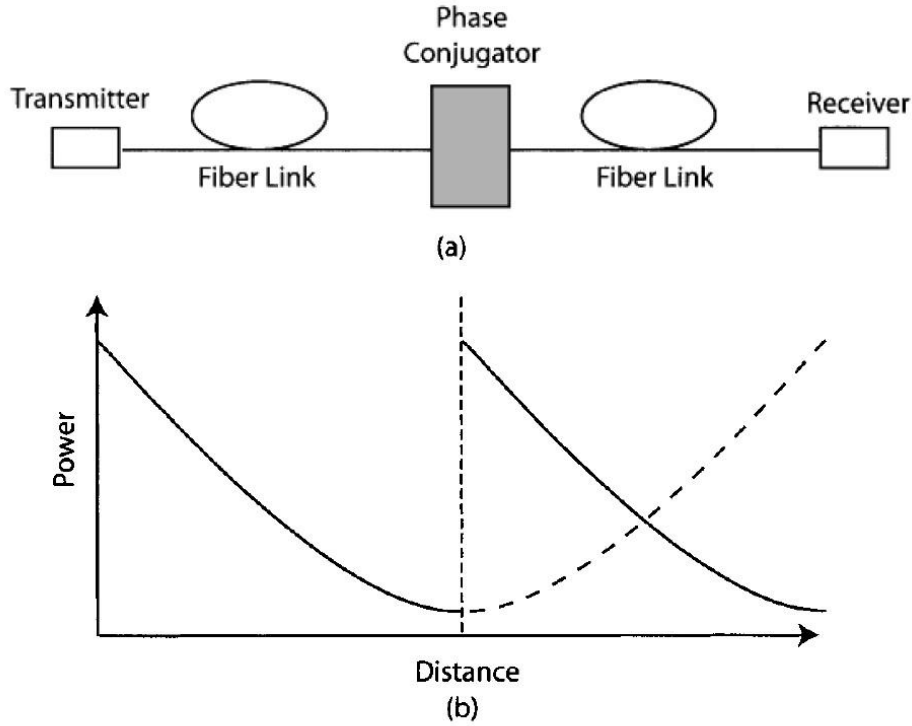


Figure (3.4) Schematic of midspan phase conjugation [91]

The following equation, where  $\beta_3 = 0$ , can be used to confirm the efficacy of midspan OIS for dispersion adjustment [93,94,95] .

$$A(z, t) = \frac{1}{2\pi} \int_{-\infty}^{\infty} \tilde{A}(0, \omega) \exp\left(\frac{i}{2}\beta_2\omega^2 z + \frac{i}{6}\beta_3\omega^3 z - i\omega t\right) d\omega \quad (3.6)$$

the optical electrical field right before the optical phase conjugated obtained it by changing.  $z = L/2$ . In this equation. The second half for the section then results from the phase-conjugated field propagation  $A^*$  [96-99].

$$A^*(L, t) = \frac{1}{2\pi} \int_{-\infty}^{\infty} \tilde{A}^*\left(\frac{L}{2}, \omega\right) \exp\left(\frac{i}{4}\beta_2 L \omega^2 - i\omega t\right) d\omega \quad (3.7a)$$

where  $\tilde{A}^*\left(\frac{L}{2}, \omega\right)$  represent the Fourier Transform of  $A^*(L/2, t)$  expressed as

$$\tilde{A}^*\left(\frac{L}{2}, \omega\right) = \tilde{A}^*(0, -\omega) \exp\left(-i\omega^2 \beta_2 \frac{L}{4}\right) \quad (3.7b)$$

When this formula is put back into the previous equation (3.6), one discovers that  $A(L, t) = A^*(0, t)$ .

The observed input optical field is the pulse form is restored as a result of complete recovery to its input form with the exception of a phase reversal brought about by the OSI [100]. The midspan spectral inversion method is another name for the Optical Phase Conjugate(OPC) method because the signal spectrum produced when OPC is applied becomes the input stream's mirror image.

### 3.5 Compensation Design Based Optical Spectrum Inversion (OSI)

The nonlinear processes include self-phase modulation (SPM) and cross phase modulation, causes the transmitted signal to phase fluctuation and shows itself by nonlinear phase shift of propagating signals in optic fiber [101,102].

Self-phase modulation and cross phase modulation effects are reducing the signal quality in the majority of light wave systems, particularly if the signal is transmitted over very long distances utilizing several optical semiconductor amplifiers.

It appears that the optical phase Conjugate method can simultaneously correct for the Group velocity dispersion and SPM. It is simple to demonstrate that in the absence of fiber losses, the GVD and SPM are both properly equalized.

In a loss pulse spreading across fiber is controlled by [ 103-105]

$$\frac{\partial A}{\partial Z} + i \frac{\beta_2}{2} \frac{\partial^2 A}{\partial t^2} = j\gamma |A|^2 \cdot A - \frac{\alpha}{2} A \quad (3.8)$$

Where  $\alpha$  represent fiber attenuation when  $\alpha = 0$  .

Taken as a complex inverse of the aforementioned equation. and swap  $z$  for  $-z$ ,  $A^*$  satisfies the same equation. The description of propagation conjugated signal in optical fiber as signal propagate in reverse direction to undo distortions result from dispersion and nonlinear parameters of optical fiber [106].

SPM and GVD can both be simultaneously restitution for by middle span OSI.

When we consider that the SPM and XPM produce the phase shift are power-dependent, the cause becomes immediately clear [107].

As a result, the first half of the link experiences significantly larger phase shifts than the second, and OSI is unable to considering non-linear influences.

the effects of fiber losses using the calculation above. The sub.  $A(z, t) = B(z, t) \exp(-\alpha z)$ , and rewrite the equation as [108-111]

$$\frac{\partial B}{\partial z} + i \frac{\beta_2}{2} \frac{\partial^2 B}{\partial t^2} = j\gamma P(Z) |B|^2 B \quad (3.9)$$

where the signal  $p(z) = \exp(-\alpha z)$ .

With a  $z$ -dependent nonlinear parameter, lack of fiber's impact is theoretically equal to the loss-free circumstance. The complex conjugate was taken for the above equation and the dimensions changing from  $z$  to  $-z$ , we can get a good XPM cross remuneration is possible if  $p(z) = \exp(\alpha z)$  after phase. Conjugation. ( $z > L/2$ ).

A main necessary for the optical phase conjugation. methods to work is

$p(z) = p(L - z)$ . if  $\alpha \neq 0$  the condition cannot be satisfied [112].

One may believe that the issue can be resolved by boosting the signal following OSI so that it reaches parity with the entrance power before. being linked in the second fiber connection portion. Although such a strategy lessens the effects of SPM, it does not fully compensate for it. By take that the transmission of a signal the that is phase-conjugated is similar to that of a time-back signal, the reasoning may be understood. Since  $p(z) = p(L - z)$  in the equation above perfect SPM correction is only possible if the power fluctuations near the midspan point, where the OSI is performed, are symmetric. Optical amplification is unable to fulfill this requirement [113].

If the wave amplified frequently sufficient for the electricity does not significantly change during each amplification stage, one can get near to SPM and XPM correction. Bidirectional pumping combined with distributed Raman amplification, which can deliver  $p(z)$  near to 1 over the whole range, can also be useful [114,115].

Employing dispersion-decreasing fibers with  $\beta_2$  decreasing along the fiber length will result in perfect adjustment of both GVD and SPM, XPM.

Assume that  $\beta_2$  in the aforementioned a function is an expression of  $z$  in order to demonstrate how such a strategy can be put into practice. By undergoing the change [116,34]. Using the parameter  $\xi$  as  $\xi = \int_0^z P(z) dz$  the final equation has the form

$$\frac{\partial B}{\partial \xi} + i \frac{b(\xi)}{2} \frac{\partial^2 B}{\partial t^2} = j\gamma |B|^2 B \quad (3.10)$$

where  $b(z) = \beta_2(z)/p(z)$

Both GVD and SPM can be replaced if  $b(\xi) = b(\xi_L - \xi)$ , where  $\xi_L$  is the value of  $\xi$  at  $z = L$ .

When  $\beta_2(z)$  drops exactly in the same manner as  $p(z)$ , keeping steady in their ratio, this condition is automatically met [117].

While the  $p(z)$  decreases exponentially, the dispersion and self-Phase Modulation and cross Phase Modulation  $M$  are equalizing (compensated) in a fiber whose GVD declines as dispersion increases  $e^{-\alpha z}$ . This method is quite flexible and works even when using in line amplifiers [118].

### 3.6 Implementation The Optical Spectrum Inversion

In this section deals with analysis photonic phases conjugation produced by dual pump extremely nonlinear fiber performance. All analysis equation based on Schrödinger nonlinear equations described above.

The solutions of Schrödinger equation achieved and performance analysis done under assumption the pump power govern fiber nonlinearities by controlling on phase nonlinearly by refractive index effects and a results control on the power of signal and idler.

The idler waves produce by optical phase conjugation in four wave mixing techniques by using highly nonlinear fiber medium, one from important properties of idler signal that have phase conjugated revers the phase of input signals.

The another important properties of idler wave it has the ability to transport identical information to the input signal but invers in phase.

The signals propagate in dielectric media with highly nonlinear according to Schrödinger equation and can expressed as [119,120]:

$$\begin{aligned} \frac{\partial A^*(z, t)}{\partial Z} + \frac{\alpha}{2} A^*(z, t) + \beta_1 \frac{\partial A^*(z, t)}{\partial t} - \frac{j}{2} \beta_2 \frac{\partial^2 A^*(z, t)}{\partial t^2} - \frac{1}{6} \beta_3 \frac{\partial^3 A^*(z, t)}{\partial t^3} \\ = j\gamma |A^*(z, t)|^2 \cdot A^*(z, t) \end{aligned} \quad (3.11)$$

The sign \* represent the conjugate and the negative sign in the equation express revers effect for chromatic dispersion and Kerr effect. This will contribute to cancel the effect of dispersion and fiber nonlinearities after the OSI blocks. As a result, the transmission impairments in optical fiber at fully symmetric will be compensate.

The proposed design consists from two pump sources followed by two semiconductor amplifiers, all undesired amplifies spontaneous emission signals filtered by using optical filter. The two optical pump sources and optical input signal as shown in figure (3.5) are launched together by optical coupler where the output of the coupler injected into highly nonlinear fiber according to the four wave mixing process the idler wave will produce and the parameter values of the proposed system in table (3.1).

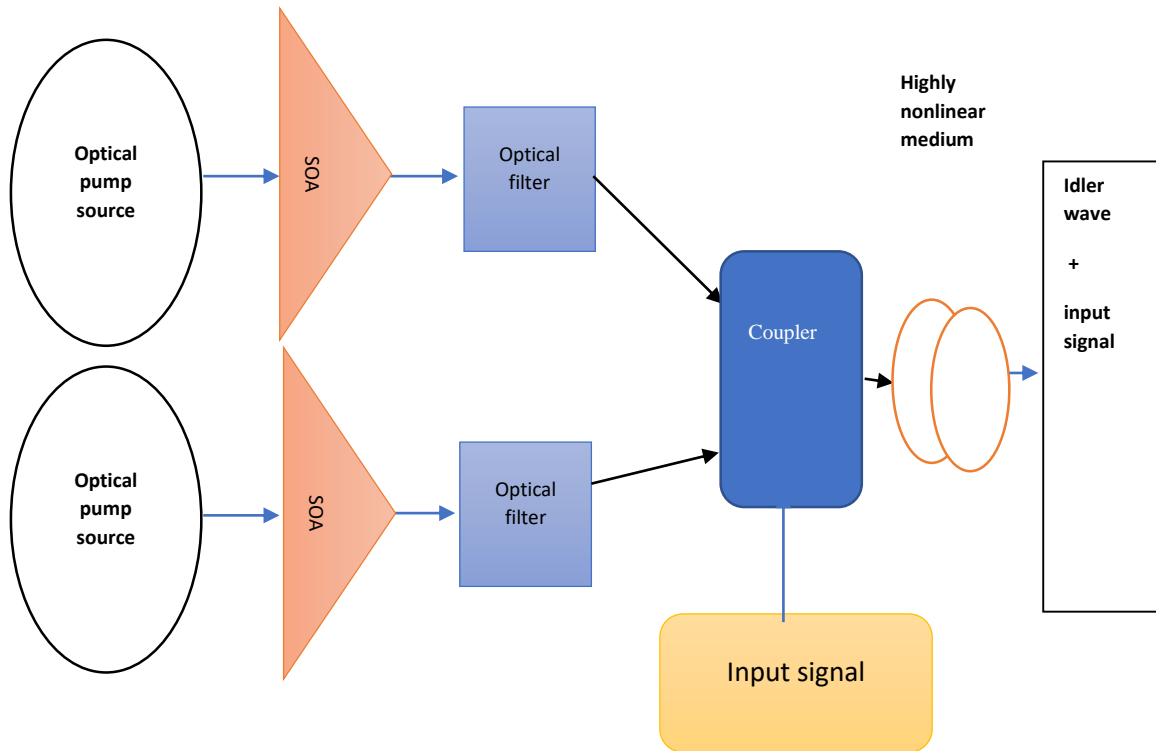


Figure (3.5) The proposed compensated design

The three signals, two pump and one input data signal and the result idler signal all of them can be described mathematically by using nonlinear Schrödinger equations. the Figure (3.6) represent the spectrum of the output from nonlinear medium.

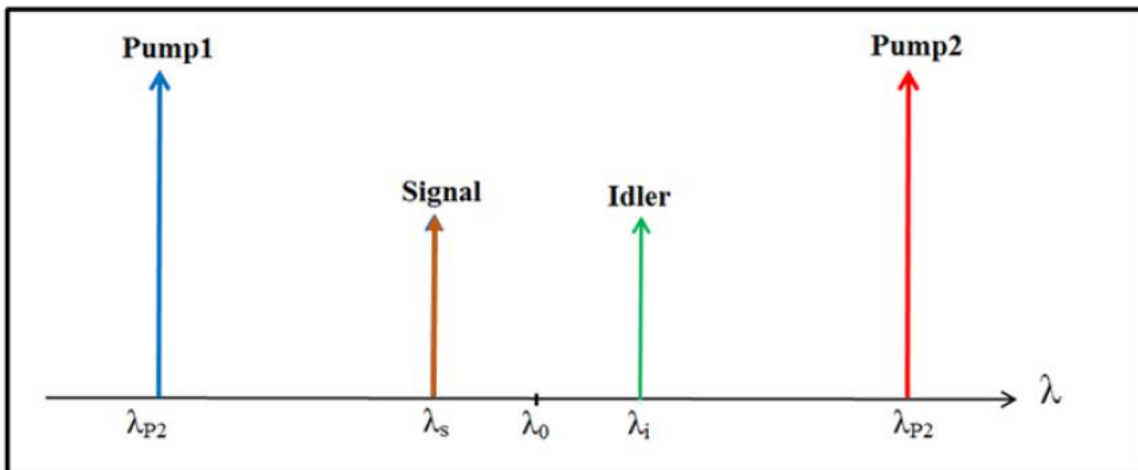


Figure (3.6) Optical spectrum of the signals

Table (3.1) Represent the Parameter values of the proposed system

parameter	HNLF-OSI
Pump. power 1 (w)	0.8
Pump. power 2 (w)	0.8
Pump wavelength 1(nm)	1600
Pump wavelength 2(nm)	1650
Attenuation coefficient of HNLF (dB/Km)	0.4
Nonlinear Coefficient of the HNLF ( $w^{-1}, km^{-1}$ )	10
Nonlinear Refractive index ( $m^2/W$ )	$22 \cdot 10^{-21}$
Effective core area of HNLF( Mm)	11
Group velocity dispersion (Ps/nm/Km)	16.75
Dispersion slop of HNLF (Ps/nm <sup>2</sup> /Km)	0.2

### 3.6.1 Effect of two pump source

The use of dual (two) pump source in proposed system give many benefit such as highly and flat gain at using optical fiber amplifier [121]. And also give highly conversion and bandwidth at used spectrum. The description of propagated signals in high nonlinear medium govern by Schrödinger equations and these equations are very difficult and complicated to solved analytically therefore we used the numerical methods and by using software package mat labs to solve this model.

### 3.6.2 Approximate analysis of the FWM-OSI system

The analysis in this paragraph based on approximate solution of the proposed mathematical model that govern propagating wave in nonlinear optic fibers

according to four wave mixing process. All fields of four wave in optical nonlinear fiber are linearly co polarized along propagation axis in the z- direction [122]. The angular frequencies of four waves are  $\omega_{p1}$ ,  $\omega_{p2}$ ,  $\omega_s$ ,  $\omega_i$  respectively. The intensity of pump waves is more than data input signal (prob signals) by ten times, ignore the fiber attenuation during propagating because using semiconductor optical amplifier according to above assumption can get the following model [123,124].

$$\frac{dA_{p2}(z)}{dz} = j\gamma[2p_1 + p_2]A_{p2}(z) \quad (3.12)$$

Where  $p_{p1} = |A_{p1}(0)|^2$  and  $p_{p2} = |A_{p2}(0)|^2$  launched pump power at  $z=0$ . The approximate analytical solution according to split step Fourier transform SSFT

$$\begin{aligned} A_{p1}(z) &= A_{p1}(0)\exp(j\gamma[p_{p1} + 2p_{p2}]z) \\ A_{p2}(z) &= A_{p2}(0)\exp(j\gamma[2p_{p1} + p_{p2}]z) \end{aligned} \quad (3.13)$$

To solve the complex amplitude of input signal and idler signal can simplify the Schrödinger equations that represent the propagation in optical fiber according to above assumption and get the propagate equations as [125,126]

$$\begin{aligned} \frac{dA_s(z)}{dz} &= 2j\gamma \left( [p_{p1} + p_{p2}]A_s(z) + A_i^*(z)A_{p1}(z)A_{p2}(z)\exp(-j\Delta kz) \right) \\ \frac{dA_i^*(z)}{dz} &= -2j\gamma \left( [p_{p1} + p_{p2}]A_s^*(z) + A_s(z)A_{p1}^*(z)A_{p2}^*(z)\exp(j\Delta kz) \right) \end{aligned} \quad (3.14)$$

The approximate solution is [127]

$$\begin{aligned} A_s(z) &= A_s(0) \left( \cos(gz) + \frac{jk}{2g} \sinh(gz) \right) \times \exp \left( j \frac{3\gamma(p_{p1} + p_{p2}) - \Delta k}{2} z \right) \\ A_i^*(z) &= A_s(0) \left( \frac{-j2\gamma A_{p1}^*(0)A_{p2}^*(0)}{g} \right) \sinh(gz) \\ &\quad \times \exp \left( -j \frac{3\gamma(p_{p1} + p_{p2}) - \Delta k}{2} z \right) \end{aligned} \quad (3.15)$$

The parameter coefficient of the gain is  $g$  showed as [128]:

$$g = \sqrt{4\gamma^2 p_{p1} p_{p2} - \left(\frac{\Lambda k}{2}\right)^2} \quad (3.16)$$

nonlinear Phase loss  $\Lambda k$  expressed as  $\Lambda k = \Delta k + \gamma(p_{p1} + p_{p2})$  the expression of power signal as [129]:

$$p_s(z) = p_s(0) \left[ \cosh^2(gz) + \frac{\Lambda k^2}{4g^2} \sinh^2(gz) \right] \quad (3.17)$$

The idler and pulse are affected the same effect in highly nonlinear fiber where both signals are amplifying. Therefore, the power of idler can be obtained as  $p_i(z) = p_s(z) - p_s(0)$  [130]. The output power near the fiber's terminus and according to previous analysis the idler wave expressed as [131]:

$$p_i(L) = p_s(0) \left[ \left( 1 + \frac{k^2}{4g^2} \right) \sinh^2(gL) \right] \quad (3.18)$$

from this equation introduce the final form of power for the idler wave, where the power of the wave produce after injected input signal power into the fiber, the contributions of pump waved in part of energy to the idler and input signal. From the previous analysis note the idler power proportional directly to square of fiber length at  $gl \ll 1$ . While when the  $gl \gg 1$  the growth becomes exponentially. The idler wave has the same information except it reverses in phase [131-133]

### 3.7 Neural Network Artificially (NN)

The intricacy of the human brain surpasses that of any other known structure in the cosmos [134]. It has roughly 86 billion cells, which are linked by trillions of synapses, or connections. This is where human intelligence first emerged. Nevertheless, further study of its workings is still needed. In addition to studying biological neural networks (BNNs) [135], studies on artificial neural networks

(ANNs) have been conducted to imitate the human brain based on a streamlined mathematical model that can be controlled on a wide scale.

Being one of computer science's most active subfields, Artificial intelligence (AI) focuses on modeling the nervous system's architecture [136] using artificial neural networks (ANNs). It creates connections between neurons at several layers of the neural network and improves their robustness and generalizability [137].

Throughout the 1980s, ANN's study has advanced significantly. Furthermore, it has effectively solved a number of real-world issues in the fields of pattern recognition that are challenging for modern computers to resolve., Robustly smart robots with autonomous control, prediction and estimation, biomedicine, economics, etc. [138].

Biological neurons, the constituent parts of BNNs, are the biological equivalents of artificial neurons. Billions of different types and sizes of neurons make up BNNs.

A generalized biological neuron having four basic units is shown in Figure (3.7) a. are first dendrites, second axons, third soma, and synapses [139-141].

ANNs use a condensed model derived from BNNs. The McCulloch and Bates-invented simple informal natural neuron acts as the ANN's computational unit in this model [142].

The task requires the simultaneous stimulation of many artificial neurons. As seen in Figure (3.7) b, an artificial neuron receives one or more inputs ( $x$ ) from other neurons, and the inputs are added together to form an output ( $y$ ) that is delivered to more neurons on the axons [143-145].

separated by a nonlinear function called an activation function or transfer function ( $f$ ), which is a weighted function ( $w$ ).; A step function, sigmoid function, etc. can be used as the activation function. The following is the artificial neuron's mathematical form [146,147]:

$$y_i = f\left(\sum_{i=0}^n w_{ij}x_i\right) \quad (3.19)$$

Figure (3.7) c depicts a typical feed-forward ANN architecture. Information only transfers in the forward direction in this network [148-150].

A series of artificial neurons are combined to form the input layer. The input signal is routed through one or more hidden layers in artificial neural networks.

The results are provided by the output layer at the conclusion of this architecture. ANN may learn to carry out a task by a series of training with examples, in contrast to the existing von Neumann computer that does tasks by pre-designing the software [151,152]. The supervised learning approach, for instance, updates weights with backpropagation errors between known target values and output values as a conventional learning process [153].

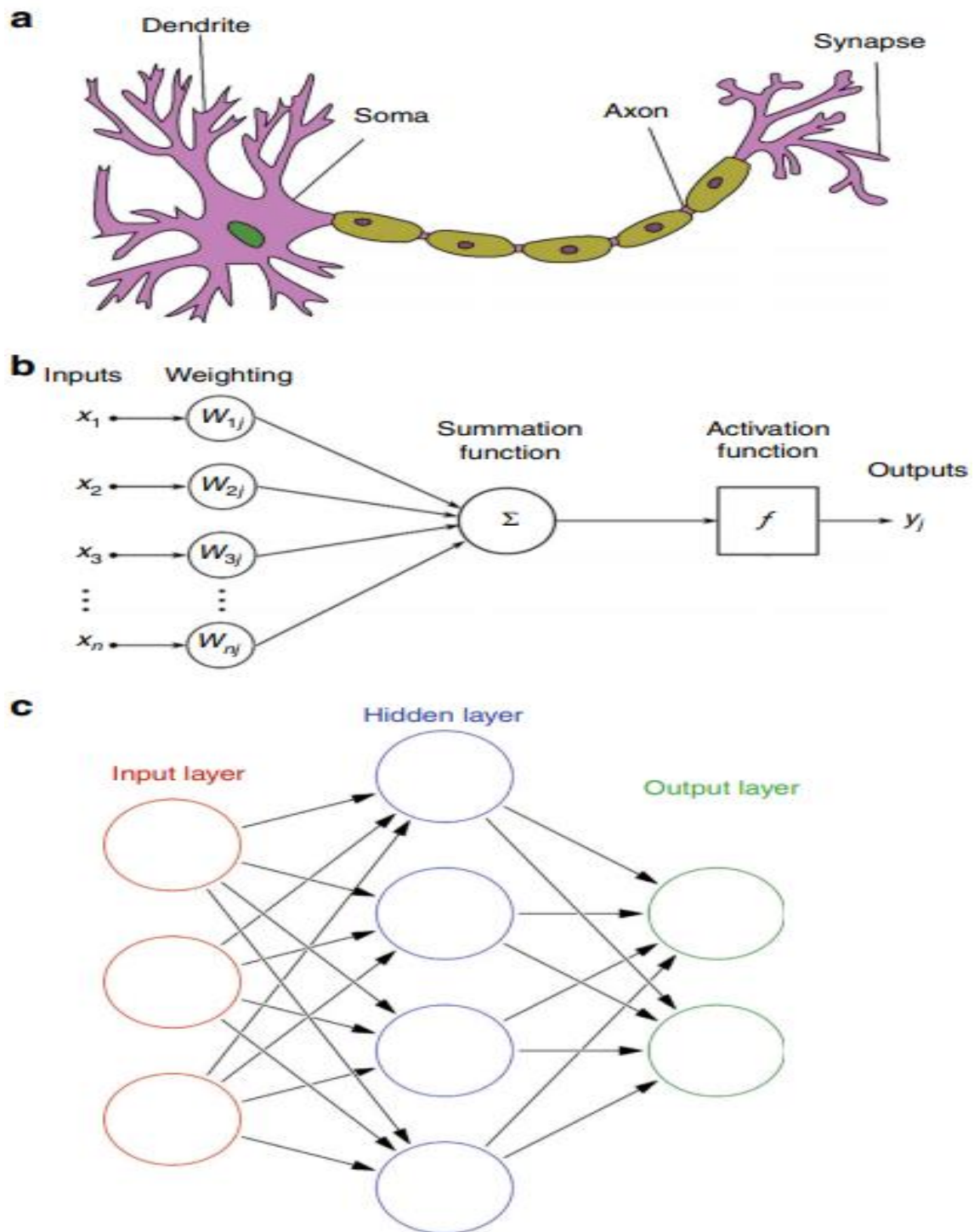


Figure (3.7) Artificial neural network operation theory. (A) A diagram of a biological neuron. (b) A schematic illustration of a synthetic neuron. (c) Feed-forward artificial neural networks' architecture [154]

### 3.8 Optical Neural Network (ONN)

Due to their unique characteristics, such as their inherent huge parallelism, quick transmission speed, and lack of mutual interference, photons are the ideal bearers of information [155,156].

Since optical techniques may multiplex signals in time, space, polarization, angular momentum, wavelength, and fields, they may be used to solve issues with electronics. Since optical or fiber waveguides have already replaced copper interconnections in computer chips and data centers, research and development in optical interconnection technology may help artificial neural networks that are based on software and electronics simulations perform better [157,158].

An artificial neural network that is physically built by using optical (electrical) components is known as an optical neural network (ONN). According to the physical implementation method, ONN can be categorized, as illustrated in Figure (3.8). [159,160, 161].

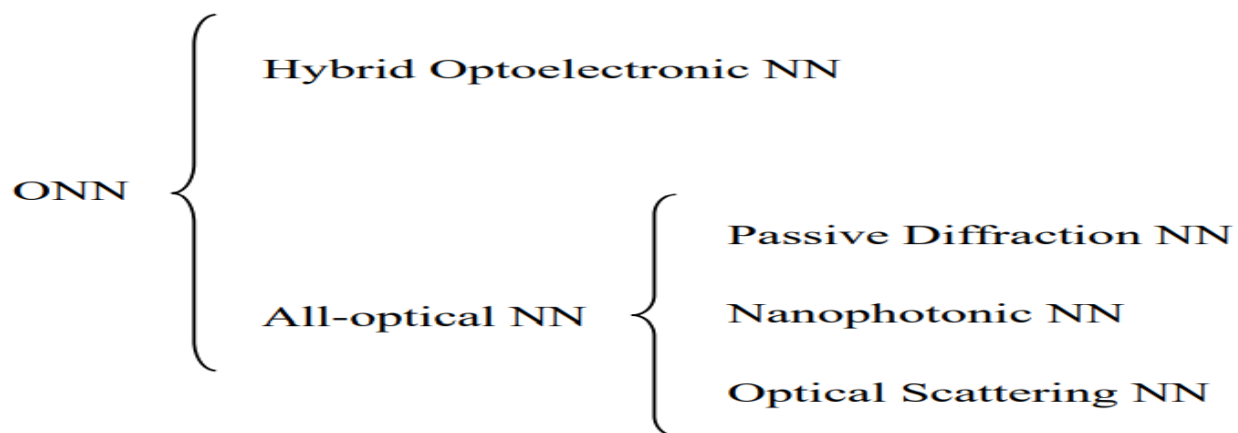


**Figure (3.8) The classification of optical neural network**

ONN can be divided into a hybrid optical electronic neural network (HONN) and an all-optical neural network (AONN) according to different physical implementation methods.

### 3.8.1 Hybrid optic-electronic neural network (HONN)

HONN is a type of ONN that uses photoelectric conversion devices to transmit data during computation. Its main feature is to use optical devices to process the partial layer, and then the optical calculation results are fed into the traditional neural network of the remaining layers via photoelectric conversion [163,164].

### 3.9 Challenge for Implementing All-Optical Neural Network (AONN)

AONN is a type of ONN that does not use photoelectric switching devices to transmit data in the computing process. All computing is achieved through optical devices [165].

According to the main use of optical devices, AONN can be divided into three types of neural networks, namely, nanoscale neural network, passive diffraction neural network, and optical scattering neural network [166].

### 3.10 Training Algorithms (Backpropagation Algorithm)

Nearly all neural networks are trained using a backpropagation process and block diagram of the NN system as shown in figure (3.9). It is difficult to implement this technique optically since it demands that the nonlinear lattice elements respond differently depending on whether light is propagating forward or backward. Current ONNs are already receiving training in response to these difficulties, often with the use of digital computers [167].

As a result, optics' immense benefits are still largely unrealized. A still-unsolved issue is the creation of fully visually trained ONNs to benefit from these advantages. A realistic instruction strategy that can back-propagate an erroneous signal across nonlinear neurons in a single optical pass is tested and presented [168].

Through gradient descent, the backpropagation method seeks to reduce the loss function that quantifies how far the performance of the present network departs from the ideal [169].

The steps following are repeated until convergence to achieve this:

- (1) information dissemination over a network
- (2) Analyze the gradients of the loss function at the output layer in relation to the network parameters.
- (3) returning these gradients to all earlier layers

The direction in which the parameter is updated minimizes the loss function. The aforementioned matrix multiplication, which translates information between layers, is necessary for forward propagation (step 1), as is a suitable nonlinear activation function that is applied to each neuron independently [170-172].

Recent work has also acknowledged optical nonlinearity, even though this nonlinearity has so far largely been used digitally in hybrid optoelectronic systems at the expense of repeatedly measuring and creating the photocurrent state.

Neuronal nonlinearity poses difficulties. This is because the activation function derivatives for each neuron at the input current value, which are required to regulate the backpropagation signal, are not readily available in ONN.

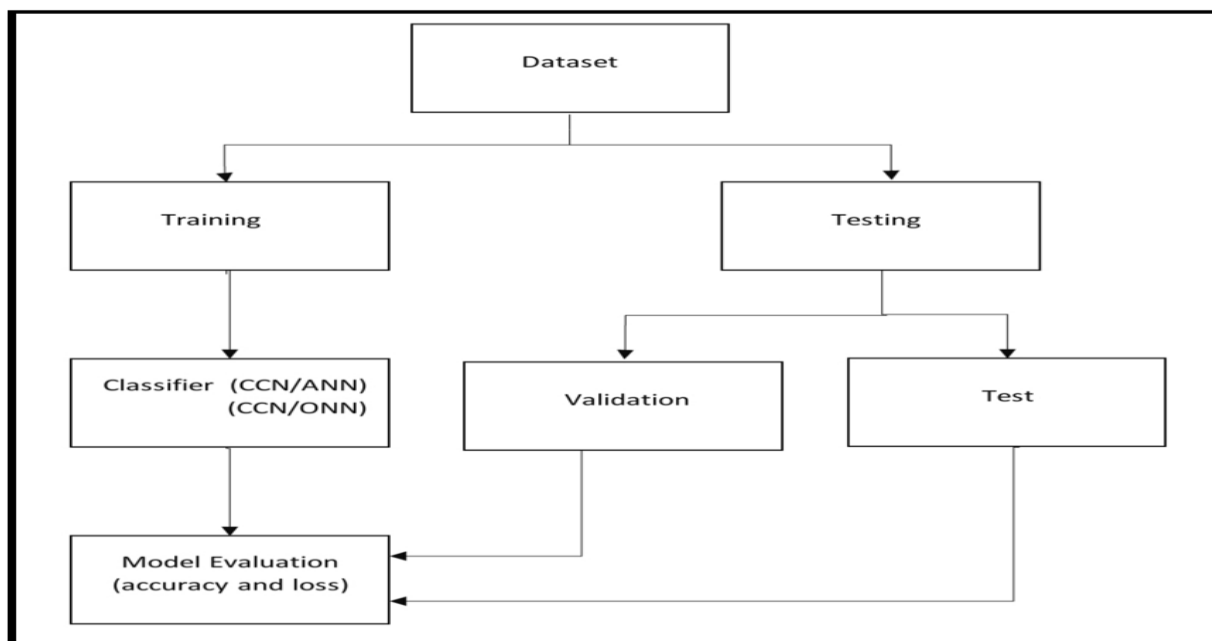


**Figure (3.9): Block diagram of the neural network system**

### 3.11 Optical Neural Network Implementation

The implementation method requires high computing resources. So the proposed system was implemented using the following software requirements.

- Software

Optisystem ver. 19. Operating System: Windows 10. 64. bit., Programming Language: Python and development Environment: Pycharm 2022.1.

Python scripts are used to program neural networks using some of the most recent automatic differentiation modules. These libraries significantly speed up our processing. Python's pickle file is used to serialize and unserialise sequence items, the Numpy library loads data into arrays, the Matplotlib tool plots the study's findings, and the PyTorch module creates actual neural networks as shown in figure (3.10), from by introducing a library called Torchvision, this library gives us some useful things like data loaders, datasets and data converters for raster images.



### 3.12 Training Network

The following steps are the structures of the training network.

1. The images would be supplied 64 (`batch_size_train`) times during one iteration from 60000, training records.
2. Utilizing forward propagating, the researcher would next feed the `batch_size_train` into the network.
3. Deliver the network output that represents the predicted class names. In addition to the actual values, the loss would be produced as a variable object by the loss function.
4. After that, the researcher carried out the backward propagating by using the loss variable's back-propagation algorithm to calculate the update of the variables.
5. The researcher is now able to use the optimizer's update function to change the model parameters since the optimizer already contains a reference to the network and access to the variables and calculated gradients.

Furthermore, in addition to the aforementioned actions, the researcher also wishes to use a verification dataset to test the network's performance. By checking if it is trying to predict to the training data, users can see how effectively it has so far generalized to new data. In the conclusion of each period, he tests the performance just on the testing set. The test is carried out with the same training steps except that the usage `batch_size_test = 128` for both data set one, and data set two. `Batch_size_test = 1000`, and the back-propagation is not used. The whole proposed method can be illustrated in flow chart in figure (3.11).

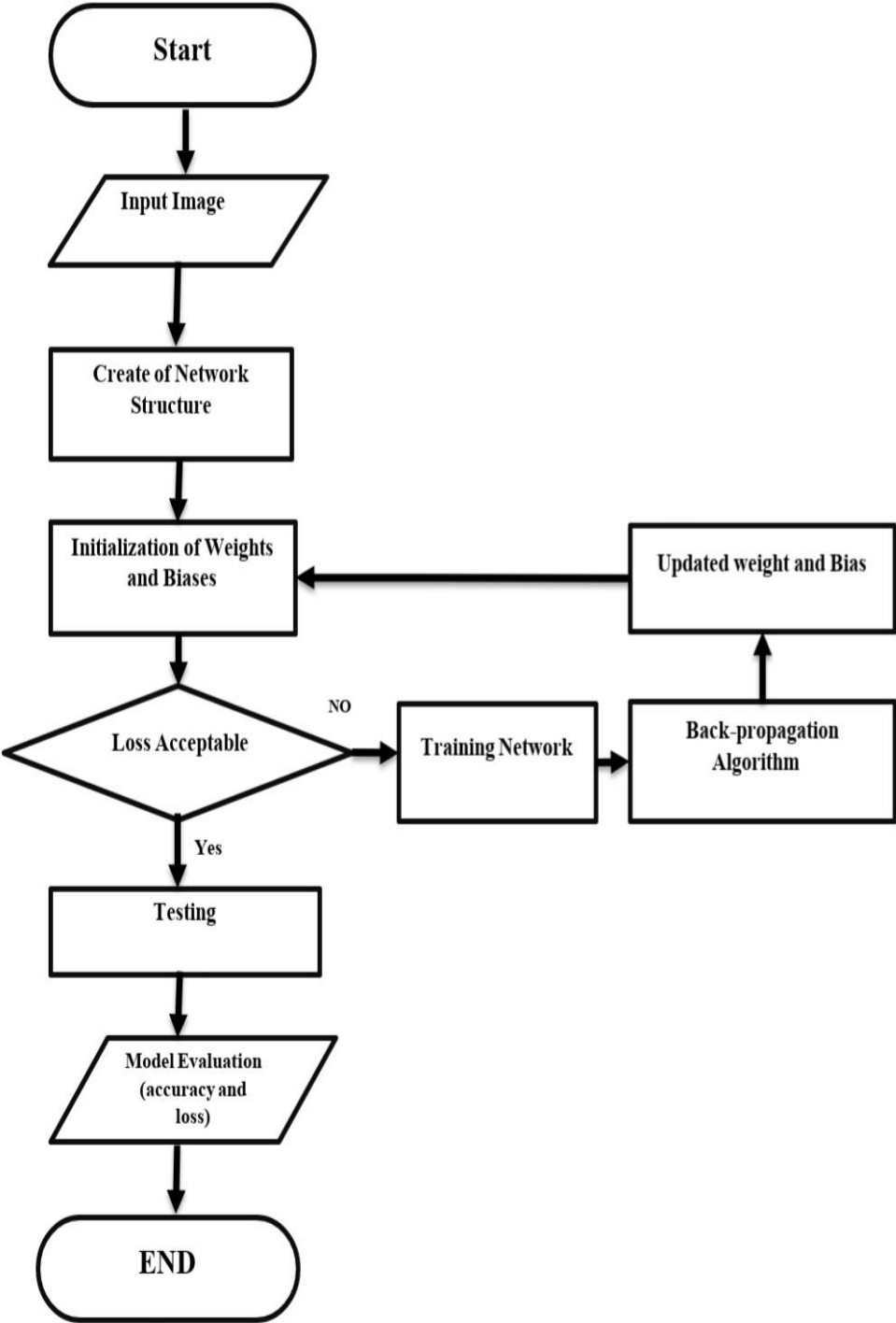


Figure (3.11): Process of the neural network system

### 4.1 Introduction

In this chapter, the results of the proposed techniques are described to mitigate the optical fiber linear impairments and nonlinear impairments are presented according to design techniques. The results showed a good performance of compensated algorithms at high bit rate optical fiber transmission systems for different fiber lengths and data rates.

### 4.2 Fiber losses compensator

The design of fiber compensator for linear and nonlinear effects in optical fiber have been designed based on HNLFF optical inversion spectrum compensator. The expanded in the fiber to the home (FTTH) system or any optical fiber application in communication or other fiber application such as medical application is based on reduction the losses in optical fiber system therefore need to develop a new design to mitigate the optical fiber losses such as linear optical fiber and nonlinear fiber. The optical phase conjugation method is used has because it low cost, fast response in optical spectrum and good performance.

In this section, describe and explain more than one scenario for the design optical phase conjugation by using nonlinear medium.

### 4.3 Compensation of linear fiber impairments by DCF OOK

The first compensation was achieved by adding linear fiber losses compensator DCF in optical fiber system without using OSI compensator of optical fiber system. The linear fiber losses can be divided into two main parts according to nonlinear Schrödinger equations that governing pulse propagation in optical fiber where the first effect represent a dispersion in optical fiber and the second one is attenuation effect due to propagate the pulse in the optical fiber. Where the dispersion causes a pulse broadening as a result from Group velocity dispersion, material dispersion, and polarization dispersion. This effect will limit the bit rate of data transmitted in optical fiber due to inter symbol interferences (ISI) between the transmitted signals. While

the other effect causes a power reduction of transmitted signal can be compensated by adding optical amplifier have a gain equal to the of power losses by optical fiber. The proposed system design shows in figure (4.1). Without OSI are reported as shown below for different bitrate, different optical fiber channel length.

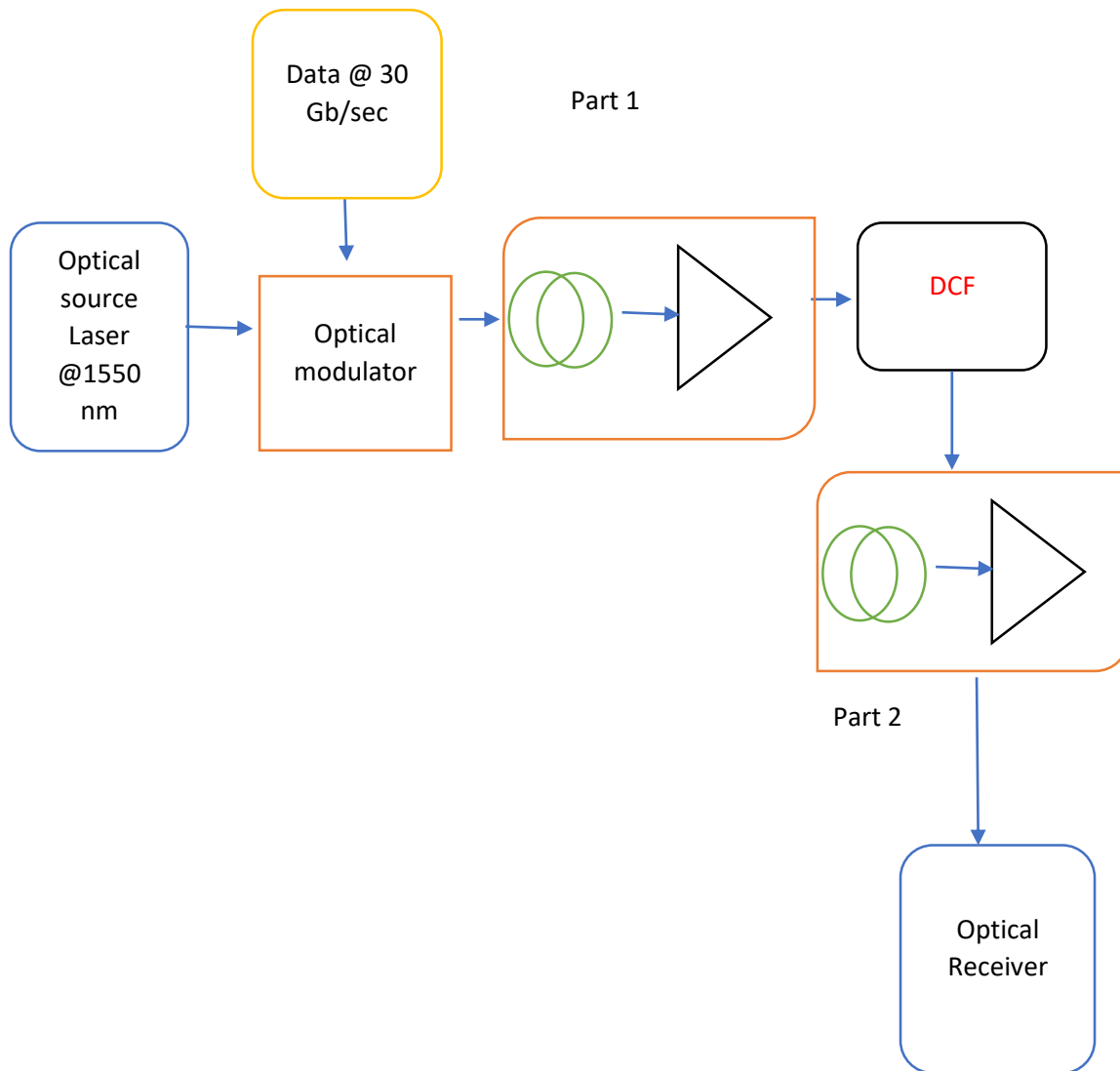


**Figure 4.1 Simulation of optical fiber system with DCF only**

The simulated system using Optisystem ver 19 with Matlab package where the system consists of optical source (laser) CW at wavelength 1550 nm with power 1mW and frequency 193THz, data rate at frequency reach up to 30 Gb/sec modulated by Mach Zinder modulator (MZM) and send over optical fiber at different lengths as recorded in table 4.1. Divided the fiber channel into two optical fiber parts between them at the middle distance putting OSI compensator based on optical spectrum inversion (phase conjugation) the first optical fiber channel part produce accumulated dispersion effect in the optical system and the optical compensator the OPC will invert the spectrum of the propagated signal through OSI compensator immediately as shown in figure (4.1) the pulse propagate continue propagate passing through the second part of the fiber channel. The results for the simulated system are reported in table (4.1) and figure (4.2).

**Table 4.1: 200 Km Fiber Length, with dispersion compensation fiber DCF only at BitRate 30 Gb/s**

<b>Effect of BR (Bit Rate)</b>	
<b>Bitrate 30 Gb/s</b>	
<b>Laser power(mW)</b>	<b>Q-Factor</b>
0.01	4.803
0.015849	4.814
0.039811	4.818
0.063096	4.822
0.079433	4.826
0.1	4.830
0.158489	4.832
0.199526	4.834

## Chapter Four: Results and Discussion

---

0.251189	4.837
0.316228	4.840
0.398107	4.841
0.501187	4.845
0.562341	4.846
0.630957	4.850
0.707946	4.854
0.794328	4.856
0.891251	4.857
0.933254	4.858
1	4.859
1.584893	4.860
2.511886	4.862
3.981072	4.868
5.011872	4.875
5.623413	4.877
6.309573	4.878
7.079458	4.880
7.943282	4.875
8.912509	4.860
10	4.855
19.95262	4.800
25.11886	4.770
31.62278	4.700

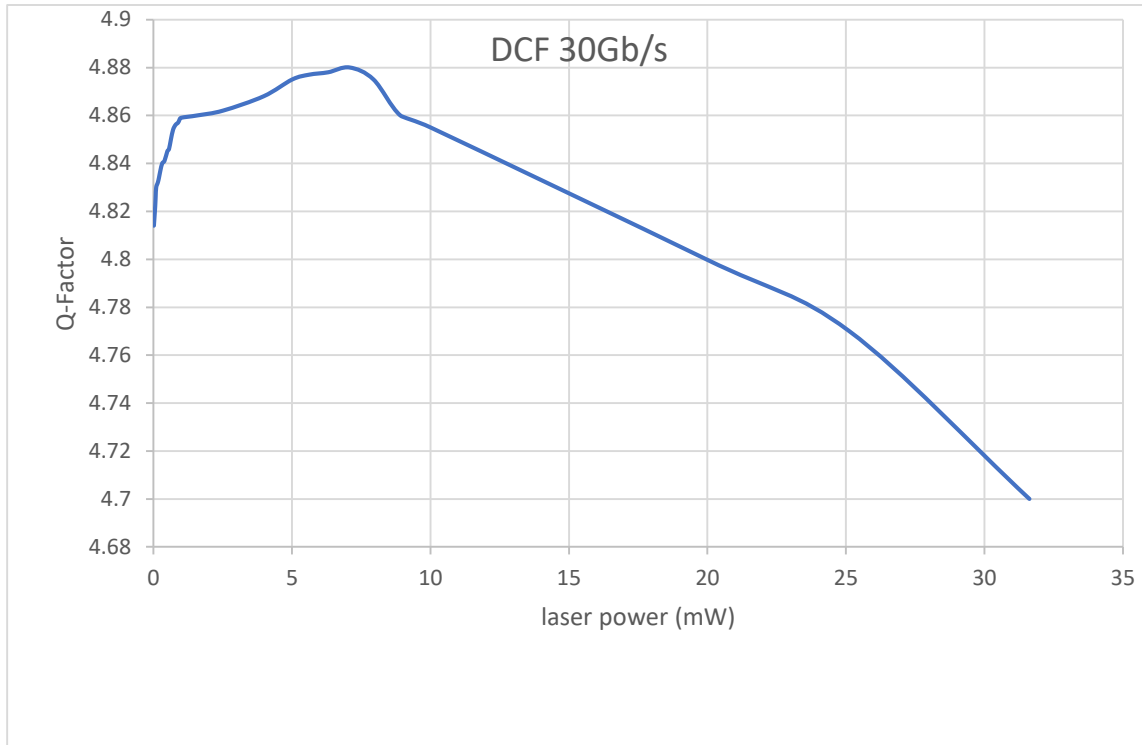


Figure 4.2: Illustrate dispersion compensation fiber DCF at 30 Gb/s

Table 4.2: 200 Km Fiber Length, with Dispersion compensation fiber DCF, at bit rate 60 Gb/s

Bit Rate 60 Gb/s	
Laser power( mW)	Q-Factor
0.01	0
0.015849	0
0.039811	0
0.063096	0
0.079433	0
0.1	0
0.158489	0
0.199526	0

## Chapter Four: Results and Discussion

---

0.251189	0
0.316228	0
0.398107	0
0.501187	0
0.562341	0
0.630957	0
0.707946	0
0.794328	0
0.891251	0
0.933254	0
1	0
1.584893	0
2.511886	0
3.981072	0
5.011872	0
5.623413	0
6.309573	0
7.079458	0
7.943282	0
8.912509	0
10	0
19.95262	0
25.11886	0

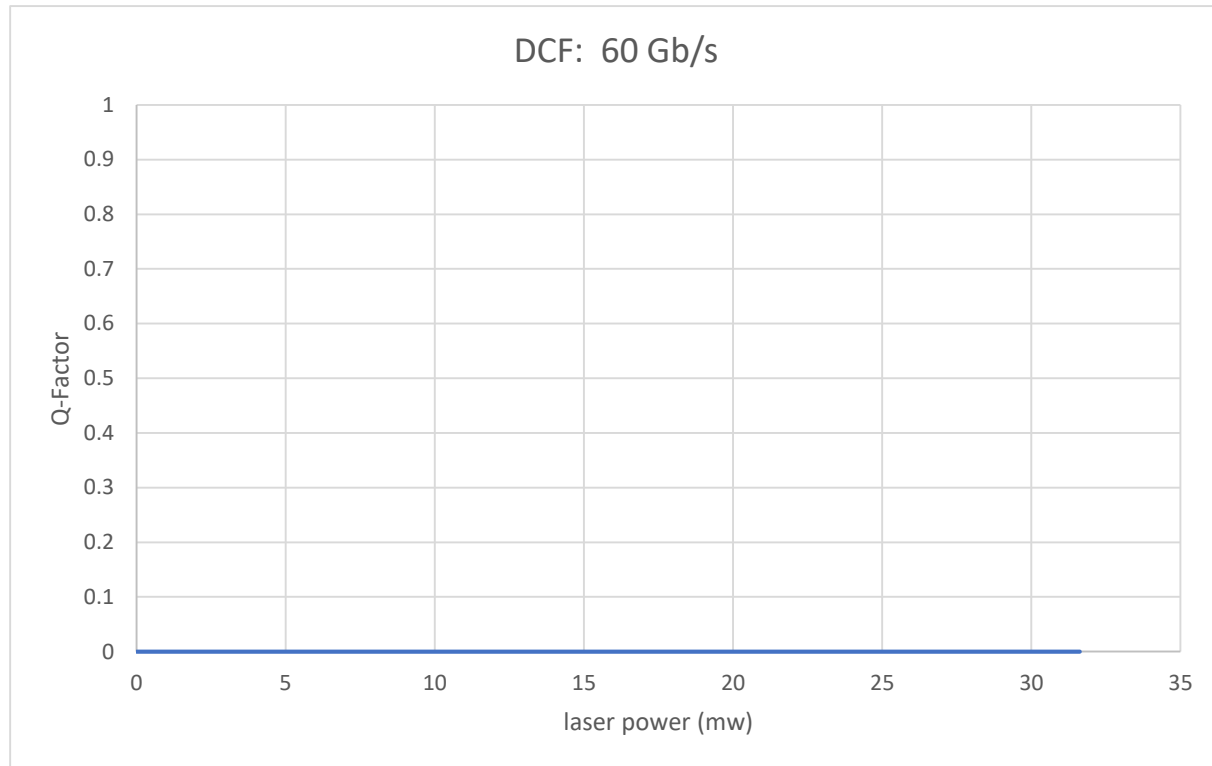


**Figure 4.3: Illustrate dispersion compensation fiber DCF at 60 Gb/s**

From the above results can find the system degradation at high bit rate 60 Gb/s and the Q- factor of the simulated system becomes approach to zero because linear losses in optical fiber accumulated over fiber length 200 Km due to dispersion and attenuation effect. Therefore, we need to introduce the design for OSI compensator as shown in figure 4.4.

#### **4.4. One OSI (MiD fiber) Compensation control**

The method of optical phase inversion or spectrum inversion, creates a signal spectrum that is the complex conjugate of the input signal spectrum, the impairments caused by linear effect in optical fiber channel are perfectly offset by the impairments in the other half of the optical fiber and also the nonlinear impairments in first part compensated by the second part of the optical fiber. Figure (4.4) depicts

the system's block diagram utilizing midway OSI. A third-order nonlinear medium is used for the Four-wave mixing procedure to create this optical inversion spectrum by phase conjugated signal. All the results were compared with reference [56,95,173] and gave a good agreement with the same input parameters.

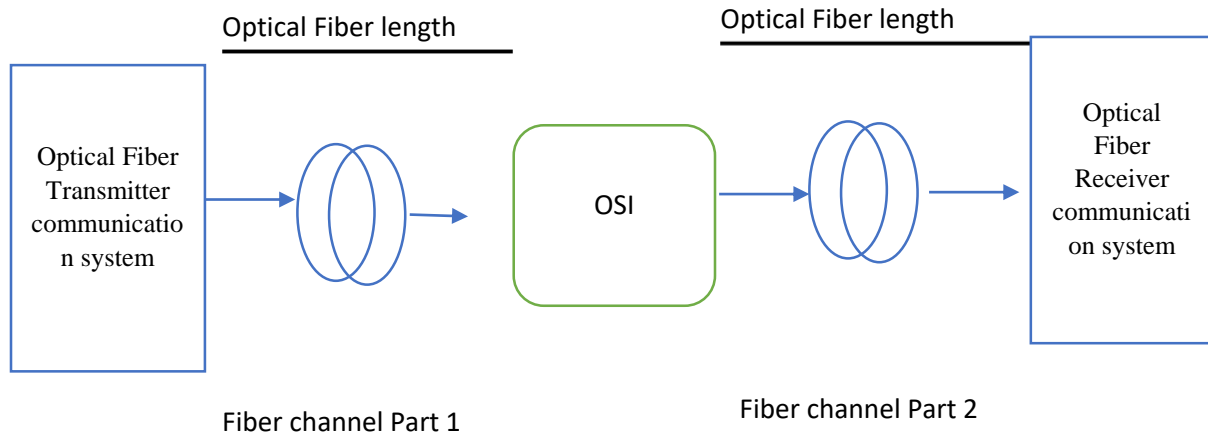


**Figure (4.4) Schematic diagram of MiD fiber OSI Compensation control**

### 4.5 Compensation using MID-HNLF-OSI OOK at Different Bitrate

The optical fiber telecommunication system consists of three parts transmitter, receiver, fiber channel and using the OSI device itself with dispersion compensation by using dispersion compensation fiber DCF incorporated in fiber link with attenuation compensation carried out using fiber system listed in Figure 4.5 as a schematic of the simulated set-up for the proposed work. The simulation of the proposed work demonstrated at high bit rate (30 Gb/s,60 Gb/s) was demonstrated at Opti system 19 software package and MATLAB Release 2019a.

An orthogonally pumped four wave mixing technique was used by the optical phase conjugation as explained in chapter three, device to enable polarization independent conjugation of the signal band, as shown in Figure (4.5). Two pump lasers sources in spectrum 1541.45 nm and 1535.04 nm are used in the system. To reduce amplified

out-of-band spontaneous emission, the pump wavelengths used, which are subsequently passed through the broadband optical filter, have a full width at half maximum (FWHM) of 0.3 nm amplified spontaneous emission (ASE) the system parameters.

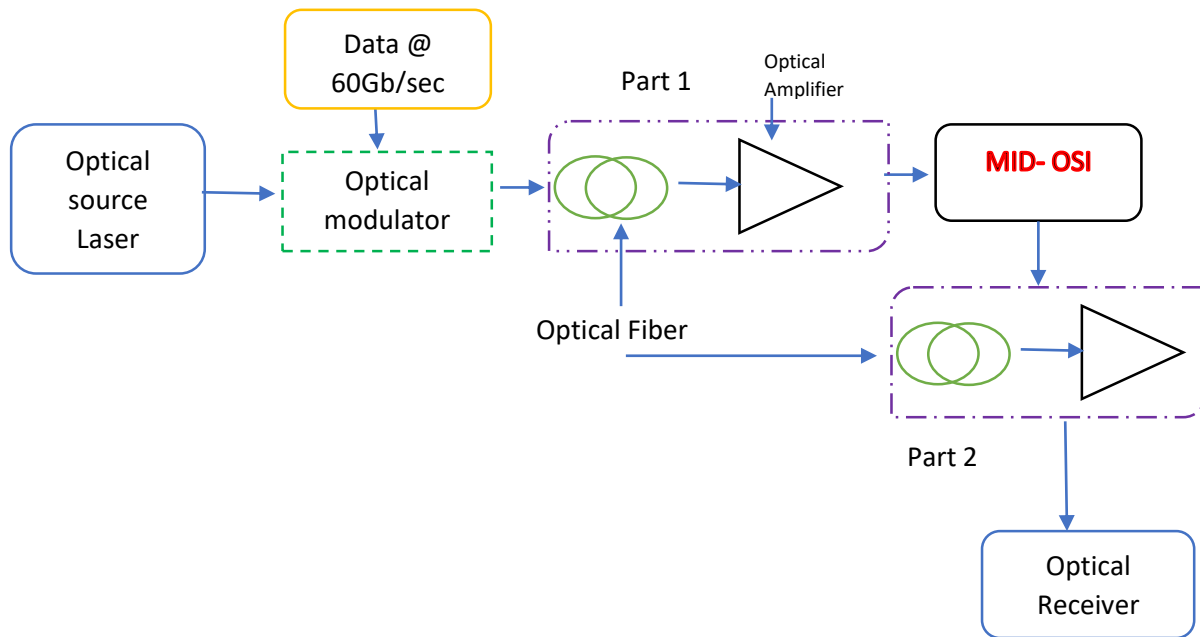


**Figure 4.5 Simulation of optical fiber system with MID-OSI**

This figure illustrates the effect of located OSI by optical phase conjugation compensator at the mid- distance in the optical fiber channel, the OSI enhance the performance of the system at the same fiber length 200Km, and the same optical power for the laser carrier, the performance evaluation of OSI compensator for 30 Gb/s produce superior performance than the system with just DCF compensator used. For input laser power 5 mW the Q-Factor for OSI reach 20, while in DCF equal to 4.8 as shown in figure (4.6) and table (4.3).

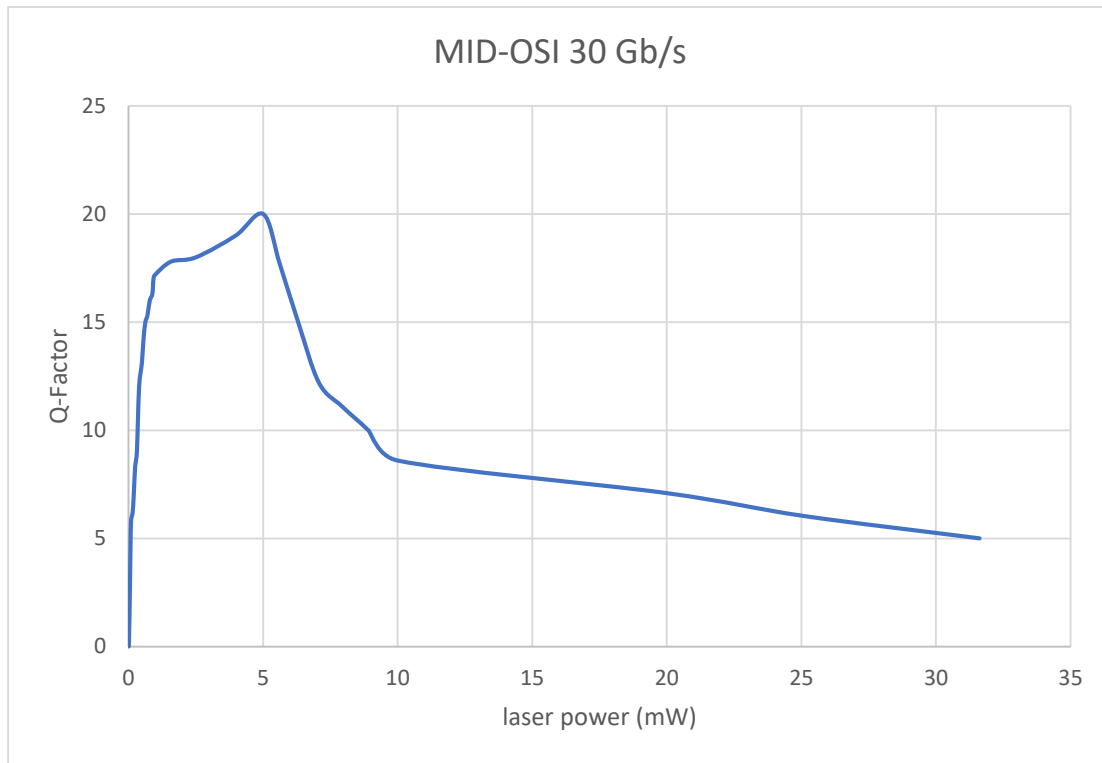


Figure 4.6 Illustrate MiD-OSI compensation fiber at 30 Gb/s

Table 4.3: 200 Km Fiber Length, with MiD-OSI fiber, at bitrate 30 Gb/s

BitRate 30 Gb/s	
Laser power( mW)	Q-Factor
0.01	0
0.015849	0
0.039811	1.3
0.063096	3.2
0.079433	4.6
0.1	5.8

## Chapter Four: Results and Discussion

---

0.158489	6.2
0.199526	7
0.251189	8.3
0.316228	9
0.398107	12
0.501187	13.1
0.562341	14.2
0.630957	15
0.707946	15.3
0.794328	16
0.891251	16.3
0.933254	17
1	17.2
1.584893	17.8
2.511886	18
3.981072	19
5.011872	20
5.623413	17.7
6.309573	15
7.079458	12.2
7.943282	11.1
8.912509	10
10	8.6
19.95262	7.1
25.11886	6.03

Figure (4.7) and table (4.4) illustrate the performance at high bit rate reach 60 Gb/s for the same modulation technique On-OFF key (OOK) and fiber length 200 Km and the same of laser input power can see the effect of adding MID-OSI compensator if are compared with the same system parameters. The performance of the system was preferred than DCF compensator as shown in figures (4.2) (4.3) where in these figures the Q-factor approach to zero for the same input optical power

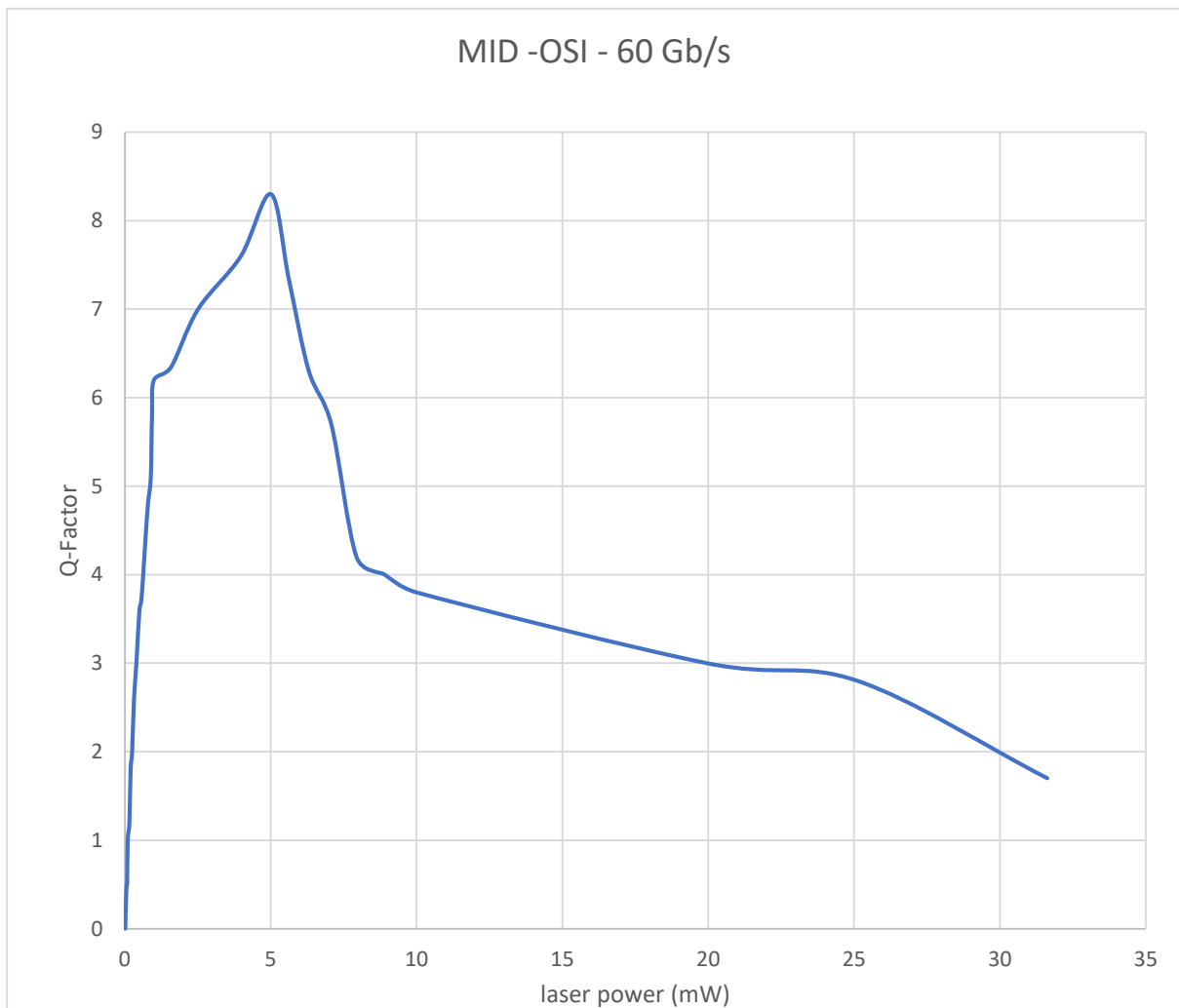


**Table 4.4: Length 200 Km Fiber, with MiD-OSI fiber, at bitrate 60 Gb/s**

## Chapter Four: Results and Discussion

---

<b>BitRate 60 Gb/s</b>	
<b>Laser power( mW)</b>	<b>Q-Factor</b>
0.01	0
0.015849	0
0.039811	0.3
0.063096	0.49
0.079433	0.5
0.1	1
0.158489	1.2
0.199526	1.8
0.251189	2
0.316228	2.6
0.398107	3
0.501187	3.6
0.562341	3.7
0.630957	4
0.707946	4.4
0.794328	4.8
0.891251	5.1
0.933254	5.8
1	6.2
1.584893	6.345
2.511886	7
3.981072	7.6
5.011872	8.3

5.623413	7.34
6.309573	6.3
7.079458	5.7
7.943282	4.2
8.912509	4
10	3.8
19.95262	3
25.11886	2.8

### 4.6 Compensation using MID-HNLF-OSI OOK at Different Fiber Length

In this section the fiber length effect was described at fiber length 200 Km, 400 Km by using MiD- OSI by phase-conjugation of light in the middle of the length of fiber MID- OSI. An orthogonally pumped four wave mixing technique was used by the phase inversion in optics as explained in chapter three, device to enable polarization independent conjugation of the signal band, as shown in Figure (4.5). Two pump laser sources in spectrum 1541.45 nm and 1535.04nm are used in the system. To reduce amplified out-of-band spontaneous emission, the pump wavelengths used, which are subsequently passed through the band pass optoelectronic filter, have a Full width at half maximum (FWHM) of 0.3 nm (ASE). Table (4.5) and figure (4.8) illustrate the effect of OSI compensator on fiber length at 200 Km. and the table (4.6) with figure (4.9) illustrate the effect of OIS on fiber length 400 Km. All the results were compared with reference [94,117,174] and gave a good agreement with the same input parameters.

**Table 4.5: 200 Km Fiber Length, with MiD-OSI fiber, at bitrate 30 Gb/s**

<b>BitRate 30 Gb/s</b>	
<b>Laser power(mW)</b>	<b>Q-Factor</b>
0.01	0
0.015849	0
0.039811	1.3
0.063096	3.2
0.079433	4.6
0.1	5.8
0.158489	6.2
0.199526	7
0.251189	8.3
0.316228	9
0.398107	12
0.501187	13.1
0.562341	14.2
0.630957	15
0.707946	15.3
0.794328	16
0.891251	16.3
0.933254	17
1	17.2
1.584893	17.8
2.511886	18

3.981072	19
5.011872	20
5.623413	17.7
6.309573	15
7.079458	12.2
7.943282	11.1
8.912509	10
10	8.6
19.95262	7.1
25.11886	6.03

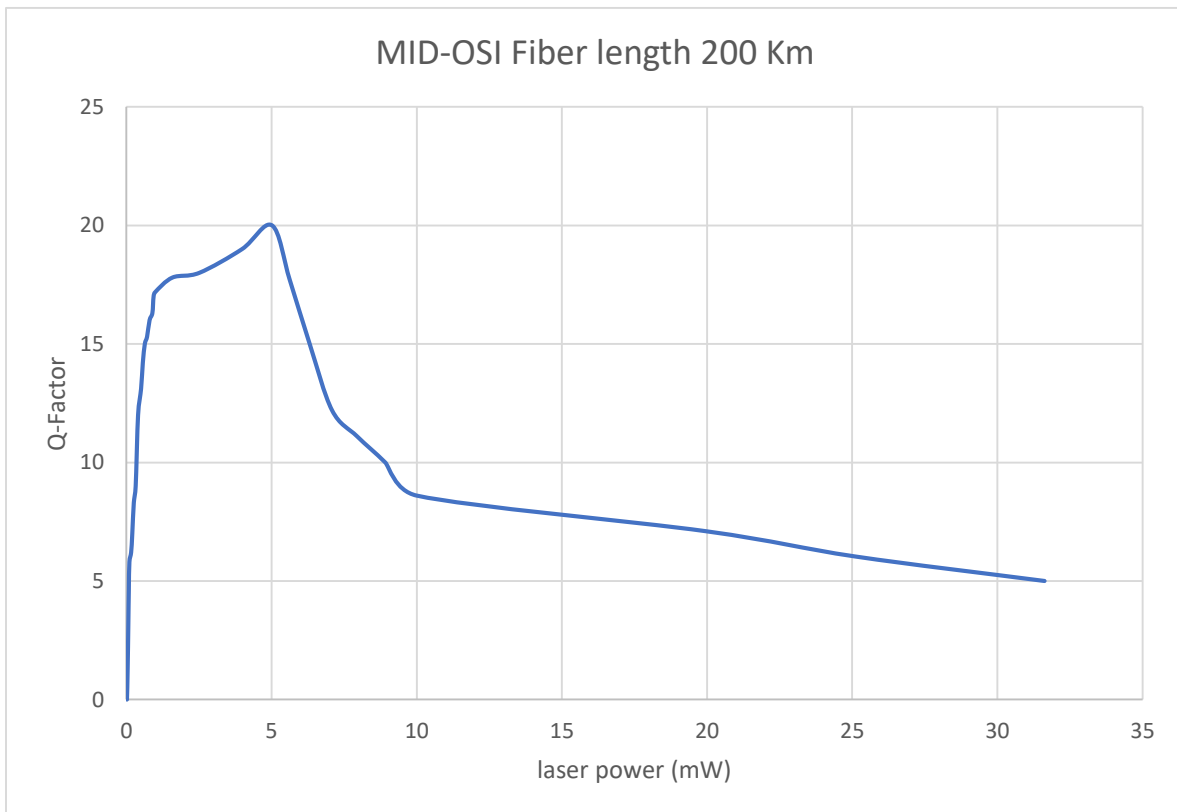


**Figure 4.8** Illustrate the effect of OSI compensator on fiber length at 200 Km.

Table 4.6: 400 Km Fiber Length, with MID-OSI fiber, at bitrate 30 Gb/s

BitRate 30 Gb/s	
Laser power( mW)	Q-Factor
0.01	0
0.015849	0
0.039811	0
0.063096	0
0.079433	2.3
0.1	3
0.158489	3.1
0.199526	3.5
0.251189	4.2
0.316228	4.5
0.398107	6
0.501187	6.4
0.562341	7
0.630957	7.5
0.707946	7.8
0.794328	8
0.891251	8.1
0.933254	8.5
1	8.7
1.584893	8.9
2.511886	9

3.981072	9.4
5.011872	10
5.623413	8.7
6.309573	7.5
7.079458	6.2
7.943282	5.1
8.912509	5
10	4.3
19.95262	3.4
25.11886	3

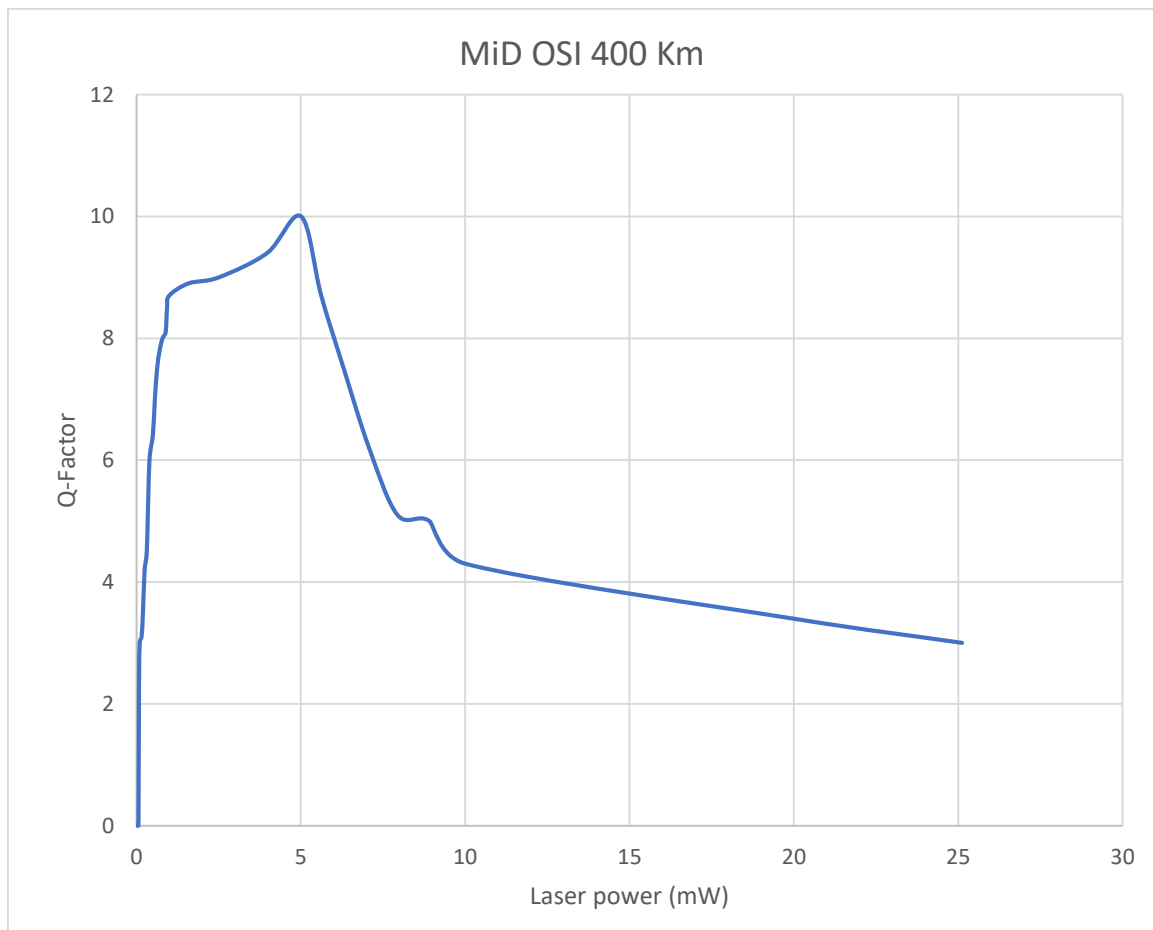


Figure 4.9 Illustrate MiD-OSI compensation fiber at 400 Km

### 4.7 Multiple-(2-OSI) Compensation Scheme for different bit rate

To determine how much better OSI by optical phase conjugation helped discretely amplified systems perform than traditional methods, simulations of single channel optical fiber communication systems were run. The simulation was achieved according to the figure (4.10) that illustrate the schematic of using multi optical phase conjugation across fiber channel to reduce and compensate the fiber nonlinear losses using two pumps lasers pump 1 and pump 2 conjugated idler and data signal. The simulated link seems to have the following parameters with a total length of 400 km of typical single mode fiber.  $\gamma = 1.2$  W/km,  $\alpha = 0.2$  dB/km, chromatic dispersion CD = 16 ps/nm/km. model for evaluating of simulations were run for various values of fiber lengths and data rates.

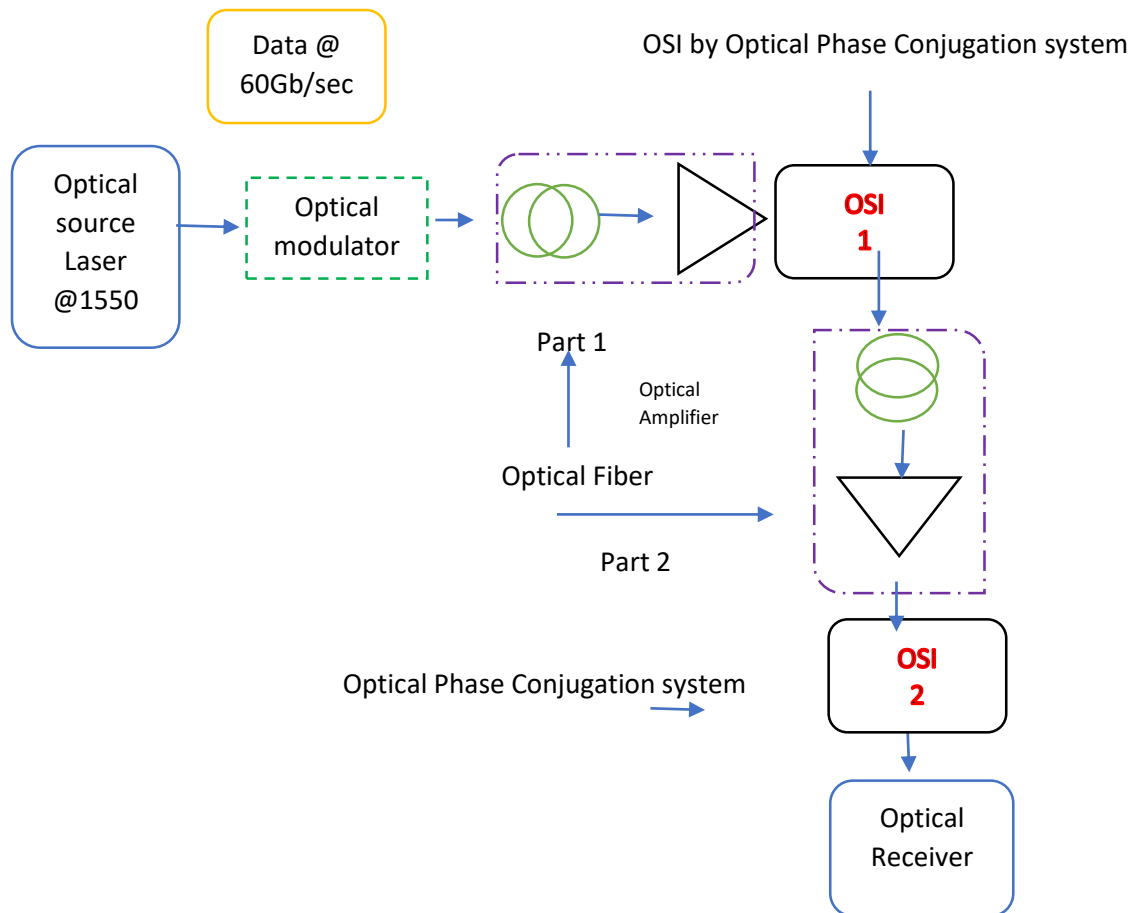


Figure 4.10 Simulation of optical fiber system with Multiple-optical OSI

**4.7.1 Effect of Multiple OSI for 40 Gb/s**

This section described the effect of adding various OSI by optical phases conjugation technique in the simulated optical fiber system the putting of Multiple OSI in the optical fiber system depend on division the fiber channel into equally parts and putting the first OSI in first part and the second OSI in the second part and so on for the remaining parts as shown in figure (4.10). The OSI achieved by optical phase conjugation and the spectrum inverted as illustrated previously and compensate the linear and nonlinear losses. This compensation will enhance the overall performance system for different bitrate reach to the range from 40 Gb/s up to 80 Gb/s as shown in table (4.7) and figure (4.11) for different bitrate at multiple OSI compensator.

**Table 4.7: 400 Km Fiber Length, with Multiple-OSI fiber, at bitrate 40 Gb/s**

<b>BitRate 40 Gb/s</b>	
<b>Laser power( mW)</b>	<b>Q-Factor</b>
0.1	0
0.125	0
0.1584	5.2
0.1995	7
0.2511	8.5
0.3162	9
0.3981	11
0.5011	12
0.6309	14.3
0.7943	15

## Chapter Four: Results and Discussion

---

1	16
1.258	18
1.584	20
1.995	21
2.511	22
3.1622	22.5
3.981	23
5.0118	23.5
6.3095	24
7.9432	25.1
10	22
12.589	20
15.848	18
19.952	17
25.118	16
31.622	15

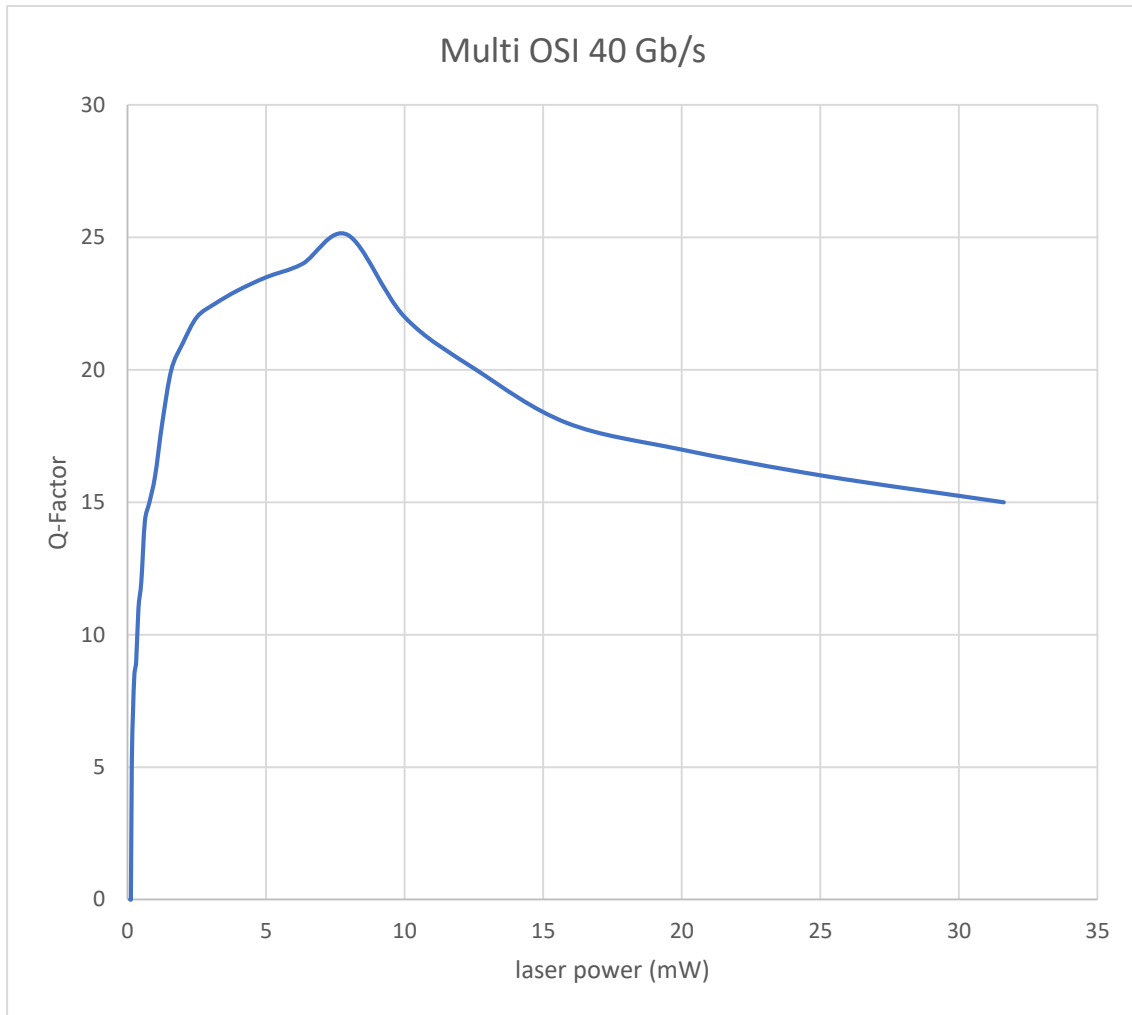


**Figure 4.11** Illustrate Multi-OSI compensation fiber at 40 Gb/s

### 4.7.2 Effect of Multiple OSI for 80 Gb/s

In this section, the enhancement of multiple OSI for a high data rate of 80 Gb/s was proposed it can see the performance of enhancement by increasing the data rate up to 80Gb/s for 400 Km fiber length as shown in table (4.8) and figure (4.12).

**Table 4.8: 400 Km Fiber Length, with Multiple-OSI fiber, at bitrate 80 Gb/s**

<b>Bit Rate 80 Gb/s</b>	
<b>Laser power( mW)</b>	<b>Q-Factor</b>
0.1	0
0.125	0
0.1584	0
0.1995	0
0.2511	6.2
0.3162	7
0.3981	9
0.5011	10
0.6309	12.3
0.7943	13
1	14
1.258	16
1.584	18
1.995	19
2.511	20
3.1622	20
3.981	21
5.0118	21.5
6.3095	22
7.9432	23.3
10	20
12.589	18

15.848	16
19.952	15
25.118	14
31.622	13

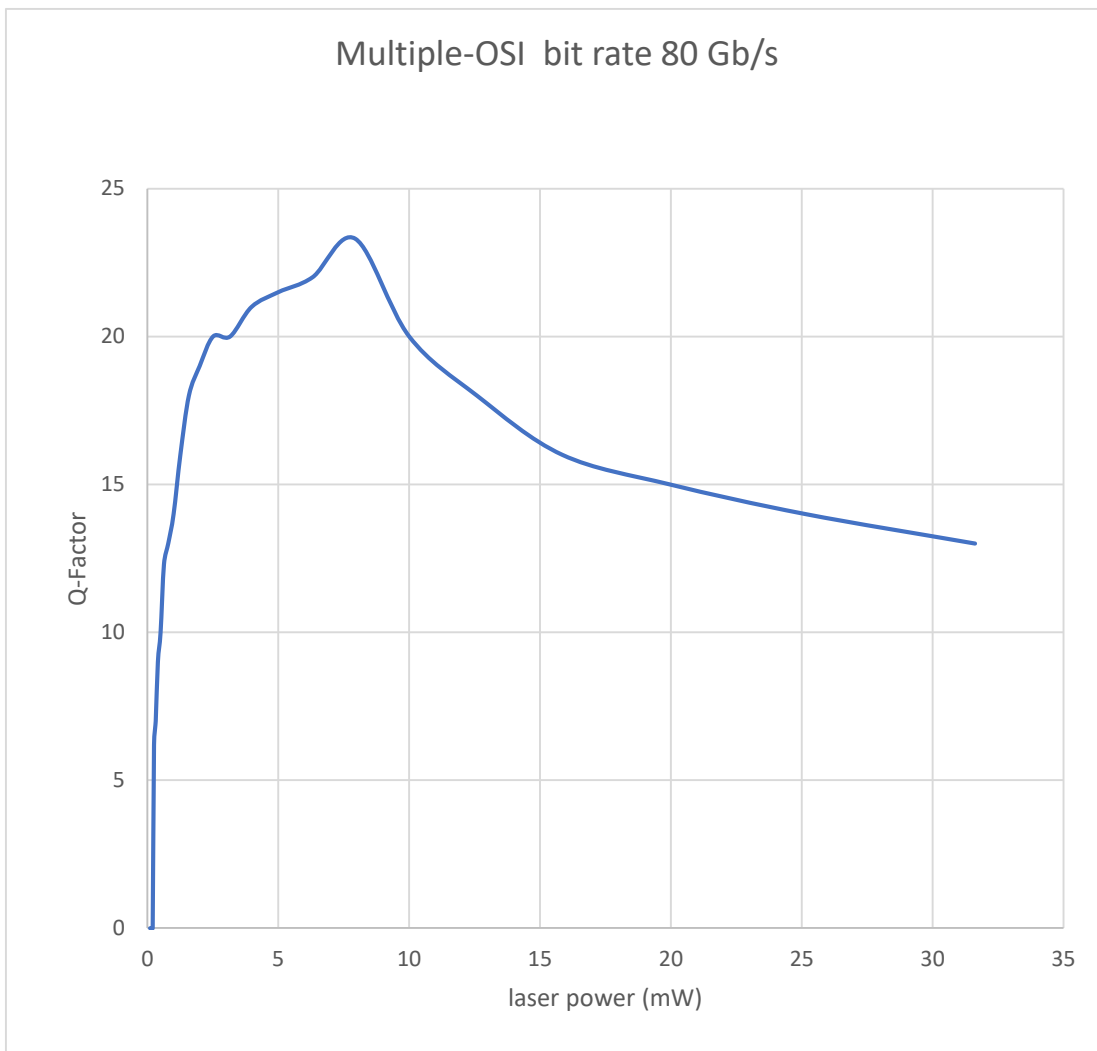


**Figure 4.12** Illustrate Multi-OSI compensation fiber at 80Gb/s

### 4.8 Multiple-(2-OSI) Compensation Scheme for different Fiber length

#### 4.8.1 Effect of Multiple OSI for 200 Km

In this section the 200 Km fiber length has been investigated based on numerical simulation of the proposed system as shown in table 4.9, for fiber with 2-OSI in the figure (4.10). The result shows a good performance in the figure (4.13).

**Table 4.9: 200 Km Fiber Length, with Multiple-OSI fiber, at bitrate 80 Gb/s**

BitRate 80 Gb/s	
Laser power( mW)	Q-Factor
0.1	0
0.125	4
0.1584	4.5
0.1995	5
0.2511	10.2
0.3162	11
0.3981	13
0.5011	14
0.6309	16.2
0.7943	17
1	18
1.258	20
1.584	22
1.995	23
2.511	24
3.1622	24

3.981	25
5.0118	26
6.3095	26.5
7.9432	27.2
10	24
12.589	22
15.848	20
19.952	19
25.118	18
31.622	22

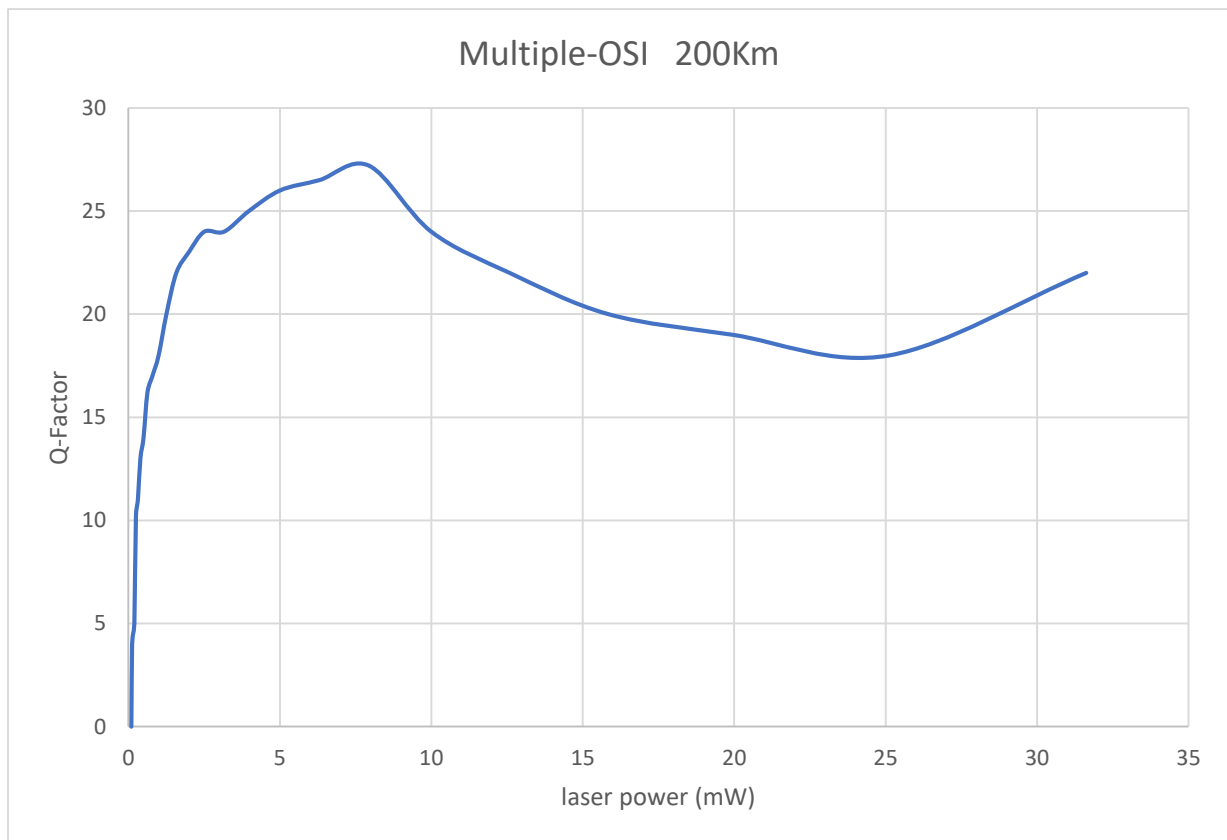


Figure 4.13 Illustrate Multi-OSI compensation fiber at 200Km

### 4.8.2 Effect of Multiple OSI for 400 Km

The enhancement of the proposed system by add the contribution of 2-OSI in fiber system showed in table (4.10) and figure (4.14) for the best performance after the evaluation for long fiber channel length and maximum bitrate where at high bitrate the linear losses such as dispersion increased and for longer fiber channel the linear and nonlinear fiber losses accumulated and increased therefore can see the contribution of 2-OSI for reduction the overall fiber losses as shown in figure (4.14).

**Table 4.10: 400 Km Fiber Length, with Multiple-OSI fiber, at bitrate 80 Gb/s**

Bit Rate 80 Gb/s	
Laser power( mw)	Q-Factor
0.1	0
0.125	0
0.1584	0
0.1995	0
0.2511	6.2
0.3162	7
0.3981	9
0.5011	10
0.6309	12.3
0.7943	13
1	14
1.258	16
1.584	18
1.995	19

2.511	20
3.1622	20
3.981	21
5.0118	21.5
6.3095	22
7.9432	23.3
10	20
12.589	18
15.848	16
19.952	15
25.118	14
31.622	13

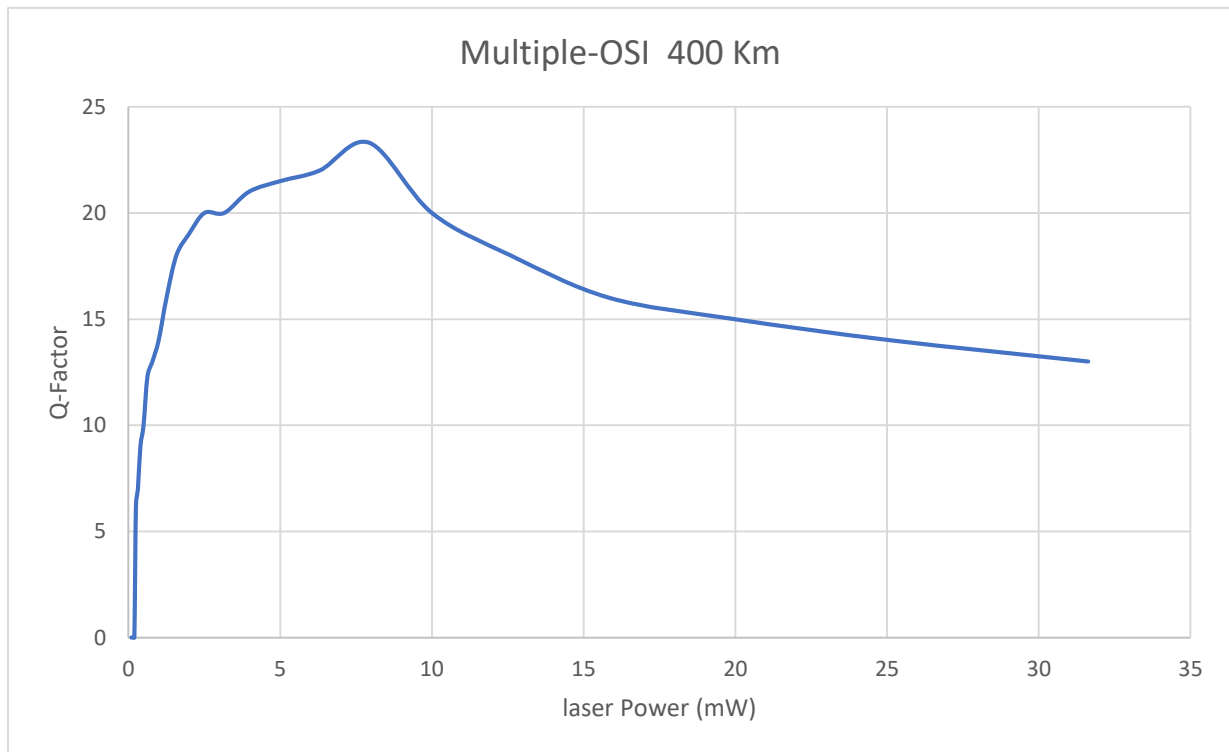


Figure 4.14 Illustrate Multi-OSI compensation fiber at 400Km 80Gb/s

### 4.9 Compensation Using Artificial Neural Networks (ANN)

This section represents nonlinear weakening compensation in optical fiber systems using artificial neural network techniques. The first section presents a model of the optical system incorporating nonlinear effects, which was modelled using Optisystem simulation software ver. 19. This model serves as a basis for understanding the nonlinear effects that occur in optical fiber systems and their impact on signal quality.

In this section compensator of fiber linear and nonlinear effects was introduced as proposed system based on neural networks to eliminate the losses. Where a compensator was designed for linear and nonlinear losses of optical fibers based on artificial intelligence networks and matlab package. All the results in neural network were compared with reference [38,44,175] and give a good agreement with the same input parameters.

#### 4.9.1 Neural network compensator

The field of neural networks has been a significant growth in its applications in fiber optic systems in recent years. These the usage of neural networks to address a wide range of challenges encountered in fiber optic systems, including nonlinear compensation, correction for dispersion of colors and polarization mode divergence. Several neural network architectures have been used in these applications, such as convolutional neural networks (CNNs), feedforward neural networks, and recurrent neural networks. These architectures have been used to model these defects and improve the performance of optical fiber systems.

It should be noted that although neural networks offer a promising solution to compensate for the nonlinear weakness in optical communication, there are also some limitations to their use. One major limitation is the need for a large amount of data to train the network. In addition, the complexity of the network and the computational resources required can also be limitations. Despite these limitations,

the use of neural networks to compensate for nonlinear weaknesses in visual communication is a promising area of research that is expected to see continued growth in the future.

An artificial neural network (ANN) was only utilized as a comparison criterion in this section. As a result, taught the artificial neural network to classify the photos these photos contain a signal that has been digitally altered using an algorithm like phase-shift keying or quadrature amplitude modulation is depicted in a constellation diagram. It depicts the signal as a two-dimensional xy-plane scatter diagram in the complex plane at symbol sampling instants. The angle of a point, measured counterclockwise from the horizontal axis, shows the phase shift of the carrier wave from a reference phase in a manner akin to that of a phasor diagram. If the location of bits' changes due to losses by linear or nonlinear effects in fiber, the ONN will set up the position of bits to correct position because the magnitude or power of the signal is represented by the distance of a location from the origin. This section uses the ReLU activation function in the convolutional layer with an input picture of (28 28) pixels, three hidden layers (512, 256, and 128), and an output of 10 different number classes. The y-coordinate indicates an accuracy value and a loss value, whereas the x-coordinate reflects the number of epochs, if the accuracy curve and loss curve were used to estimate network performance. The system parameters as follows:

1. Batch\_Size\_Train = 128.
2. Batch\_Size\_Test = 256.
3. Number of epochs data set one = 50.  
Number of epochs data set two = 50.
4. Seed = 5 (i.e. five activation functions).  
Seed 0 (indicates to SA (approx.) activation function).  
Seed 1 (indicates to SA (exact) activation function).

Seed 2 (indicates to ReLU activation function).

Seed 3 (indicates to Tanh activation function).

Seed 4 (indicates to sigmoid activation function).

5. Learning Rate =  $10^{-5}$ .

### 4.9.2 Neural network results

Table (4.11) illustrates the results of validation of the first datasets and second dataset.

**Table (4.11): Results of ANN.**

Activation Function	First Dataset	Second Dataset
SA (approx.)	(95 $\pm$ 1) %	(96.14 $\pm$ 1)%
SA (exact)	(96 $\pm$ 1) %	(97.28 $\pm$ 1)%
ReLU	(96.68 $\pm$ 1) %	(97.22 $\pm$ 1)%
Tanh	(98.6 $\pm$ 1) %	(98.16 $\pm$ 1)%
Sigmoid	(97.62 $\pm$ 1) %	(97.30 $\pm$ 1)%

The convolutional neural network used to predict the performance of optic fiber shown in figure (4.15). Processed the nonlinear effect in fiber to enhanced the overall system performance CNN was trained on a dataset of nonlinear measurements taken from an optical fiber, and was able to accurately predict the nonlinearity of the fiber. The network was able to learn complex nonlinear relationships in the data and generalize well to unseen measurements the results as shown in figures for the accuracy and loss of first dataset in ANN, figure (4.16), (4.17) illustrates the accuracy and loss curves of training of the dataset.

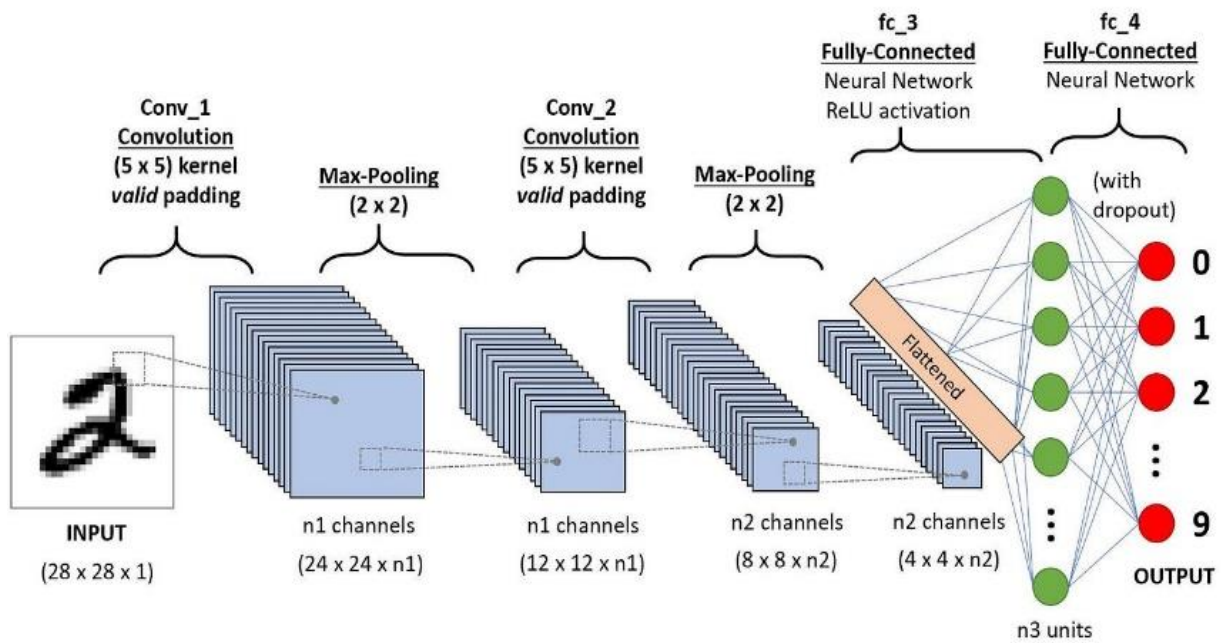


Figure 4.15 A CNN sequence to classify handwritten digits [175]

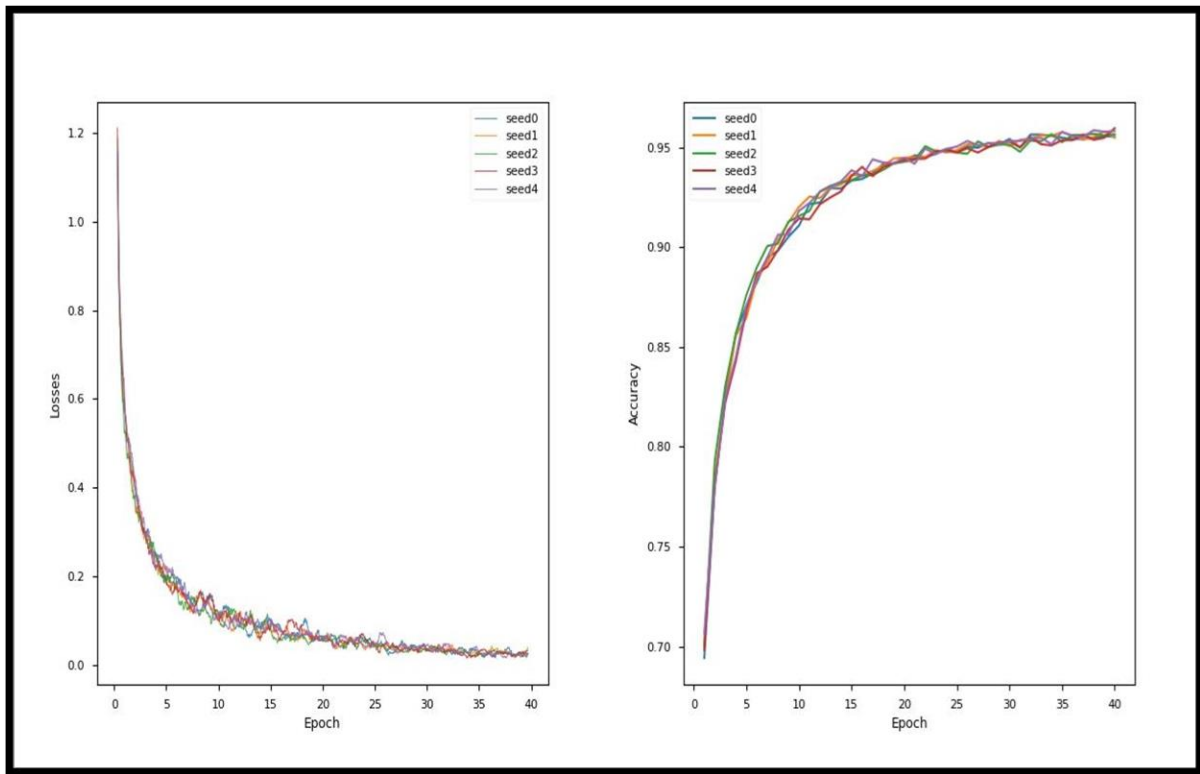
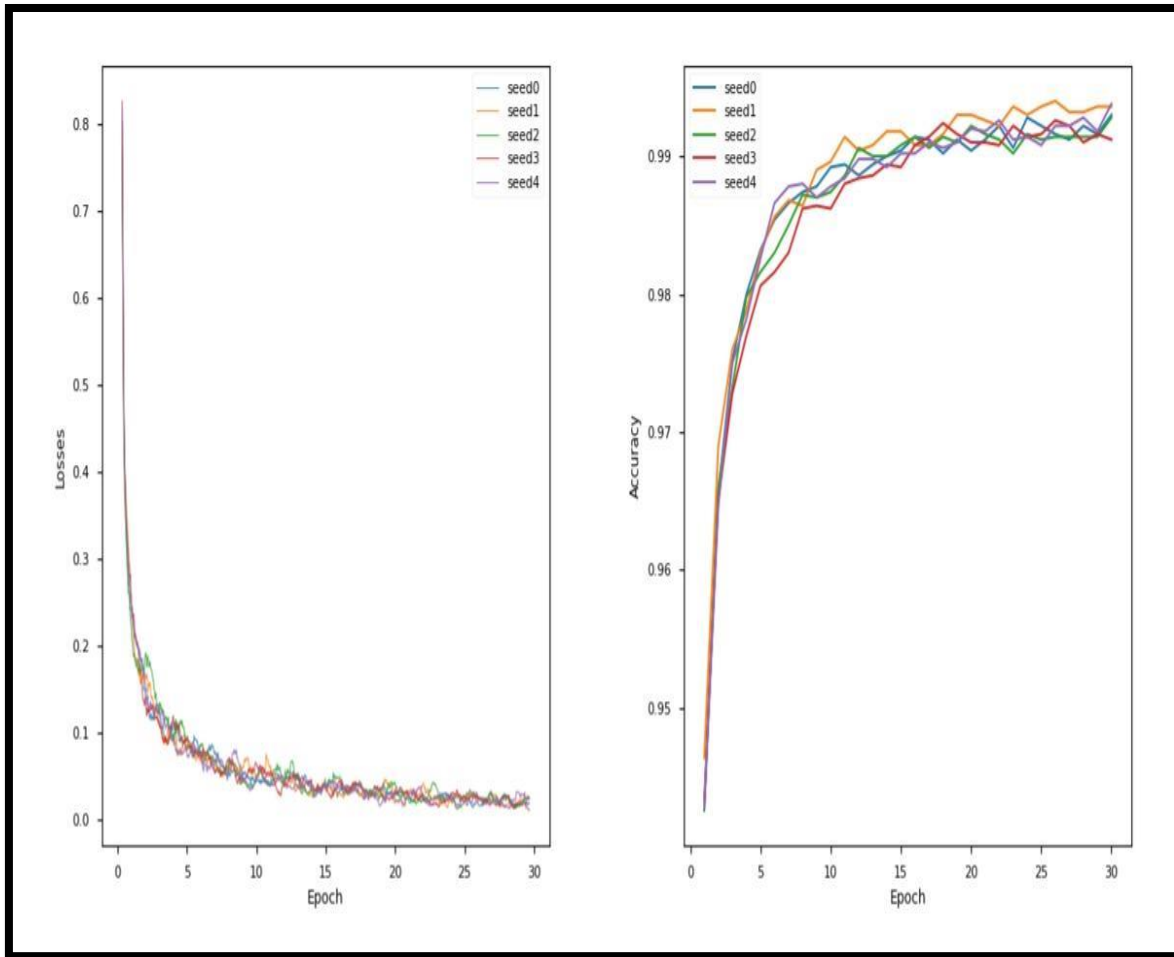


Figure 4.16 The losses and accuracy of first dataset in ANN



**Figure 4.17** The losses and accuracy of second dataset in ANN.

The accuracy of the system rises with the fall in loss due to an inverse relationship between them, as shown by the results in table (4.11) and the graphs in figures (4.16), (4.17).

### **4.10 Results and Discussion of Optical Neural Network (ONN)**

To look into how optical neural networks are trained and how approximation derivatives affect the effectiveness of the network.

The researcher used the fiber parameters and signal power dataset to categorize the photos of constellation diagram. In this section, employed a convolutional layer with SA non-linear activation functions, an input picture of, three hidden layers (512, 256,

and 128), and an output layer of 4 neurons for additionally, the employed the accuracy curve and loss curve to assess the performance of the network; the y-coordinate denotes the accuracy and loss values, respectively, while the x-coordinate denotes the number of epochs. The sets the system parameters as follows:

1. Batch\_Size\_Train = 64.

2. Batch\_Size\_Test = 128.

Batch\_Size\_Test = 1000.

3. Number of epochs data set one = 40

Number of epochs data set two = 40.

4. Seed = 5 (i.e. five activation functions).

Seed 0 (indicates to SA (approx.) activation function).

Seed 1 (indicates to SA (exact) activation function).

Seed 2 (indicates to ReLU activation function).

Seed 3 (indicates to Tanh activation function).

Seed 4 (indicates to sigmoid activation function).

5. Choosing the learning rate is very difficult, so the researcher trained dataset at different learning rates ( $10^{-3}$ ,  $10^{-4}$ ) .To find out which one fits the network best.

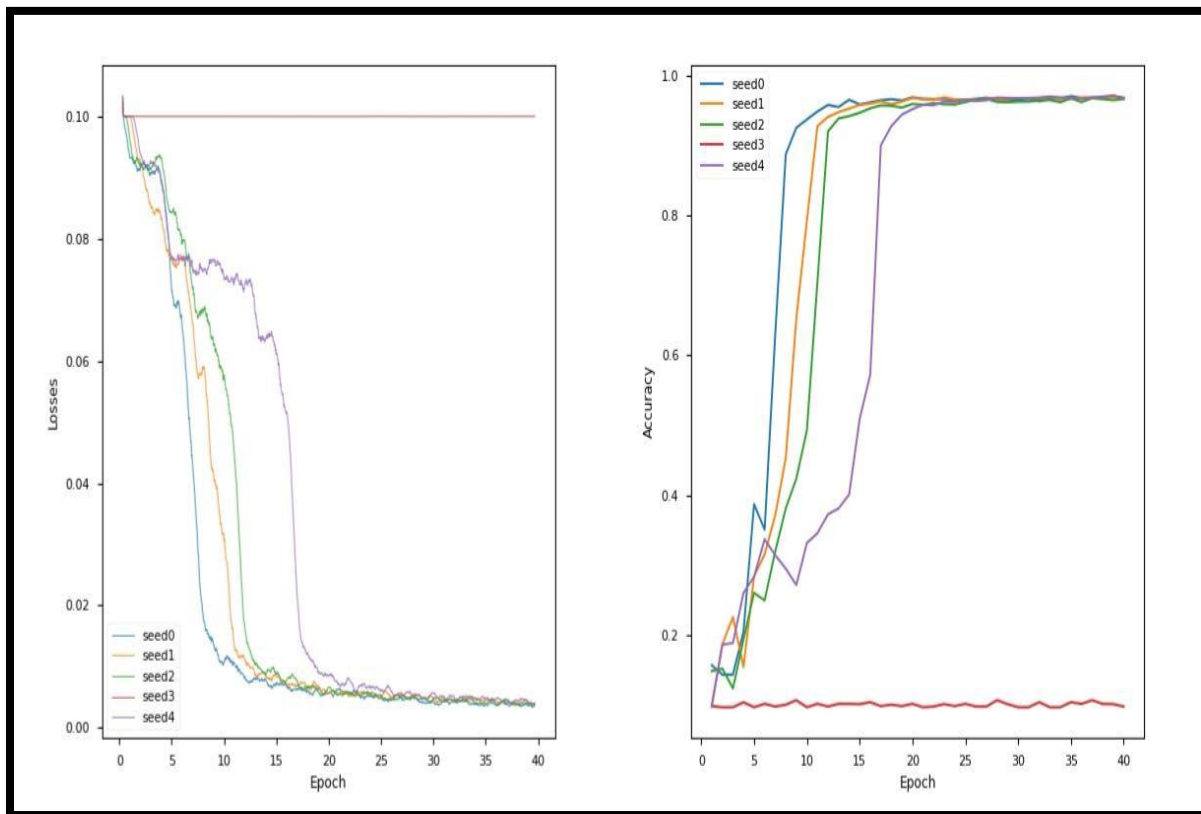
### ***5.1 Learning rate $10^{-3}$ .***

Table (4.12) illustrates the results of validation of the second dataset at learning rate  $10^{-3}$ .

**Table (4.12): Results of dataset in ONN (learning rate  $1 \times 10^{-3}$ ).**

Activation Function	first Dataset
SA (approx.)	(98.04 $\pm$ 0.1) %
SA (exact)	(98.78 $\pm$ 0.1) %
ReLU	(98.12 $\pm$ 0.1) %
Tanh	(98.32 $\pm$ 10) %
Sigmoid	(98.60 $\pm$ 0.1) %

Figure (4.18) illustrates the accuracy and loss curves of training of the first data set at learning rate  $1 \times 10^{-3}$ .



**Figure 4.18 The accuracy and loss of first dataset in ONN**

It is noticed that through the results in table (4.12) and the graphs in figure (4.18), and that the high learning rate led to learning a set of sub-optimal activation function (as in Tanh) because of high speed or unstable training process. Figure 4.18 illustrate the relationship between the loses of the system and the training process we can see the losses decreases while the training of the system. Early neural network models calculated the difference between the actual output and the expected output which was used to determine the error. At the moment, several formulas have appeared for calculating errors in neural networks, these formulas are called Loss Functions. When using various loss functions, this can lead to a different error values for the same prediction, therefore the type of loss function has a major impact on the output of the network.

Accuracy is a metric for the performance of a model. It is typically expressed as a percentage. The number of correct predictions over the total number of predictions is known as accuracy. Although the value is frequently linked to overall or end model accuracy, it is frequently graphed and tracked during the training phase. It is noticed that the accuracy of the system increases (i.e. increase to nearly optimal levels) with the decrease in loss. This indicates that the medium learning rate is suitable for training the system.

### **5.2 Learning rate $1 \times 10^{-4}$ .**

Table (4.13) illustrates the results of validation of the second dataset at learning rate  $1 \times 10^{-4}$ .

Table (4.13): Results of second dataset in ONN (learning rate  $1 \times 10^{-4}$ ).

Activation Function	Second Dataset
SA (approx.)	(99.04 $\pm$ 0.1) %
SA (exact)	(99.06 $\pm$ 0.1) %
ReLU	(98.68 $\pm$ 0.1) %
Tanh	(99.64 $\pm$ 0.1) %
Sigmoid	(98.90 $\pm$ 0.1) %

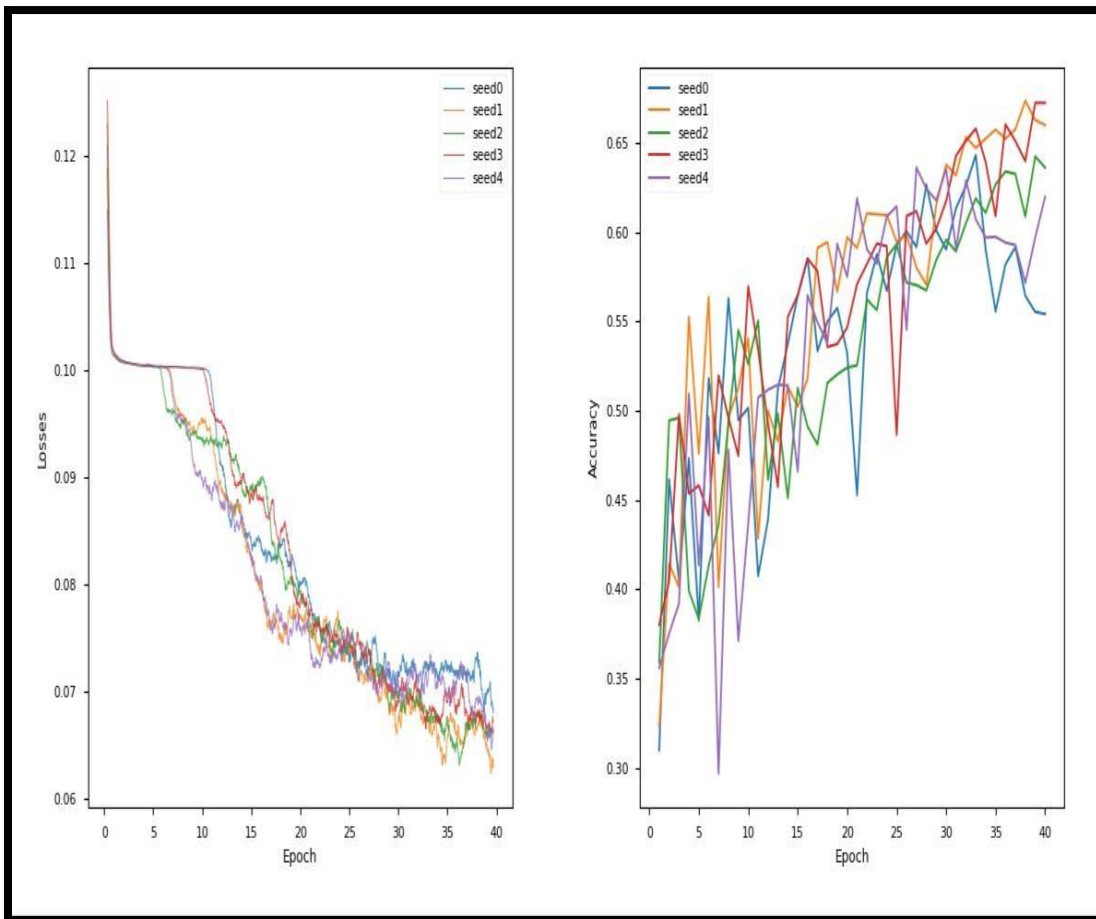


Figure 4.19 The accuracy and loss of second dataset in ONN

Figure (4.19) illustrate the system performance evaluation at second data set training where the ONN produce a loss where the loss is a value that symbolizes the total of the model errors. The loss will be considerable if the errors are high, indicating that the model does not perform well. The lower the loss is, the better model performs we can note the losses decreases as the training process progress and the system produce a good performance. So that from results table (4.13) and figure (4.19) it is noticed the high learning rate led to learning a set of sub-optimal activation function (as in Tanh) because of high speed or unstable training process.

### **4.11 Comparison between Optical Neural Networks (ONNs) and Artificial Neural Networks (ANNs).**

While categorical cross entropy (CCE) serves as the baseline for ANNs, the mean absolute error (MAE) loss function is employed to train ONNs.

This choice was made because soft max in CCE needs offline computation, but gradients for MAE loss may easily be calculated for an optical setup. The ANNs use CCE since it is the go-to method for classification problems in the deep learning arena. The outcomes of optical neural networks and artificial neural networks are shown in Table (4.14).

**Table (4.14): A comparison between Artificial Neural Networks (ANNs) and Optical Neural Networks (ONNs).**

Activation Function	Results of ANNs		Results of ONNs	
	First Dataset	second Dataset	First Dataset $1 \times 10^{-3}$	Second Dataset $1 \times 10^{-4}$
SA (approx.)	$(95 \pm 1) \%$	$(96.14 \pm 1)\%$	$(98.04 \pm 0.1) \%$	$(99.04 \pm 0.1) \%$
SA (exact)	$(96 \pm 1) \%$	$(97.28 \pm 1)\%$	$(98.78 \pm 0.1) \%$	$(99.06 \pm 0.1) \%$
ReLU	$(96.68 \pm 1) \%$	$(97.22 \pm 1)\%$	$(98.12 \pm 0.1) \%$	$(98.68 \pm 0.1) \%$
Tanh	$(98.6 \pm 1) \%$	$(98.16 \pm 1)\%$	$(98.92 \pm 10) \%$	$(99.64 \pm 0.1) \%$
Sigmoid	$(97.62 \pm 1) \%$	$(97.30 \pm 1)\%$	$(98.60 \pm 0.1) \%$	$(98.90 \pm 0.1) \%$

It is noticed that through the results in table (4.14) the accuracy of ANNs is almost close to the accuracy of ONNs. As for the value of the loss ONNs is much better than the value of the loss of ANNs, as well as for the processing speed in the implementation of ONNs, it was faster than the speed of the implementation of ANNs and the reason is due to the distinctive characteristics of ONNs compared to ANNs.

The neural networks perform a process of training on the outputs of the optical system, and then they are trained to correct the power and phase values of the signal passing through the optical fiber visual and modify the transmission signal accordingly. The overall performance of the fiber system will also enhance. the

performance target was achieved, with the accuracy reaching up to 98% for the training and testing data as illustrated in figure (4.20).

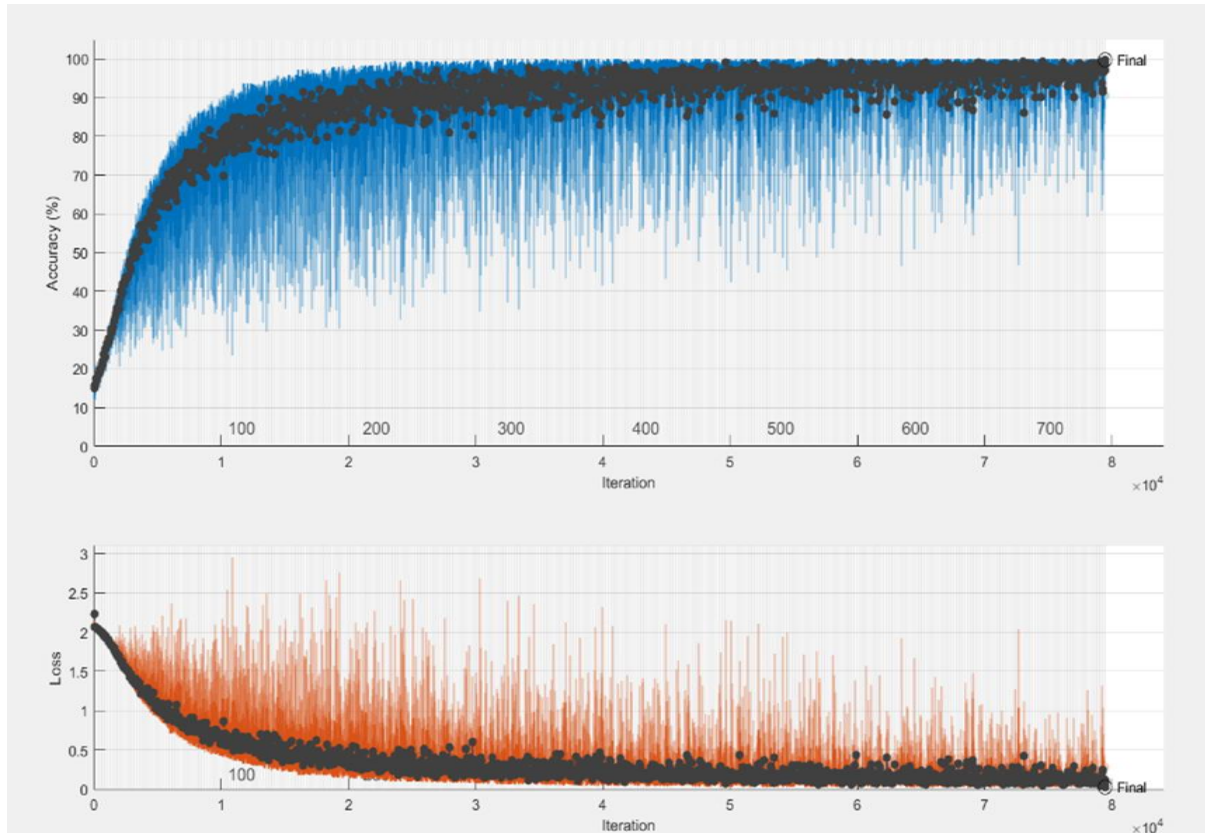


**Figure 4.20 Training of convolutional neural network**

Table (4.15) represents the performance evaluation of the proposed system at a variety of fiber lengths by changing the number of spans in order to assess how effective the ONN compensating method and also changing the laser power. This will be done in order to investigate and evaluate the performance of the proposed system at a variety of fiber lengths and laser power. At the end of investigation of ONN learning compensation based on two efficient algorithms that were employed in this work to address and solve the problems that the optical fiber

**Table 4.15** Illustrate the performance enhancement of the system for different laser power and fiber length

Laser power (dBm)	Fiber length (Km)	BER *10 <sup>-3</sup>
-20	100	0.00612
	500	0.0718
	1000	0.0175
-15	100	0.00614
	500	0.0780
	1000	0.0509
-10	100	0.00652
	500	0.08124
	1000	0.1235
1	100	0.00759
	500	0.09897
	1000	0.1789
8	100	0.00703
	500	0.0993
	1000	0.18954
10	100	0.0087
	500	0.167
	1000	0.1991
20	100	0.00908
	500	0.18561
	1000	0.203

### 5.1 Conclusions

As the need for channel capacity rises, fiber nonlinearity has been discovered to be one of the reasons limiting optical fiber systems. This research makes a contribution to our understanding of how fiber nonlinearity affects optical fiber system performance.

The proposed work produces the most important conclusions where the conclusions that can be obtained from the proposed work can be summarized as follows:

- i) Through this study, the researcher concluded that the use of optical neural networks in processing data systems is a good method for its distinctive properties, such as high speed, bandwidth, high correlation, internal balanced processing, and low power consumption which makes it a very promising method to be used in the future.
- ii) The saturable absorption (SA) nonlinear activation function depends on the optical depth, so choosing the optical depth is critical. The researcher noticed from the results that the saturable absorption (SA) nonlinear activation function achieves the best results at medium optical depths, but at very low and very high optical depths, the results are not at the desired level.
- iii) Effect of using dispersion compensation fiber DCF in optical fiber system can illuminate the linear losses of optical fiber and non-compensate the nonlinear losses.
- iv) Introduce a new proposal model for optical phase conjugation to compensate the linear and nonlinear fiber losses
- v) The proposed solution of fiber nonlinearities gives the preferable performance of optical fiber in communication and medical applications

### 5.2 Suggestions for future works

- i) Development of an optical phase conjugation device that omits the HNLF in favor of photonic crystal fiber.
- ii) Design new optical spectrum inversion OSI based on optical neural network system
- iii) Use different pump sources for the design of Optical spectrum inversion (phase conjugation)
- iv) Using the developed Multi OSI system to solved the nonlinear losses at higher bitrate and different fiber lengths

## References

---

- [1] S. Sugumaran, R. Bhura, U. Sagar, and P. Arulmozhivarman, "Performance analysis of FWM efficiency and Schrödinger equation solution," *Int. J. Eng. Technol.*, vol. 5, no. 2, pp. 1665–1671, 2013.
- [2] S. Kanprachar, "Modeling and Analysis of the Effects of Impairments in Fiber Optic Links," Thesis, 1999.
- [3] F. Da Ros., "Nonlinearity Compensation through Optical Phase Conjugation for Improved Transmission Reach/Rate," *Int. Conf. Transparent Opt. Networks*, vol. 2, no. 22, pp. 2114–2115, 2018.
- [4] H. Eliasson, P. Johannisson, M. Karlsson and P. A. Andrekson, "Mitigation of nonlinearities using conjugate data repetition," *Optics Express*, vol. 23, no. 3, pp. 2392-2402, 2015.
- [5] X. Xiao, S. Gao, Y. Tian, H. Yan, and C. Yang, "The effect of optical phase conjugation on inter- and intra-channel nonlinearities in ultrahigh-speed transmission systems," *Opt. Transm. Switch. Subsystems III*, vol. 6021, p. 602130, 2005.
- [6] Cristiani, Ilaria' "Compensation of nonlinear effects in optical communication systems through phase-conjugation." 2009 IEEE LEOS Annual Meeting Conference Proceedings. IEEE, 2009.
- [7] J. C. Cartledge, F. P. Guiomar, F. R. Kschischang, G. Liga, and M. P. Yankov, "Digital signal processing for fiber nonlinearities" *Opt. Express*, vol. 25, no. 3, p. 1916, 2017.
- [8] A. Kurtinaitis and F. Ivanauskas, "Finite Difference Solution Methods for a System of the Nonlinear Schrödinger Equations," *Nonlinear Anal. Model. Control*, vol. 9, no. 3, pp. 247–258, 2004.
- [9] S. Kumar Orappanpara Soman, "A tutorial on fiber Kerr nonlinearity effect and its compensation in optical communication systems," *J. Opt. (United Kingdom)*, vol. 23, no. 12, 2021.

## References

---

- [10] J. Toulouse, "Optical nonlinearities in fibers: Review, recent examples, and systems applications," *J. Light. Technol.*, vol. 23, no. 11, pp. 3625–3641, 2005.
- [11] Supe, A. and Porins, J. "Methods for Estimation of Optical Fiber Non-Linearity Using Self-Phase Modulation Effect" *Latvian Journal of Physics and Technical Sciences*, vol.48, no.6, pp.29-40 ,2012.
- [12] J. B. H. Tahar, "Theoretical and Simulation Approaches for Studying Compensation Strategies of Nonlinear Effects Digital Lightwave Links Using DWDM Technology," *J. Comput. Sci.*, vol. 3, no. 11, pp. 887–893, 2007.
- [13] H. F. Arnoldus and T. F. George, "Theory of optical phase conjugation in Kerr media," *Phys. Rev. A*, vol. 51, no. 5, pp. 4250–4263, 1995
- [14] D. S. Hsiung, thesis "Fast and Efficient Optical Phase Conjugation Using a Degenerate Raman System in Rubidium," MIT 1997.
- [15] S. Kanprachar, "Modeling and Analysis of the Effects of Impairments in Fiber Optic Links," Thesis, 1999.
- [16] Guang, "Optical phase conjugation: Principles, techniques, and applications," *Prog. Quantum Electron.*, vol. 26, no. 3, pp. 131–191, 2001
- [17] Claudio "nonlinear effect in optical fiber "thesis 2001.
- [18] B. Xu, "Study of Fiber Nonlinear Effects on Fiber Optic Communication Systems by," Engineering, 2003.
- [19] Kurtinaitis and F. Ivanauskas, "Finite Difference Solution Methods for a System of the Nonlinear Schrödinger Equations," *Nonlinear Anal. Model. Control*, vol. 9, no. 3, pp. 247–258, 2004.
- [20] J. Toulouse, "Optical nonlinearities in fibers: Review, recent examples, and systems applications," *J. Light. Technol.*, vol. 23, no. 11, pp. 3625–3641, 2005.
- [21] X. Xiao, S. Gao, Y. Tian, H. Yan, and C. Yang, "The effect of optical phase conjugation on inter- and intra-channel nonlinearities in ultrahigh-speed

## References

---

- transmission systems,” *Opt. Transm. Switch. Subsystems III*, vol. 6021, p. 602130, 2005.
- [22] J. B. H. Tahar, “Theoretical and Simulation Approaches for Studying Compensation Strategies of Nonlinear Effects Digital Lightwave Links Using DWDM Technology,” *J. Comput. Sci.*, vol. 3, no. 11, pp. 887–893, 2007.
- [23] I. Cristiani, “Compensation of nonlinear effects in optical communication systems through phase-conjugation,” *Conf. Proc. - Lasers Electro-Optics Soc. Annu. Meet.*, no. May 2014, pp. 751–752, 2009.
- [24] A. Supe and J. Porins, “Optisko šķiedru nelinearitātes novērtējuma metodes, izmantojot signāla fāzes pašmodulācijas efektu,” *Latv. J. Phys. Tech. Sci.*, vol. 48, no. 6, pp. 29–40, 2011.
- [25] S. Sugumaran, R. Bhura, U. Sagar, and P. Arulmozhivarman, “Performance analysis of FWM efficiency and Schrödinger equation solution,” *Int. J. Eng. Technol.*, vol. 5, no. 2, pp. 1665–1671, 2013.
- [26] Salah Al-Deen, M. M. Shellal, and A. C. Kadhim, “Simulation of Gaussian Pulses Propagation Through Single Mode Optical Fiber Using MATLAB,” *Iraqi J. Sci.*, vol. 54, no. 3, pp. 601–606, 2013.
- [27] M. Gazeau, “Numerical simulation of nonlinear pulse propagation in optical fibers with randomly varying birefringence,” *J. Opt. Soc. Am. B*, vol. 30, no. 9, p. 2443, 2013.
- [28] H. Eliasson, “Mitigation of nonlinear fiber distortion using phase conjugation Mitigation of nonlinear fiber distortion using phase conjugation,” 2016.
- [29] J. C. Cartledge, F. P. Guiomar, F. R. Kschischang, G. Liga, and M. P. Yankov, “Digital signal processing for fiber nonlinearities [Invited],” *Opt. Express*, vol. 25, no. 3, p. 1916, 2017.
- [30] Adnan S. Abbas, Mazin M. Elias, and Raad. S. Fyath”Comprehensive Analysis of HNLFF-Based Optical Phase Conjugation in the Presence of Polarization

- Misalignment” Jour of Adv Research in Dynamical & Control Systems, Vol. 10, 04-Special Issue, 2018.
- [31] Francesco Da Ros, Metodi P. Yankov, Edson P. da Silva, Mads Lillieholm Pawel M. Kaminski, P. Guan<sup>1</sup>, Hao Hu<sup>1</sup>, Anders T. Clausen<sup>1</sup>, Michael Galili<sup>1</sup>, and Leif K. Oxenløwe “Nonlinearity Compensation through Optical Phase Conjugation for Improved Transmission Reach/Rate” ICTON 2018
- [32] P. M. Kaminski, “Lumped Compensation of Nonlinearities based on Optical Phase Conjugation,” *J. Light. Technol.*, vol. 40, no. 3, pp. 681–691, 2022.
- [33] J. Wang, Y. Du, C. Liang, Z. Li, and J. Fang, “Performance evaluation of highly nonlinear fiber (HNLF) based optical phase conjugation (OPC) in long haul transmission of 640 Gbps 16-QAM CO-OFDM,” *Photonics*, vol. 8, no. 2, pp. 1–9, 2021.
- [34] S. Kumar Orappanpara Soman, “A tutorial on fiber Kerr nonlinearity effect and its compensation in optical communication systems,” *J. Opt. (United Kingdom)*, vol. 23, no. 12, 2021.
- [35] Fan Sun, Feng Wen, BaojianWu, Yun Ling and Kun Qiu “Optical Phase Conjugation Conversion through a Nonlinear Bidirectional Semiconductor Optical Amplifier Configuration” *Photonics* 2022, 9, 164.
- [36] A. Jha, C. Huang, H. T. Peng, W. Zhang, B. Shastri, and P. R. Prucnal, “High-speed time series prediction and classification on an all-optical neural network,” *Opt. InfoBase Conf. Pap.*, vol. 1, no. c, pp. 2–4, 2016.
- [37] G. Fennessy, "Optical Neural Networks.", 16 May 2018. arXiv: 1805.06082v1 [cs.CV].
- [38] J. Chang, V. Sitzmann, X. Dun, W. Heidrich, and G. Wetzstein, “Hybrid optical-electronic convolutional neural networks with optimized diffractive optics for image classification,” *Sci. Rep.*, vol. 8, no. 1, pp. 1–10, 2018.

- [39] S. Geoffroy-Gagnon, F. Shokraneh, and O. Liboiron-Ladouceur, “Analysis of an analog optical neural network,” *Front. Opt. - Proc. Front. Opt. + Laser Sci. APS/DLS*, no. January 2020, pp. 10–12, 2019.
- [40] R. Hamerly, L. Bernstein, A. Sludds, M. Soljačić, and D. Englund, “Large-Scale Optical Neural Networks Based on Photoelectric Multiplication,” *Phys. Rev. X*, vol. 9, no. 2, pp. 1–12, 2019.
- [41] M. Y.-S. Fang, S. Manipatruni, C. Wierzynski, A. Khosrowshahi, and M. R. DeWeese, “Design of optical neural networks with component imprecisions,” *Opt. Express*, vol. 27, no. 10, p. 14009, 2019.
- [42] M. Paraschiv, R. Padrino, P. Casaris, and A. F. Anta, "Very Small Neural Networks for Optical Classification of Fish Images and Videos", 2020.
- [43] H. Zhang, M. Gu, X. D. Jiang, J. Thompson, H. Cai, S. Paesani, R. Santagati, A. Laing, Y. Zhang, M. H. Yung, Y. Z. Shio, F. K. Muhammad, G. Q. Lo, X. S. Luo, B. Dong, D. L. Kwong, L. C. Kwek & A. Q. Liu., “An optical neural chip for implementing complex-valued neural network,” *Nat. Commun.*, vol. 12, no. 1, pp. 1–11, 2021.
- [44] T. Wang, S. Y. Ma, L. G. Wright, T. Onodera, B. C. Richard, and P. L. McMahon, “An optical neural network using less than 1 photon per multiplication,” *Nat. Commun.*, vol. 13, no. 1, pp. 1–8, 2022.
- [45] N. A. Kudryashov, “Mathematical model of propagation pulse in optical fiber with power nonlinearities,” *Optik (Stuttg.)*, vol. 212, no. April, p. 164750, 2020.
- [46] Y. Z. Pchelkina and I. V. Alimenkov, “The solutions of the equations of pulse propagation in optical fibers,” *J. Phys. Conf. Ser.*, vol. 574, no. 1, 2014.
- [47] S. M. K. Chaitanya and P. Rajesh Kumar, “Kidney images classification using cuckoo search algorithm and artificial neural network,” *Int. J. Sci. Technol. Res.*, vol. 9, no. 3, pp. 6127–6132, 2020.

## References

---

- [48] R. Verma and P. Garg, “Qualitative Analysis of Self Phase Modulation (SPM),” vol. 4, no. 2, pp. 330–333, 2013.
- [49] S. H. Saeid, “Computer simulation and performance evaluation of single mode fiber optics,” *Lect. Notes Eng. Comput. Sci.*, vol. 2198, pp. 1007–1012, 2012.
- [50] Ryan, Cooper, and Tauer “principle of phase conjugation “springer 2013.
- [51] F. George, “Theory optical Kerr,” vol. 51, no. 5, 1995.
- [52] A. Yariv, D. Fekete, and D. M. Pepper, “Compensation for channel dispersion by nonlinear optical phase conjugation,” *Opt. Lett.*, vol. 4, no. 2, p. 52, 1979.
- [53] L. N. Venkatasubramani, A. Sobhanan, A. Vijay, R. D. Koilpillai, and D. Venkitesh, “Optical Phase Conjugation Using Nonlinear SOA for Nonlinearity and Dispersion Compensation of Coherent Multi-Carrier Lightwave Systems,” *IEEE Access*, vol. 9, pp. 44059–44068, 2021.
- [54] R. Hamerly, L. Bernstein, A. Sludds, M. Soljačić, and D. Englund, “Large-Scale Optical Neural Networks Based on Photoelectric Multiplication,” *Phys. Rev. X*, vol. 9, no. 2, pp. 1–12, 2019.
- [55] F. Sun, F. Wen, B. Wu, Y. Ling, and K. Qiu, “Optical Phase Conjugation Conversion through a Nonlinear Bidirectional Semiconductor Optical Amplifier Configuration,” *Photonics*, vol. 9, no. 3, 2022.
- [56] H. Zhang, M. Gu, X. D. Jiang, J. Thompson, H. Cai, S. Paesani, R. Santagati, A. Laing, Y. Zhang, M. H. Yung, Y. Z. Shio, F. K. Muhammad, G. Q. Lo, X. S. Luo, B. Dong, D. L. Kwong, L. C. Kwek & A. Q. Liu., “An optical neural chip for implementing complex-valued neural network,” *Nat. Commun.*, vol. 12, no. 1, pp. 1–11, 2021.
- [57] J. Wang, Y. Du, C. Liang, Z. Li, and J. Fang, “Performance evaluation of highly nonlinear fiber (HNLF) based optical phase conjugation (OPC) in long haul transmission of 640 Gbps 16-QAM CO-OFDM,” *Photonics*, vol. 8, no. 2, pp. 1–9, 2021.

## References

---

- [58] A. Krizhevsky, I. Sutskever, and G. E. Hinton, "ImageNet classification with deep convolutional neural networks," *Commun. ACM*, 2017.
- [59] G. S. He, "Optical phase conjugation: Principles, techniques, and applications," *Prog. Quantum Electron.*, vol. 26, no. 3, pp. 131–191, 2002.
- [60] Kaminski, Pawel M., et al. "Lumped compensation of nonlinearities based on optical phase conjugation." *Journal of Lightwave Technology* 40.3 (2021): 681-691.
- [61] B. Y. Zel'dovich, N. F. Pilipetsky, and V. V. Shkunov, "OPC in Four-Wave Mixing," vol. 1, pp. 144–170, 1985.
- [62] D. Zhang and Z. Tan, "A Review of Optical Neural Networks," *Appl. Sci.*, vol. 12, no. 11, 2022.
- [63] P. A. Birdi, Yashika, Tanjyot Aurora, "Study of Artificial Neural Networks and neural implants," *Int. J. Recent Innov. Trends Comput. Commun.*, vol. 1(4), pp. 258–62, 2013.
- [64] M. Ducloy, "Nonlinear Optical Phase Conjugation," *Festkoerperprobleme*, no. October 1982, pp. 35–60, 1982.
- [65] F. Da Ros, "Nonlinearity Compensation through Optical Phase Conjugation for Improved Transmission Reach/Rate," *Int. Conf. Transparent Opt. Networks*, vol. 2018-July, no. 22, pp. 2014–2015, 2018.
- [66] A. S. Abbas, "Mitigation of Distortion in WDM Systems Based on Optical Phase Conjugation," p. 128, 2017.
- [67] H. Eliasson, P. Johannisson, M. Karlsson and P. A. Andrekson, "Mitigation of nonlinearities using conjugate data repetition," *Optics Express*, vol. 23, no. 3, pp. 2392-2402, 2015.
- [68] X. Xiao, S. Gao, Y. Tian, H. Yan, and C. Yang, "The effect of optical phase conjugation on inter- and intra-channel nonlinearities in ultrahigh-speed

## References

---

- transmission systems,” *Opt. Transm. Switch. Subsystems III*, vol. 6021, p. 602130, 2005.
- [69] J.P. Huignard and A. Brignon, “Overview of Phase Conjugation,” *Phase Conjug. Laser Opt.*, pp. 1–17, 2005.
- [70] A. H. Jarah and D. I. A. Murdas, “Optical nonlinear impairment compensation based on Deep Neural Network (DNN) for coherent modulation systems,” *Period. Eng. Nat. Sci.*, vol. 10, no. 1, pp. 431–441, 2022.
- [71] H. Eliasson, S. L. I. Olsson, M. Karlsson and P. A. Andrekson, “Mitigation of nonlinear distortion in hybrid Raman/phase-sensitive amplifier links,” *Optics Express*, vol. 24, no. 2, pp. 888-900, 2016.
- [72] M. Pradeep Doss, T. Sridarshini, and M. Valliammai, “Performance analysis and dispersion compensation in ultra-Long-Haul 10Gbps optical system by OPC,” *Commun. Comput. Inf. Sci.*, vol. 269 CCIS, no. PART I, pp. 545–549, 2012.
- [73] J. Wang, Y. Du, C. Liang, Z. Li, and J. Fang, “Performance evaluation of highly nonlinear fiber (HNLF) based optical phase conjugation (OPC) in long haul transmission of 640 Gbps 16-QAM CO-OFDM,” *Photonics*, vol. 8, no. 2, pp. 1–9, 2021.
- [74] Kaminski, P. M., Da Ros, F., Yankov, M. P., Hansen, H. E., Ulvenberg, J. B., Schou, C. K., ... & Galili, M. (2021). Lumped compensation of nonlinearities based on optical phase conjugation. *Journal of Lightwave Technology*, 40(3), 681-691.
- [75] G. S. He, “Optical phase conjugation: Principles, techniques, and applications,” *Prog. Quantum Electron.*, vol. 26, no. 3, pp. 131–191, 2002.
- [76] J. Wang, Y. Du, C. Liang, Z. Li, and J. Fang, “Performance evaluation of highly nonlinear fiber (HNLF) based optical phase conjugation (OPC) in long

## References

---

- haul transmission of 640 Gbps 16-QAM CO-OFDM,” *Photonics*, vol. 8, no. 2, pp. 1–9, 2021.
- [77] F. Sun, F. Wen, B. Wu, Y. Ling, and K. Qiu, “Optical Phase Conjugation Conversion through a Nonlinear Bidirectional Semiconductor Optical Amplifier Configuration,” *Photonics*, vol. 9, no. 3, 2022.
- [78] H. F. Arnoldus and T. F. George, “Theory of optical phase conjugation in Kerr media,” *Phys. Rev. A*, vol. 51, no. 5, pp. 4250–4263, 1995.
- [79] S. Kanprachar, “Modeling and Analysis of the Effects of Impairments in Fiber Optic Links,” Thesis, 1999.
- [80] A. S. Abbas, “Mitigation of Distortion in WDM Systems Based on Optical Phase Conjugation,” p. 128, 2017.
- [81] S. Sugumaran, R. Bhura, U. Sagar, and P. Arulmozhivarman, “Performance analysis of FWM efficiency and Schrödinger equation solution,” *Int. J. Eng. Technol.*, vol. 5, no. 2, pp. 1665–1671, 2013.
- [82] M. González-Herráez and T. Sylvestre, “Nonlinear effects in optical fibers,” *Adv. Fiber Opt.*, pp. 145–170, 2011.
- [83] CRISTIANI, Ilaria, et al. Compensation of nonlinear effects in optical communication systems through phase-conjugation. In: 2009 IEEE LEOS Annual Meeting Conference Proceedings. IEEE, 2009. p. 751-752.
- [84] J. C. Cartledge, F. P. Guiomar, F. R. Kschischang, G. Liga, and M. P. Yankov, “Digital signal processing for fiber nonlinearities [Invited],” *Opt. Express*, vol. 25, no. 3, p. 1916, 2017.
- [85] J. Toulouse, “Optical nonlinearities in fibers: Review, recent examples, and systems applications,” *J. Light. Technol.*, vol. 23, no. 11, pp. 3625–3641, 2005.
- [86] J. B. H. Tahar, “Theoretical and Simulation Approaches for Studying Compensation Strategies of Nonlinear Effects Digital Lightwave Links Using DWDM Technology,” *J. Comput. Sci.*, vol. 3, no. 11, pp. 887–893, 2007.

## References

---

- [87] S. Kumar Orappanpara Soman, “A tutorial on fiber Kerr nonlinearity effect and its compensation in optical communication systems,” *J. Opt.* (United Kingdom), vol. 23, no. 12, 2021.
- [88] A. Supe and J. Porins, “Optisko šķiedru nelinearitātes novērtējuma metodes, izmantojot signāla fāzes pašmodulācijas efektu,” *Latv. J. Phys. Tech. Sci.*, vol. 48, no. 6, pp. 29–40, 2011.
- [89] S. Al, D. Adnan, M. M. Shellal, and A. C. Kadhim, “Simulation of Gaussian Pulses Propagation Through Single Mode Optical Fiber Using MATLAB,” *Iraqi J. Sci.*, vol. 54, no. 3, pp. 601–606, 2013.
- [90] M. Gazeau, “Numerical simulation of nonlinear pulse propagation in optical fibers with randomly varying birefringence,” *J. Opt. Soc. Am. B*, vol. 30, no. 9, p. 2443, 2013.
- [91] S. H. Saeid, “Computer simulation and performance evaluation of single mode fiber optics,” *Lect. Notes Eng. Comput. Sci.*, vol. 2198, pp. 1007–1012, 2012.
- [92] S. P. Singh, “Progress in Electromagnetics Research, PIER 73, 249–275, 2007,” pp. 249–275, 2007.
- [93] I. Powe, “study of Fiber Nonlinearities and Effect of Phase input power and chirping Factor on received power,” MSc thesis Deemed University 2012.
- [94] G. P. Agrawal, “Nonlinear fiber optics,” *Nonlinear Fiber Opt.*, pp. 1–728, 2019.
- [95] B. Xu, “Study of Fiber Nonlinear Effects on Fiber Optic Communication Systems by,” *Engineering*, 2003.
- [96] Y. Z. Pchelkina and I. V. Alimenkov, “The solutions of the equations of pulse propagation in optical fibers,” *J. Phys. Conf. Ser.*, vol. 574, no. 1, 2014.
- [97] M. González-Herráez and T. Sylvestre, “Nonlinear effects in optical fibers,” *Adv. Fiber Opt.*, pp. 145–170, 2011.

## References

---

- [98] N. A. Kudryashov, "Mathematical model of propagation pulse in optical fiber with power nonlinearities," *Optik (Stuttg.)*, vol. 212, no. April, p. 164750, 2020.
- [99] R. Verma and P. Garg, "Qualitative Analysis of Self Phase Modulation (SPM)," vol. 4, no. 2, pp. 330–333, 2013.
- [100] G. P. Agrawal, "Nonlinear fiber optics," *Nonlinear Fiber Opt.*, pp. 1–728, 2019.
- [101] Huignard, Jean-Pierre, and Arnaud Brignon. "Overview of phase conjugation." *Phase Conjugate Laser Optics* (2004): 1.
- [102] A. H. Jarah and D. I. A. Murdas, "Optical nonlinear impairment compensation based on Deep Neural Network (DNN) for coherent modulation systems," *Period. Eng. Nat. Sci.*, vol. 10, no. 1, pp. 431–441, 2022.
- [103] J.-P. Huignard and A. Brignon, "Overview of Phase Conjugation," *Phase Conjugate. Laser Opt.*, pp. 1–17, 2005, doi: 10.1002/0471728446.ch1.
- [104] XIAO, Xiaosheng, et al. The effect of optical phase conjugation on inter-and intra-channel nonlinearities in ultrahigh-speed transmission systems. In: *Optical Transmission, Switching, and Subsystems III*. SPIE, 2005. p. 759-767.
- [105] Ryan, Cooper, and Tauer, "principle of phase conjugation "springer 2013.
- [106] H. Eliasson and H. Eliasson, "Mitigation of nonlinear fiber distortion using phase conjugation Mitigation of nonlinear fiber distortion using phase conjugation," 2016.
- [107] D. S. Hsiung, "Fast and Efficient Optical Phase Conjugation Using a Degenerate Raman System in Rubidium," p. 70, 1997.
- [108] A. S. Abbas, "Mitigation of Distortion in WDM Systems Based on Optical Phase Conjugation," p. 128, 2017.

## References

---

- [109] M. Ducloy, “Nonlinear Optical Phase Conjugation,” *Festkoerperprobleme*, no. October 1982, pp. 35–60, 1982.
- [110] D. Zhang and Z. Tan, “A Review of Optical Neural Networks,” *Appl. Sci.*, vol. 12, no. 11, 2022.
- [111] B. Y. Zel’dovich, N. F. Pilipetsky, and V. V. Shkunov, “OPC in Four-Wave Mixing,” vol. 1, pp. 144–170, 1985.
- [112] KAMINSKI, Pawel M., et al. Lumped compensation of nonlinearities based on optical phase conjugation. *Journal of Lightwave Technology*, 2021, 40.3: 681-691.
- [113] G. S. He, “Optical phase conjugation: Principles, techniques, and applications,” *Prog. Quantum Electron.*, vol. 26, no. 3, pp. 131–191, 2002.
- [114] J. Wang, Y. Du, C. Liang, Z. Li, and J. Fang, “Performance evaluation of highly nonlinear fiber (HNLF) based optical phase conjugation (OPC) in long haul transmission of 640 Gbps 16-QAM CO-OFDM,” *Photonics*, vol. 8, no. 2, pp. 1–9, 2021.
- [115] F. Sun, F. Wen, B. Wu, Y. Ling, and K. Qiu, “Optical Phase Conjugation Conversion through a Nonlinear Bidirectional Semiconductor Optical Amplifier Configuration,” *Photonics*, vol. 9, no. 3, 2022.
- [116] L. N. Venkatasubramani, A. Sobhanan, A. Vijay, R. D. Koilpillai, and D. Venkitesh, “Optical Phase Conjugation Using Nonlinear SOA for Nonlinearity and Dispersion Compensation of Coherent Multi-Carrier Lightwave Systems,” *IEEE Access*, vol. 9, pp. 44059–44068, 2021.
- [117] A. Yariv, D. Fekete, and D. M. Pepper, “Compensation for channel dispersion by nonlinear optical phase conjugation,” *Opt. Lett.*, vol. 4, no. 2, p. 52, 1979.
- [118] F. George, “Theory optical Kerr,” vol. 51, no. 5, 1995.

## References

---

- [119] M. Pradeep Doss, T. Sridarshini, and M. Valliammai, “Performance analysis and dispersion compensation in ultra-Long-Haul 10Gbps optical system by OPC,” *Commun. Comput. Inf. Sci.*, vol. 269 CCIS, no. PART I, pp. 545–549, 2012.
- [120] F. Project, “Orthogonal Frequency-Division Multiplexing for Optical Communications a Dissertation Submitted to the Department of Electrical Engineering and the Committee on Graduate Studies of Stanford University in Partial Fulfillment of the Requirements for the Degr,” Final year Proj., no. September, p. 160, 2011.
- [121] M. L. Hafiane, Z. Dibi, and O. Manck, “On the Capability of Artificial Neural Networks to Compensate Nonlinearities in Wavelength Sensing,” *Sensors*, vol. 9, no. 4, pp. 2884–2894, 2009.
- [122] G. P. Agrawal, “Lightwave Technology: Telecommunication Systems” John Wiley & Sons 2018.
- [123] S. P. Singh, R. Gangwar, and N. Singh, “Nonlinear scattering effects in optical fibers,” *Prog. Electromagn. Res.*, vol. 74, pp. 379–405, 2007.
- [124] Z. Kriszti, “Nonlinear wave propagation and ultrashort pulse compression in step-index and microstructured fibers,” 2007, [Online]. Available: <http://libra.msra.cn/Publication/14070518/nonlinear-wave-propagation-and-ultrashort-pulse-compression-in-step-index-and-microstructured-fibers>
- [125] B. Xu, “Study of Fiber Nonlinear Effects on Fiber Optic Communication Systems by,” *Engineering*, 2003.
- [126] *Fiber-Optic Communications Systems, Third Edition.*, vol. 6. 2002.
- [127] S. P. Singh, “Progress in Electromagnetics Research, PIER 73, 249–275, 2007,” pp. 249–275, 2007.
- [128] M. Moshinsky dissertation, “nonlinear pulse propagation through an optical fiber theory and experiment 2004.

## References

---

- [129] M. N. Chughtai, “Nonlinear Phase Noise in Fiber Optical Communication,” 2009.
- [130] M. Y. Hamza, “Mitigation of SPM and GVD Effects in Fiber Optic Communications by Dispersion- and Power-Map Co-Optimization Using Genetic Algorithm,” no. June, 2009.
- [131] M. Y. Hamza, “Mitigation of SPM and GVD Effects in Fiber Optic Communications by Dispersion- and Power-Map Co-Optimization Using Genetic Algorithm,” no. June, 2009.
- [132] M. Borecki, “Intelligent fiber optic sensor for estimating the concentration of a mixture-design and working principle,” *Sensors*, vol. 7, no. 3, pp. 384–399, 2007.
- [133] B. Li and Y. Chen, “On exact solutions of the nonlinear Schrödinger equations in optical fiber,” *Chaos, Solitons and Fractals*, vol. 21, no. 1, pp. 241–247, 2004.
- [134] M. J. Li, “Fiber designs for reducing stimulated Brillouin scattering,” 2006 *Opt. Fiber Commun. Conf. 2006 Natl. Fiber Opt. Eng. Conf.*, vol. 2006, no. 4, pp. 2–4, 2006.
- [135] T. Hohage and F. Schmidt, “On the Numerical solution of Nonlinear Schrodinger Type Equations in Fiber Optics,” *ZIB-Report*, vol. 04, no. Januar, p. 25, 2002.
- [136] X. Deng, “A modified split-step Fourier scheme for fiber-optic communication system and its application to forward and backward propagation,” pp. xi, 57, 2010.
- [137] M. Malekiha, “Analysis of Nonlinear Effects and Their Mitigation in Fiber-Optic Their Mitigation in Fiber-Optic,” 2011.
- [138] Z. Kriszti, “Nonlinear wave propagation and ultrashort pulse compression in step-index and microstructured fibers,” 2007,

## References

---

- [139] S. Christa, V. Suma, and L. Madhuri, “Data preprocessing using intelligent agents,” *Adv. Intell. Syst. Comput.*, vol. 199 AISC, pp. 197–204, 2013.
- [140] T. V. Andersen, “Applications of Nonlinear Optics and Optical Fibers PhD thesis,” *Opt. Express*, no. April, 2006.
- [141] T. Carmon, “Nonlinear Optics and Solitons,” 2003.
- [142] O. V Sinkin, “Calculation of Bit Error Rates in Optical Fiber Communications Systems in the Presence of Nonlinear Distortion and Noise by,” *System*, 2006.
- [143] J. Shoer, “Simulation of a Passively Modelocked All-Fiber Laser with Nonlinear Optical Loop Mirror by,” *Components*, no. May, 2006.
- [144] M. Saeed, “Determining optimal fibre-optic network architecture using bandwidth forecast, competitive market, and infrastructure-efficient models used to study last mile,” no. June, p. 66, 2011, [Online]. Available: <https://tspace.library.utoronto.ca/handle/1807/31425>
- [145] M. Rusu, *Frequency Conversion Using Ultrafast Fiber Lasers*. 2006.
- [146] R. G. Molla, “Nonlinear Fiber Optics for Bio-Imaging,” p. 467, 2001.
- [147] M. Y. Hamza, “Mitigation of SPM and GVD Effects in Fiber Optic Communications by Dispersion- and Power-Map Co-Optimization Using Genetic Algorithm Department of Computer Science A thesis submitted to the Department of Computer Science, Lahore University of Management,” no. June, 2009.
- [148] R. Gangopadhyay and S. Chandra, “DWDM Transmission Systems and Networks: Experiments by Simulation,” pp. 101–110, 2004.
- [149] F. Čertík, “Using Matlab Tools for Simulation of the optical transmission medium,” *Tech. Comput. Bratislava 2012 [elektronický zdroj] 20th Annu. Conf. Proceedings. Bratislava*, p. 7.11., 2012.
- [150] T. J. Xia, “Optical channel capacity - From Mb/s to Tb/s and beyond,” *Opt. Fiber Technol.*, vol. 17, no. 5, pp. 328–334, 2011.

## References

---

- [151] M. González-Herráez and T. Sylvestre, “Nonlinear effects in optical fibers,” *Adv. Fiber Opt.*, pp. 145–170, 2011.
- [152] Xu, Runqin, “A survey of approaches for implementing optical neural networks.” *Optics & Laser Technology* 136 (2021): 106787.
- [153] Zhang, Qiming, "Artificial neural networks enabled by nanophotonics." *Light: Science & Applications* 8.1 (2019): 1-14.
- [154] Xiong, Jianmin, Zejun Zhang, and Jing Xu. "Advances and marine applications of optical neural network." *Seventh Symposium on Novel Photoelectronic Detection Technology and Applications*. Vol. 11763. International Society for Optics and Photonics, 2021.
- [155] Guo, Xianxin, "Backpropagation through nonlinear units for the all-optical training of neural networks." *Photonics Research* 9.3 (2021): B71-B80.
- [156] I. Neokosmidis, “Propagation limitations in all-optical networks due to nonlinear effects,” 2019.
- [157] O. A. Note, “Matlab component Creating a component to handle optical signals OptiSystem Application Note”.
- [158] L. Franzens, U. Innsbruck, and T. U. Berlin, “Lecture on Time-Splitting Spectral Methods for Nonlinear Schrödinger Equations Mechthild Thalhammer Analytical and Numerical Aspects of Evolution Equations”.
- [159] Q. Lin, “Polarization and Fiber Nonlinearities,” New York, 2006.
- [160] Z. M. Liao and P. Agrawal, Dissertation “Design of High-Capacity Fiber-Optic Transport Systems Zhi Ming Liao,” 2001.
- [161] A. Kurtinaitis and F. Ivanauskas, “Finite Difference Solution Methods for a System of the Nonlinear Schrödinger Equations,” *Nonlinear Anal. Model. Control*, vol. 9, no. 3, pp. 247–258, 2004.
- [162] J. E. Kardontchik and S. Wurster, “300 meters on installed MMF Part III: Link Simulations,” no. November, 1999.

## References

---

- [163] J. F. COOPER, “Chapter I,” *The Deerslayer*, pp. 13–29, 2019, doi: 10.2307/j.ctvjsf5ms.9.
- [164] Huang, C., Fujisawa, S., de Lima, T. F., Tait, A. N., Blow, E. C., Tian, Y., ... & Prucnal, P. R. (2021). A silicon photonic–electronic neural network for fibre nonlinearity compensation. *Nature Electronics*, 4(11), 837-844.
- [165] S. Sugumaran, R. Bhura, U. Sagar, and P. Arulmozhivarman, “Performance analysis of FWM efficiency and Schrödinger equation solution,” *Int. J. Eng. Technol.*, vol. 5, no. 2, pp. 1665–1671, 2013.
- [166] M. González-Herráez and T. Sylvestre, “Nonlinear effects in optical fibers,” *Adv. Fiber Opt.*, pp. 145–170, 2011.
- [167] C. C. Figura, “Second Order Nonlinear Optics in Ionically Self-Assembled Thin Films, Chapter One: An Introduction to Nonlinear Optics, Second Order Nonlinear Applications, and Nonlinear Materials,” PhD Diss. Blacksburg, Virginia, pp. 1–24, 1999.
- [168] T. V. Andersen, “Applications of Nonlinear Optics and Optical Fibers PhD thesis,” *Opt. Express*, no. April, 2006.
- [169] O. V Sinkin, “Calculation of Bit Error Rates in Optical Fiber Communications Systems in the Presence of Nonlinear Distortion and Noise by,” *System*, 2006.
- [170] G. P. Agrawal, “Nonlinear fiber optics,” *Nonlinear Fiber Opt.*, pp. 1–728, 2019.
- [171] S. Kanprachar, “Modeling and Analysis of the Effects of Impairments in Fiber Optic Links,” Thesis, 1999.
- [172] K. N. Modi, “Modeling, Detection and Signal Design for Multichannel Fiber Optic Communications,” Thesis 2009.
- [173] L. McCarthy, M. E., Turitsyn, S. K., Phillips, I., Lavery, D., Xu, Tllis, A. D. “Optical and Digital Phase Conjugation Techniques for Fiber Nonlinearity

## References

---

- Compensation” Opto-Electronics and Communications Conference (OECC),2015.
- [174] Reach/Rate F.Ros, M.Yankov,E. da Silva<sup>1</sup>, Mads Lillieholm, Pawel M. Kaminski<sup>1</sup>,P. Guan, Hao Hu, Anders T. Clausen<sup>1</sup>, Michael Galili, and Leif K. Oxenløwe ,” Nonlinearity Compensation through Optical Phase Conjugation for Improved Transmission” IEEE conference ICTON 2018.
- [175] Chaoran Huang, Shinsuke Fujisawa, Thomas Ferreira de Lima, Alexander N. Tait “Silicon photonic-electronic neural network for fibre nonlinearity compensation” journal of Nature Electronics, Vol.4, No.11, PP837-844, 2021.